Investigating the temporally dynamic mechanisms of T-cell regulation during helminth infection

A thesis presented by

Catherine Beth Ducker

In partial fulfilment of the requirements for the degree of Doctor of Philosophy (PhD) in Immunology.

Department of Life Sciences, Imperial College London

July 2020

Declaration of Originality

The work contained in this thesis is my own; all work that is not my own has been appropriately referenced.

C.B.Ducker
July 2020

Copyright declaration

The copyright of this thesis rests with the author. Unless otherwise indicated, its contents are licensed under a Creative Commons Attribution-Non Commercial 4.0 International Licence (CC BY-NC). Under this licence, you may copy and redistribute the material in any medium or format. You may also create and distribute modified versions of the work. This is on the condition that: you credit the author and do not use it, or any derivative works, for a commercial purpose. When reusing or sharing this work, ensure you make the licence terms clear to others by naming the licence and linking to the licence text. Where a work has been adapted, you should indicate that the work has been changed and describe those changes. Please seek permission from the copyright holder for uses of this work that are not included in this licence or permitted under UK Copyright Law.

Acknowledgements

I would like to thank my supervisor, Dr Masahiro Ono, for all his help and guidance throughout my PhD. I have learnt and grown as a scientist due to his mentorship; skills that will stay with me as I progress in my career. I am grateful to the MRC for funding my PhD and allowing me to undertake the research of my choosing. I would also like to thank Dr David Bending for all his help at the start of my PhD and instilling in me the importance of networking at conferences. I am grateful to Professor Murray Selkirk, Dr Corinna Schnoeller and Dr Rita Berkachy for sharing with me their expertise and resources. Finally, I would like to thank the other members of the Ono lab, Dr Bahire Kalfaoglu, Alina Paduraru, and Jehanne Hassan.

Many friends have made my PhD an unforgettable experience. Honourable mentions go to Kathryn Farrell, Emily Whettlock and Carys Davies for your relentless friendship; Dr Josh Blight for the ridiculous number of GIFs and harassing me into finishing this thesis; and to Dr Heather Ang for her help, no matter the time of day or duration, especially when faced with a broken flow cytometer in the late evening/s.

My placement year during my BSc was instrumental in my decision to undertake a PhD. I loved my year and I know that my career will continue to be heavily influenced by my time there; I would like to thank the whole team. In particular, I would like to thank my mentor and supervisor at the time, Dom, for his patience and friendship. I would also like to thank Riccardo for his help and guidance upon hearing that I was interested in parasite-immune interactions going forward.

Finally, I need to thank my family. Thank you for your unconditional support, for never expecting too much, and for always being there (and of course the ridiculous amount of coffee).

I hope that you, the reader, find my thesis of interest. I hope that I give you pause for thought.

Abstract

Tolerance mechanisms are vital for maintaining immune homeostasis in the intestinal system. The intestinal system must remain primed against pathogens whilst nutrients are absorbed without an inappropriate inflammatory response. Regulatory T-cells (Treg) are a key cell type for maintaining tolerance, primarily acting to suppress inflammatory T-cell responses. This mechanism is exploited by helminth parasites, including *Heligmosomoides polygyrus* (*H. polygyrus*), in order to suppress the anti-helminth T-cell response and establish chronic infection. *H. polygyrus* infection therefore provides a useful model for studying the dynamics of T-cell regulation *in vivo*.

The current understanding of T-cell and Treg dynamics *in vivo* is limited. This thesis uses the novel Timer Of Cell Kinetics and Activity (Tocky) reporter system developed by the Ono Lab to overcome this knowledge-gap. Tocky reveals whether a gene of interest is actively transcribed or has previously been transcribed in real-time. Here, *Foxp3*-Tocky mice are used to report transcription of the key Treg gene *Foxp3*, and *Nr4a3*-Tocky mice are used to reveal T-cell receptor signalling through transcription of the *Nr4a3* gene.

This thesis identifies that during early primary *H. polygyrus* infection, a proportion of infection-reactive T-cells appear to induce and maintain *Foxp3* transcription. Further analyses, including transcriptomic analysis, support that activated T-cells are a source of Treg in this context. Within secondary infection, where mice exhibit resistance to re-infection, *Foxp3* transcription within Treg appears to be very similar to that in primary infection. However, the Treg pool is offset by the memory T-cell pool.

In conclusion, I demonstrate that a subset of T-cells activated in *H. polygyrus* infection up-regulate *Foxp3* transcription, potentially as a mechanism to suppress their own anti-parasite T-cell response. In secondary infection, *Foxp3* transcription is similarly initiated and maintained, however, due to disproportionate expansion of the memory T-cell population, the Treg response is ineffective.

Table of Contents

Declaration of Originality ..... - 2 -
Copyright declaration ..... - 2 -
Acknowledgements ..... - 3 -
Abstract ..... - 4 -
Table of Contents ..... - 5 -
Table of Figures ..... - 8 -
Table of Tables ..... - 9 -
Abbreviations ..... - 10 -
1 Chapter One: Introduction ..... - 12 -
1.1 The mouse mucosal system ..... - 12 -
1.1.1 Mucosal antigen recognition ..... - 13 -
1.1.2 Tolerance in the mucosal system ..... - 14 -
1.2 *Heligmosomoides polygyrus* infection ..... - 16 -
1.2.1 The anti-parasite response ..... - 17 -
1.2.2 Immune modulation ..... - 19 -
1.2.3 Life cycle ..... - 21 -
1.3 T-cells ..... - 22 -
1.3.1 T-cell activation and the role of TCR signalling ..... - 24 -
1.4 Foxp3 and regulatory T-cells ..... - 30 -
1.4.1 Regulatory T-cell suppressive mechanisms ..... - 31 -
1.4.2 Regulatory T-cell differentiation ..... - 32 -
1.5 *Heligmosomoides polygyrus* infection promotes Foxp3 expression ..... - 36 -
1.6 Thesis Aims ..... - 38 -
2 Chapter Two: Materials and Methods ..... - 40 -
2.1 Timer Of Cell Kinetics and Activity ..... - 40 -
2.2 Mice ..... - 43 -

2.3 *Heligmosomoides polygyrus* infection ..... - 44 -

2.3.1 Culturing *H. polygyrus* ..... - 44 -

2.3.2 Time Course ..... - 45 -

2.3.3 Primary vs secondary infection ..... - 45 -

2.4 Ovalbumin ..... - 45 -

2.5 Flow cytometry ..... - 45 -

2.5.1 Gating strategy ..... - 47 -

2.5.2 Tocky analysis ..... - 49 -

2.5.3 t-SNE analysis ..... - 49 -

2.6 RNA extraction ..... - 49 -

2.7 RNA-seq and analysis ..... - 50 -

2.8 Statistics ..... - 50 -

3 Chapter Three: Transcriptional dynamics of *Foxp3* during primary *Heligmosomoides polygyrus* infection ..... - 52 -

3.1 Background ..... - 52 -

3.2 Results ..... - 57 -

3.2.1 *Foxp3* transcription dynamics change during the course of infection ..... - 57 -

3.2.2 GITR is associated with *Foxp3* transcription and early parasite infection ..... - 61 -

3.2.3 The $GITR^{high}CD44^{high}$ population is enriched with infection-reactive T-cells - 65 -

3.2.4 New *Foxp3* transcription appears to originate within activated T-cells ..... - 69 -

3.2.5 Transcriptomic features of infection-reactive Treg and activated T-cells during early infection ..... - 70 -

3.3 Discussion ..... - 78 -

4 Chapter Four: A comparison of primary and secondary *Heligmosomoides polygyrus* infection ..... - 83 -

4.1 Background ..... - 83 -

4.2 Results ..... - 87 -

4.2.1 *Foxp3* is actively transcribed in T-cells upon secondary infection. ..... - 87 -

4.2.2 The T-cell subset enriched with parasite-reactive non-regulatory T-cells and Treg expands during secondary infection..... - 88 -

4.2.3 *Foxp3*-Timer transcription is active in the GITR^{high}CD44^{high} T-cell population in secondary infection..... - 92 -

4.2.4 Investigation of peripheral TCR signalling dynamics within *H. polygyrus* infection ..... - 96 -

4.2.5 TCR signalling is inhibited in CD44^{high}*Foxp3*-GFP^{-} T-cells but not CD44^{high}*Foxp3*-GFP^{+} T-cells..... - 100 -

4.2.6 TCR signalling may be inhibited by multiple mechanisms..... - 104 -

4.2.7 Tfh increase in secondary but not primary *H. polygyrus* infection ..... - 106 -

4.3 Discussion..... - 113 -

5 Chapter Five: Discussion ..... - 121 -

5.1 Key findings in context ..... - 121 -

5.1.1 A potential model explaining the delayed Treg response ..... - 123 -

5.1.2 Combining *Foxp3*-Timer and *Nr4a3*-Timer analyses ..... - 125 -

5.2 Mouse strain variation ..... - 126 -

5.3 Use of the Tocky system ..... - 128 -

5.4 Overall conclusions ..... - 129 -

6 References ..... - 130 -

Table of Figures

Figure 1.1: The small intestine environment. ..... - 13 -
Figure 1.2: The lifecycle of *H. polygyrus* ..... - 22 -
Figure 1.3: Cytokines dictate the T-cell differentiated state ..... - 23 -
Figure 1.4: TCR signal transduction ..... - 26 -
Figure 1.5: A diagram of IL-2 signalling transduction simplified ..... - 29 -
Figure 1.6: Regulatory T-cell suppressive mechanisms ..... - 32 -
Figure 1.7: Transcriptional control of the *Foxp3* gene..... - 34 -
Figure 2.1: Timer-Blue and Timer-Red analysis ..... - 42 -
Figure 2.2 : Standard gating strategy..... - 48 -
Figure 3.1: *Foxp3* transcription dynamics change during the course of infection ..... - 58 -
Figure 3.2: Day effect is unlikely to be responsible for the differences in *Foxp3* transcriptional dynamics..... - 60 -
Figure 3.3: GITR expression is associated with early parasite infection..... - 63 -
Figure 3.4: GITR expression appears to be increased in the *Foxp3*$^{-}$ T-cell population..... - 64 -
Figure 3.5 The GITR^{high}CD44^{high} T-cell population likely expands ..... - 66 -
Figure 3.6: GITR^{high}CD44^{high} T-cells are enriched with Persistent *Foxp3* transcribing cells - 67 -
Figure 3.7: Timer Locus analysis of the GITR^{high}CD44^{high} T-cell subset ..... - 69 -
Figure 3.8: t-SNE analysis of GITR^{high} CD4 T-cells..... - 71 -
Figure 3.9: Contamination of non-T-cells within some RNA-seq samples..... - 74 -
Figure 3.10: RNAseq analysis. ..... - 77 -
Figure 4.1: Infection schematic..... - 87 -
Figure 4.2: *Foxp3* transcription is activated and sustained in CD4 T-cells and *Foxp3*-Timer^{+} pre-existing Treg in 2^{o} infection..... - 89 -
Figure 4.3: The GITR^{high}CD44^{high} population expands in 2^{o} infection ..... - 91 -
Figure 4.4: The proportion of infection-reactive *Foxp3*-Timer^{-} T-cells expands disproportionately compared to infection-reactive *Foxp3*-Timer^{+} T-cells in 2^{o} infection . - 92 -
Figure 4.5: The GITR^{high}CD44^{high} T-cell subset enriched with parasite-reactive T-cells exhibit active *Foxp3* transcription ..... - 94 -

Figure 4.6: A reduced proportion of non-regulatory T-cells show CD25 expression in 2° infection ..... - 96 -
Figure 4.7: Ovalbumin administration in OT-II *Nr4a3*-Tocky mice increases TCR signalling..... - 98 -
Figure 4.8: CD44^{high}*Foxp3*-GFP^{+} T-cell TCR signalling appears to differ between 1° and 2° *H. polygyrus infection* ..... - 99 -
Figure 4.9: CD44^{high}*Foxp3*-GFP^{-} T-cell TCR signalling appears to differ between 1° and secondary *H. polygyrus* infection..... - 101 -
Figure 4.10: TCR signalling is inhibited in CD44^{high}*Foxp3*-GFP^{-} T-cells but not CD44^{high}*Foxp3*-GFP^{+} T-cells..... - 103 -
Figure 4.11: APC stimulation of the TCR may be inhibited in 1° but not 2° *H. polygyrus* infection ..... - 105 -
Figure 4.12: PD-1 expression is specifically decreased in GITR^{high}CD44^{high}*Foxp3*$^{+}$ T-cells and not GITR^{high}CD44^{high}*Foxp3*$^{-}$ T-cells..... - 107 -
Figure 4.13: Tfh increase in 2° but not 1° *H. polygyrus* infection..... - 109 -
Figure 4.14: TCR signalling increases with PD-1 expression in CD44^{high}*Foxp3*-GFP^{-} T-cells..... - 110 -
Figure 4.15: TCR signalling increases with PD-1 expression in CD44^{high}*Foxp3*-GFP^{+} T-cells..... - 112 -
Figure 5.1: Proposed mechanism of an efficient memory T-cell response to *H. polygyrus* infection ..... - 124 -

Table of Tables

Table 2.1: Mouse strains..... - 43 -
Table 2.2: Table of antibodies..... - 47 -

Abbreviations

AICD	Activation Induced Cell Death
APC	Antigen-Presenting Cell
BAC	Bacterial Artificial Chromosome
CNS	Conserved Non-coding Sequence
CTLA-4	Cytotoxic T-lymphocyte associated protein 4
DAMP	Danger Associated Molecular Pattern
DC	Dendritic Cell
DEG	Differentially Expressed Genes
DTR	Diphtheria Toxin Receptor
EAE	Experimental Autoimmune Encephalomyelitis
ER	Endoplasmic Reticulum
eTreg	activated phenotype Treg
FACS	Fluorescence Activated Cell Sorting
FCS	Foetal Calf Serum
FSC	Forward scatter
GALT	Gut Associated Lymphoid Tissue
GITR	Glucocorticoid-induced tumour necrosis factor receptor
GITRL	GITR ligand
H. polygyrus	*Heligmosomoides polygyrus*
HES	*H. polygyrus* Excretory Secretory proteins
HpARI	*H. polygyrus* alarmin release inhibitor
Hp-CPI	*H. polygyrus* Cysteine Protease Inhibitor
Hp-TGM	*H. polygyrus* TGF-β mimic
ICOS	Inducible T-cell co-stimulator
ICOSL	ICOS ligand
IDO	indoleamine 2,3-dioxygenase
IFN-γ	Interferon gamma
IgSF	Immunoglobulin Superfamily
IL	Interleukin
ILC	Innate Lymphoid Cell
IPEX	Immunodysregulation, polyendocrinopathy, enteropathy, X-linked
IRES	Internal ribosomal entry site
JAK	Janus Kinase
lpCD103$^+$DCs	Lamina propria CD103$^+$ DCs
MHC	Major Histocompatibility Complex
mLN	Mesenteric lymph nodes
mTOR	Mammalian Target of Rapamycin
NPt	New to Persistent transitioning
Nr4a	Nuclear receptor subfamily 4 group A member
PAt	Persistent to Arrested transitioning
PCA	Principle Component Analysis

PD-1	Programmed cell death-1
PD-L	Programmed death ligand
PP	Peyer's patches
pTreg	Peripheral Treg
RAR	Retinoic Acid Receptors
SHP2	SH2-containing phosphatase 2
SSC	Side scatter
STAT	Signal Transducers and Activators of Transcription
TCR	T-cell receptor
Teff	Effector T-cells
Tfh	Follicular helper T-cell
T_H	Helper T-cell
Tmem	Memory T-cell
TNF	Tumour Necrosis Factor
TNFRSF	Tumour Necrosis Factor Receptor Superfamily
Tocky	Timer Of Cell Kinetics and Activity
TRAF	TNF receptor associated factors
Treg	Regulatory T-cell
TSLP	stromal lymphopoietin
tTreg	Thymic Treg
WT	Wild Type
Zap70	Zeta-chain Associated Protein kinase 70

1 Chapter One: Introduction

A careful balance must be maintained between the inflammatory immune response and tolerance mechanisms. When this balance is disrupted, disease pathologies occur. Inappropriate immune activation may lead to autoimmunity and allergy, whereas insufficient activation can prevent the resolution of cancers and infections. Such immune homeostasis is of particular importance within the intestinal system. As a mucosal surface, the intestine is in constant contact with the external environment. It must therefore be able to absorb nutrients and tolerate the microbiota, whilst also remaining primed against pathogens. Key cells implicated in maintaining such tolerance are regulatory T-cells (Treg). However, these and other cells of the immune system may be exploited by intestinal parasites for chronic infections to persist.

1.1 The mouse mucosal system

This thesis focuses on the intestinal immune system (Figure 1.1), a part of the mucosal system. A thin epithelial cell layer covered in mucus separates the intestinal lumen from the lamina propria. Within the lamina propria, tissue-resident immune cells reside in abundance, in order to rapidly launch an immune response. These tissue-resident cells include Innate Lymphoid Cells (ILCs), Dendritic Cells (DCs), macrophages, mast cells, and both effector and memory B and T lymphocytes. These lymphocytes would have initially encountered antigen within the Gut Associated Lymphoid Tissue (GALT), which consists of organised secondary lymphoid

structures associated with the intestine. Specifically, antigen is encountered within the Peyer's patches (PP) or mesenteric lymph nodes (mLN), which act as the intestinal inductive sites. The PP are found within the lamina propria beneath the epithelial cell layer and drain, along with the lamina propria, to the mLN via lymphatic vessels.

1.1.1 Mucosal antigen recognition

Insoluble antigen from the intestinal lumen is typically taken up by M cells within the epithelial cell layer. Antigen reaches M cells more efficiently than the epithelial cell layer as M cells are not covered by the mucus barrier. These M cells allow transcytosis of antigen into

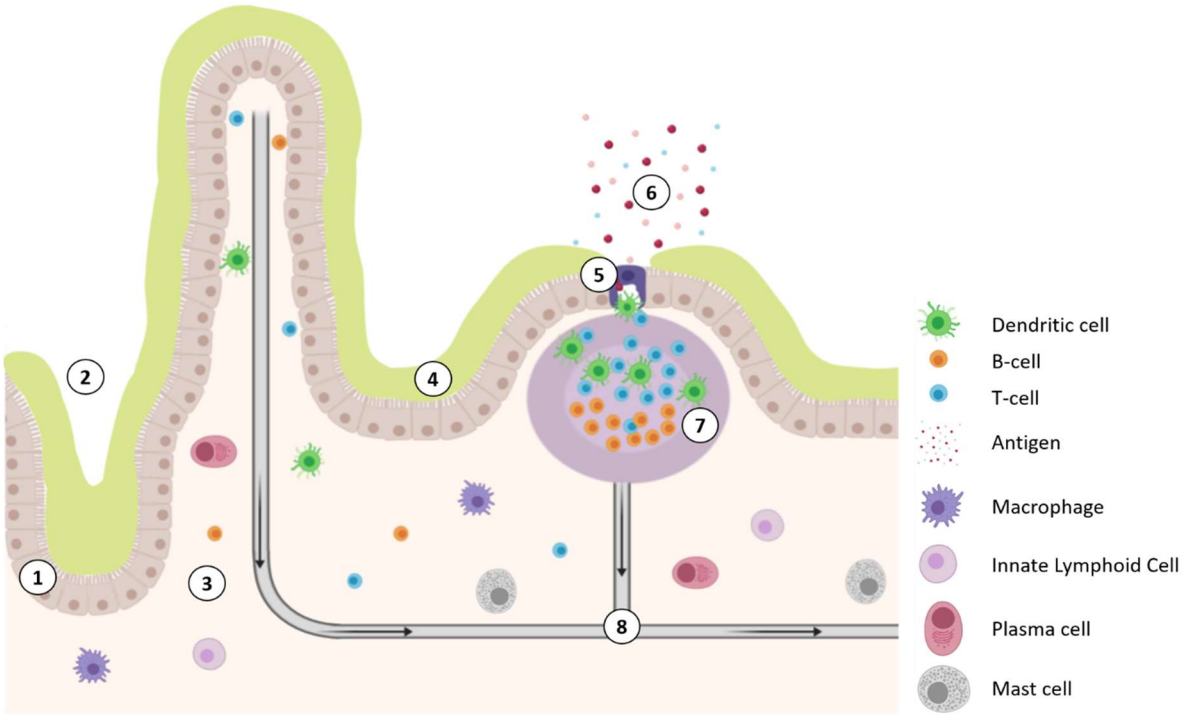


Figure 1.1: The small intestine environment. (1) A thin layer of epithelial cells separates the intestinal lumen (2) and lamina propria (3). (4) Mucus is secreted by goblet cells to prevent large particles from reaching the epithelial layer. (5) M-cells are not covered by mucus, allowing antigen (6) uptake into the Peyer's patches (7). Dendritic cells sample the antigen taken up by the M-cells and present this to T-cells within the Peyer's patch. The dendritic cells and T-cells proceed to the B-cell zone within the Peyer's patch to activate corresponding B-cells and class-switch antibody to IgA. Antigen-Presenting cells from the lamina propria and Peyer's patch drain to the mesenteric lymph nodes by lymphatic vessels (8).

the PP. In contrast, smaller soluble antigen enters the lamina propria through the epithelial barrier (reviewed by Mowat, (Mowat, 2003)). Antigen-Presenting Cells (APCs) such as DCs within the PP or lamina propria endocytose the antigen, allowing processing and presentation of antigen peptide on Major Histocompatibility Complex (MHC)-II molecules. The peptide-MHC-II complex is then presented to T-cells within the PP or mLN.

Cross-linking between the peptide-MHC-II complex and the T-cell Receptor (TCR) results in TCR signalling (further discussed in Chapter 1.3.1). If co-stimulation is not provided by an APC, T-cell anergy may occur. When combined with co-stimulation from an APC, TCR signalling leads to T-cell activation (discussed in Chapter 1.3.1). T-cells that are primed in this way within the GALT down-regulate expression of L-selectin (the homing receptor for secondary lymphoid tissue) and up-regulate $\alpha_4\beta_7$ integrin and CCR9 (Campbell and Butcher, 2002; Hammerschmidt et al., 2011; Mora et al., 2003); the intestinal homing receptors. As a result, these primed cells are able to leave the lymphoid tissue and enter the lamina propria in order to undertake their function. Alternatively, Follicular Helper T-cells (Tfh, further discussed in Chapter 4.1) do not leave the lymphoid tissue and migrate to the B-cell zone to induce antibody production and class switching.

1.1.2 Tolerance in the mucosal system

Oral tolerance specifically refers to local and systemic immune non-reactivity to food and other ingested antigens. Counterintuitively, the necessity of PP for tolerance induction is controversial (Fujihashi et al., 2001; Mowat, 2003; Pabst and Mowat, 2012; Spahn et al., 2002; Worbs, 2006), whereas it is well established that mLN are essential. Spahn *et al.* demonstrate that oral tolerance cannot be induced in mice lacking both PP and mLN, however, the

development of mLN alone restores this capacity (Spahn et al., 2002). Worbs *et al.* further show that mesenteric lymphadenectomy removes oral tolerance (Worbs, 2006).

DCs from the lamina propria and the PP drain to the mLN to interact with naïve T-cells. Here, tolerance may be induced by T-cell anergy or Treg polarisation. Friedman *et al.* proposed that high doses of antigen result in T-cell anergy, whilst multiple low doses of antigen result in active T-cell suppression (Friedman and Weiner, 1994), later concluded to be Treg activity. Subsequent studies both support and contradict this proposal and as such, it should be treated with caution (Bedoret et al., 2012; Pabst and Mowat, 2012; Siewert et al., 2008). Pabst and Mowat argue that Treg (discussed in section 1.4) are likely to be the most crucial T-cell mechanism of oral tolerance (Pabst and Mowat, 2012) due to the prevalence of Treg polarising Retinoic Acid in the mLN. The argument for a central Treg role is further supported by the loss of tolerance seen in mesenteric lymphadenectomy (Worbs, 2006).

Retinoic Acid, a nuclear receptor ligand (discussed in Chapter 1.3.1.3) that binds Retinoic Acid Receptors (RAR), is found in abundance within the mLN and lamina propria. Stroma cells, epithelial cells and lamina propria $CD103^+$ DCs ($lpCD103^+DCs$) metabolise Vitamin A into Retinoic Acid via secretion of retinaldehyde dehydrogenase. Indeed, stroma cells of the mLN are unique compared to those of other lymph nodes in this capacity (Hammerschmidt et al., 2008). $lpCD103^+DCs$ are also unique compared to other APCs in their ability to produce Retinoic Acid, as described by Sun *et al*.. The secretion of Retinoic Acid synergizes with TGF-β to enhance *Foxp3* expression and therefore increases the percentage of naïve CD4 T-cells converted to Treg. Consequently, $lpCD103^+DCs$ convert naïve CD4 T-cells to Treg more efficiently than other APCs (Sun et al., 2007).

Sun *et al.* further showed that during *in vitro* culture, an exogenous source of TGF-β is not required for lpCD103$^+$DCs to polarise Treg (Sun et al., 2007). These DCs up-regulate $\alpha_v\beta_8$ integrin expression (Worthington et al., 2011), which activates latent TGF-β. Latent TGF-β is produced by many cells of the intestine; including epithelial cells, glial cells and lymphocytes (Bauché and Marie, 2017). The increased capacity to activate TGF-β likely increases the concentration of local activated TGF-β, allowing Treg polarisation at endogenous levels. Whilst lpCD103$^+$DCs do not require exogenous TGF-β to induce Treg, additional exogenous TGF-β increases polarisation (Sun et al., 2007). The tolerogenic nature of the intestinal tissue is therefore further aided by the abundance of TGF-β. Whilst TGF-β may polarise cells to either Treg or Th17 differentiation, the prevalence of both IL-2 and Retinoic Acid in the intestinal environment favour Treg (Xiao et al., 2008). Finally, Retinoic Acid also plays a key role in the upregulation of gut homing receptors CCR9 and $\alpha_4\beta_7$ integrin (Jaensson-Gyllenbäck et al., 2011; Johansson-Lindbom et al., 2005) discussed in Chapter 1.1.1.

1.2 *Heligmosomoides polygyrus* infection

Heligmosomoides polygyrus (*H. polygyrus*) is a natural murine gastrointestinal helminth, commonly used to model human and livestock helminth infections within rodents. This is largely due to the nature of infection, where the parasite life cycle is restricted to the gastrointestinal tract. *H. polygyrus* naturally infect rodents, establishing chronic infection by employing immune modulation of the host. This immune modulation appears to be largely non-specific. Indeed, infection with *H. polygyrus* has been found to protect against various inflammatory conditions; including Experimental Autoimmune Encephalomyelitis (EAE)

(Donskow-Lysoniewska et al., 2012), peanut allergy (Bashir et al., 2002) and allergic asthma (Hartmann et al., 2009; Kitagaki et al., 2006; Wilson et al., 2005).

Susceptibility to chronic infection has been found to differ depending on the mouse genetic background. For instance, BALB/c mice expel adult worms by week 6-8 of infection. Meanwhile, C57BL/6 mice are more susceptible to infection and expel worms between 8-20 weeks post-infection (Reynolds et al., 2012). The differences in susceptibility are believed to be due to several variations in the immune response, including MHC-II haplotype (Behnke and Wahid, 1991). Later investigation identified that differences in the Th2 response and some innate immune responses between mouse strains also lead to differences in susceptibility (Filbey et al., 2014).

1.2.1 The anti-parasite response

Whilst *H. polygyrus* establish chronic infection, they are eventually cleared by the host. The anti-parasite response involves T- and B-lymphocytes, innate cells and other intestinal cells such as goblet cells. As expected within parasite infection, the primary T-cell response is CD4 in nature and Th2 polarised (Urban et al., 1991). Cytokines associated with *H. polygyrus* infection include IL-3, IL-4, IL-5 and IL-9, produced within the mLN (Svetic et al., 1993). Such a T-cell response is reported to be essential for worm clearance in primary infection (Urban et al., 1991). CD8 T-cells appear to have little role in the anti-parasite response (Urban et al., 1991).

Mice are typically resistant to secondary infection with *H. polygyrus*, and this is B-cell dependent (McCoy et al., 2008; Wojciechowski et al., 2009). A stronger and faster antibody response is further associated with mouse strains that are more resistant to *H. polygyrus*

infection (Wahid and Behnke, 1993). Interestingly, whilst circulating levels of IgG1 and IgE drastically increase during infection (Urban et al., 1991), the IgE response is not found to affect parasite clearance. Instead, IgG and IgA are the prominent antibodies associated with a successful anti-parasite response (McCoy et al., 2008). Considering the important role of B-cells, Tfh cells are recognised to play a major role in the resistance to secondary infection (King et al., 2010). The T- (including Tfh) and B-cell responses are further considered in Chapter 4.1.

ILCs have only relatively recently been described and their role in the anti-parasite response against *H. polygyrus* will likely be further elucidated. A role for ILC2s in initiating and driving the Th2 response in *H. polygyrus* infection has been suggested through expression of IL-4 (Patel et al., 2014; Pelly et al., 2016). Interestingly, very low levels of ILC2 cells are observed within the mLN of C57BL/6 mice during *H. polygyrus* infection (Hepworth et al., 2012). In a review of ILC2s during helminth infection, Löser *et al.* suggest that the low level of ILC2 cells found in the mLN of infected C57BL/6 mice may contribute to the increased susceptibility of C57BL/6 mice to primary *H. polygyrus* infection over some other strains (Loser et al., 2019).

The anti-parasite response against *H. polygyrus* has been extensively reviewed by Reynolds *et al.* (Reynolds et al., 2012). In summary, DCs are the primary subset of APC required for T-cell polarisation into the Th2 lineage during helminth infection (MacDonald and Maizels, 2008), specifically, the $CD11c^{+}$ DC subset is required for an effective Th2 response to be established in *H. polygyrus* infection (Phythian-Adams et al., 2010). Macrophages appear to be alternatively activated in *H. polygyrus* infection, with a key role in mediating tissue repair during primary infection (Loke et al., 2007). In secondary infection, alternatively activated

macrophages are required for the protective immune response, likely through arginase activity directly targeting *H. polygyrus* larvae (Anthony et al., 2006). The accumulation of mast cells within the tissue, known as Mastocytosis, is also associated with parasite clearance (Behnke et al., 1993), potentially by changing the intestinal microenvironment. Other cells of the innate immune system do not appear to have a critical role in the anti-parasite response.

1.2.2 Immune modulation

H. polygyrus are well characterised to modulate the host immune response in order to establish chronic infection. To reduce chances of early detection, *H. polygyrus* secrete *H. polygyrus* alarmin release inhibitor (HpARI). HpARI binds to activated IL-33, a key alarmin or "danger signal" secreted from damaged epithelial cells, and prevents its release from necrotic cells (Osbourn et al., 2017). HpARI is one component of *H. polygyrus* Excretory Secretory proteins (HES), secreted by *H. polygyrus* at each phase of the infection cycle. Additional components of HES, such as apyrases, also aim to prevent the initial detection of *H. polygyrus* larvae. Apyrases have been identified to reduce Danger Associated Molecular Pattern (DAMP) signalling in other helminth infections by converting pro-inflammatory ATP released from necrotic cells into AMP (Da'dara et al., 2014; Gounaris et al., 2004).

The IL-33 pathway is further targeted by *H. polygyrus*, as the IL-33 receptor (IL-33R) is a target of microRNAs found within extracellular vesicles secreted by *H. polygyrus* (Buck et al., 2014). Such targeting prevents expression of the IL-33R, and thus reduces IL-33 responsiveness. In addition, extracellular vesicles secreted by *H. polygyrus* are found to be taken up by macrophages and thus modulate gene expression within these cells. Indeed, alternative activation of macrophages appears to be somewhat suppressed and inflammatory

Tumour Necrosis Factor (TNF)-α and IL-6 limited. Sensitization to extracellular vesicles combined with alum protected against larval *H. polygyrus* infection (Coakley et al., 2017). This suggests that the role of extracellular vesicles within infection establishment is critical. It is further likely that additional microRNAs found within these extracellular vesicles have yet-undiscovered functions.

DCs are the key APC during *H. polygyrus* infection. There is some evidence that *H. polygyrus* infection may suppress DC function through the *H. polygyrus* Cysteine Protease Inhibitor (Hp-CPI). In *ex vivo* analysis, administration of Hp-CPI appeared to reduce MHC-II expression and the co-stimulatory CD86 ligand. Upon antigen presentation to CD4 T-cells, these T-cells showed a reduced proliferative capacity and a reduced inflammatory response (Sun et al., 2013). These findings suggest that DCs may have a reduced capacity to activate T-cells and thus drive the Th2 response during *H. polygyrus* infection. Other studies suggest that the migratory capacity of DCs from the lamina propria to the mLN may be impaired (Balic et al., 2009), which would further reduce antigen presentation and subsequent T-cell activation.

The ability of *H. polygyrus* to induce Treg during infection is the most well-known method of immune modulation carried out by the parasite. Indeed, administration of HES alone is protective against allergic airway inflammation in an ovalbumin model. Upon HES administration at ovalbumin sensitisation, a key effect is a reduced ratio of effector T-cells (Teff) to Treg, with a corresponding reduction in inflammatory cytokine production (McSorley et al., 2012). Treg expansion during *H. polygyrus* infection has been linked with TGF-β like activity from one component of HES (Grainger et al., 2010). The TGF-β mimic has subsequently been identified and named *H. polygyrus* TGF-β mimic (Hp-TGM)(Johnston et al., 2017). Hp-TGM is further discussed in section 1.5.

1.2.3 Life cycle

H. polygyrus spend their life cycle within the gastrointestinal tract of the host (Figure 1.2). *H. polygyrus* eggs are excreted into the host faeces. Outside of the host, the eggs hatch and progress through larval stages L1-L3 within approximately 7 days. The L3 larvae are infective, and once ingested by a murine host, penetrate the small intestine to reside within the submucosa. Within the submucosa, the larvae mature to the L4 stage by day-4 of infection, and to the adult form by day-7. At approximately day-10 of infection, *H. polygyrus* migrate to the intestinal lumen. Here they tightly coil around the intestinal villi. Male and female *H. polygyrus* are subsequently able to reproduce and excrete eggs into the host faeces (Bryant, 1973).

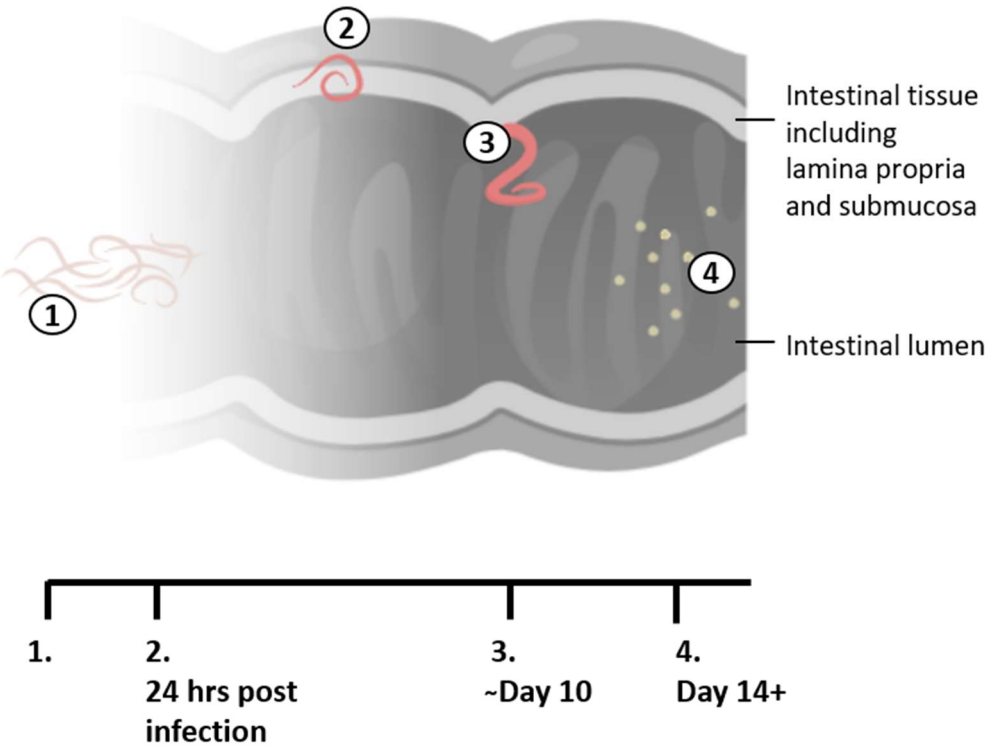


Figure 1.2: The lifecycle of H. polygyrus. L3 stage *H. polygyrus* larvae are ingested by the host (1). After 24 hours, the L3 stage larvae have reached the submucosa (2), where they mature through the L4 larval stage to the L5 stage by ~ day-7. At ~ day-10 of infection, the now adult form of *H. polygyrus* migrate to the intestinal lumen (3), where they coil around intestinal villi. After 14 days of infection, male and female *H. polygyrus* mate and secrete eggs (4) into the faeces of the host.

1.3 T-cells

This thesis focuses on CD4 T-cells. CD4 T-cells consist of helper T-cells (T_H) and Treg. T_H influence other immune cell types through the release of cytokines. Such cytokine activity may include the promotion of B-cell antibody class switching or enhancing phagocyte action. Upon T-cell activation, differentiation occurs into one of three main T_H subsets, followed by clonal expansion. The three main T_H subsets are Th1, Th2 and Th17 cells. These subsets allow for the immune response to more effectively target a specific type of pathogen. For instance, the Th1 response typically targets intracellular bacteria, whilst the Th2 response primarily functions against extracellular parasites. The differentiated fate of the T_H cell is determined by the precise cytokine environment at activation (Figure 1.3).

Th2 cells are associated with the lineage-defining transcription factor GATA3 and the expression of IL-4, IL-5 and IL-13 cytokines. IL-4 is typically considered the key cytokine required for Th2 polarisation upon T-cell activation, however, Th2 polarisation may be propagated by the presence of stromal lymphopoietin (TSLP), IL-25 and IL-33 (Fort et al., 2001; Schmitz et al., 2005; Zhou et al., 2005), each considered an alarmin associated with tissue damage and parasite infection. IL-4 is further associated with the recruitment and activation of mast cells and basophils to the site of infection; IL-5 is associated with the recruitment and activation of eosinophils and IL-13 promotes mucosal barrier integrity. Finally, a Th2 response

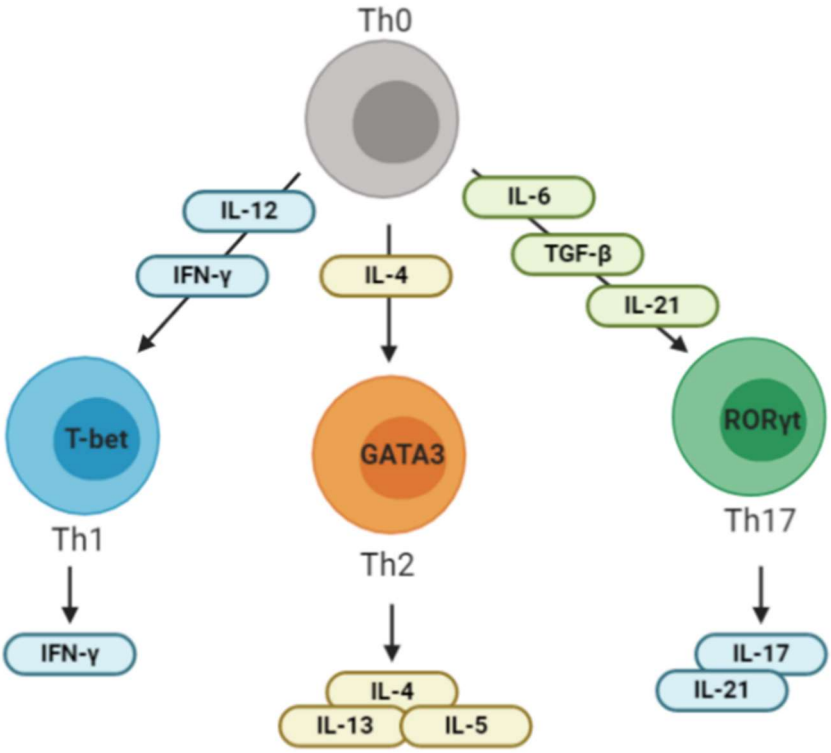


Figure 1.3: Cytokines dictate the T-cell differentiated state. Upon T-cell activation of naïve T-cells (Th0), the cytokine environment determines the subsequent Th lineage. An environment with IL-12 and IFN-γ results in Th1 cell differentiation. Th1 cells are defined by the T-bet master transcription factor. These cells typically secrete inflammatory cytokines such as IFN- γ. In the presence of IL-4, Th2 cell differentiation occurs. The master transcription factor of Th2 cells is GATA3 and these cells are associated with secretion of IL-4, IL-5 and IL-13 cytokines. An environment of IL-6, TGF-β and IL-21 promotes differentiation of the Th17 lineage; of which the master transcription factor is RORγt. These cells are associated with secretion of IL-17 and IL-21.

is associated with antibody class switching to the IgE isoform (Corry and Kheradmand, 1999). As such, the Th2 response is geared towards helminth clearance.

Upon pathogen clearance, a prolonged T-cell response is no longer necessary. The Teff pool decreases in size in what is called a contraction phase; most Teff undergo apoptosis. Some T-cells survive and differentiate into antigen-specific memory T-cells (Tmem). These Tmem are more abundant than the original naïve T-cells, allowing a more rapid T-cell

response upon re-infection. Further, Tmem exhibit an activated phenotype much more rapidly than naïve T-cells upon recognition of cognate antigen, reviewed by Macleod *et al*. (MacLeod et al., 2009). Tmem are therefore antigen-experienced T-cells that have arisen from infection or immunisation. Memory-phenotype T-cells include Tmem, however, this memory-phenotype population also contains memory-like T-cells which have not experienced foreign antigen. These cell types are phenotypically indistinguishable, however, they appear to respond differently *in vivo*, as identified by proliferation (Younes et al., 2011). These memory-like T-cells are likely to be self-reactive (Ono and Tanaka, 2015).

1.3.1 T-cell activation and the role of TCR signalling

T-cell activation requires the combination of a strong TCR signal and a co-stimulatory signal, both from an APC. Naïve T-cells are found in the G0 resting phase of cell cycle, successful combination of TCR and co-stimulatory signalling results in the T-cell entering the G1 phase of cell cycle (Pardee, 1989), preparing to proliferate and differentiate according to the cytokine environment.

The CD4 T-cell TCR is antigen-specific, recognising a short antigen peptide sequence typically of 13 or more amino acids (Lippolis et al., 2002). If the TCR has a high affinity for the presented peptide-MHC-II complex, a signalling cascade is initiated, determining the T-cell fate (Figure 1.3). Initially, a series of phosphorylation steps occur, resulting in recruitment of Zeta-chain Associated Protein kinase 70 (Zap70) from the cytoplasm and subsequent conformational change into its activated state. Zap70 activation allows transduction of the TCR signal (Yan et al., 2013).

Downstream of Zap70 activation, three key signalling pathways occur (Figure 1.4); the PI_3K pathway, the IKK pathway and the RAS/MAPK pathway, resulting in activation and translocation of NFAT and NFκB into the nucleus from the cytoplasm, and formation of the AP-1 complex within the nucleus (reviewed by Smith-Garvin *et al*. (Smith-Garvin et al., 2009)). These transcription factors are then able to bind DNA and dictate, with cytokine signalling, the transcription of downstream genes that regulate T-cell differentiation, proliferation and survival. These early genes include IL-2 (further discussed in Chapter 1.3.1.2).

In contrast to the TCR, the co-stimulatory signal is antigen non-specific. The most well-defined co-stimulation occurs through the interaction of CD80/86 on the APC surface and CD28 on the T-cell surface. Other co-modulating molecules are upregulated post-T-cell activation. Ligation of CD28 activates PI_3K, increasing AP-1 and NFκB levels and thus increasing IL-2 production. Further, PI_3K plays a role in recruiting and activating the kinase Akt. Akt promotes cell survival by inhibiting the pro-apoptotic protein Bad, which in turn prevents inhibition of the anti-apoptotic Bcl-2. Downstream of Akt activation is stimulation of the mammalian Target Of Rapamycin (mTOR) pathway, a key pathway for the regulation of macromolecular biosynthesis. Thus, Akt indirectly acts to increase the utilization of glucose and increase metabolism to meet the demand of an activated T-cell. Finally, CD28 ligation also delays the degradation of cytokine mRNA produced as a result of TCR signalling, increasing the cytokine output (Bour-Jordan et al., 2011). The role of co-stimulation in Treg generation is discussed in Chapter 1.4.2.

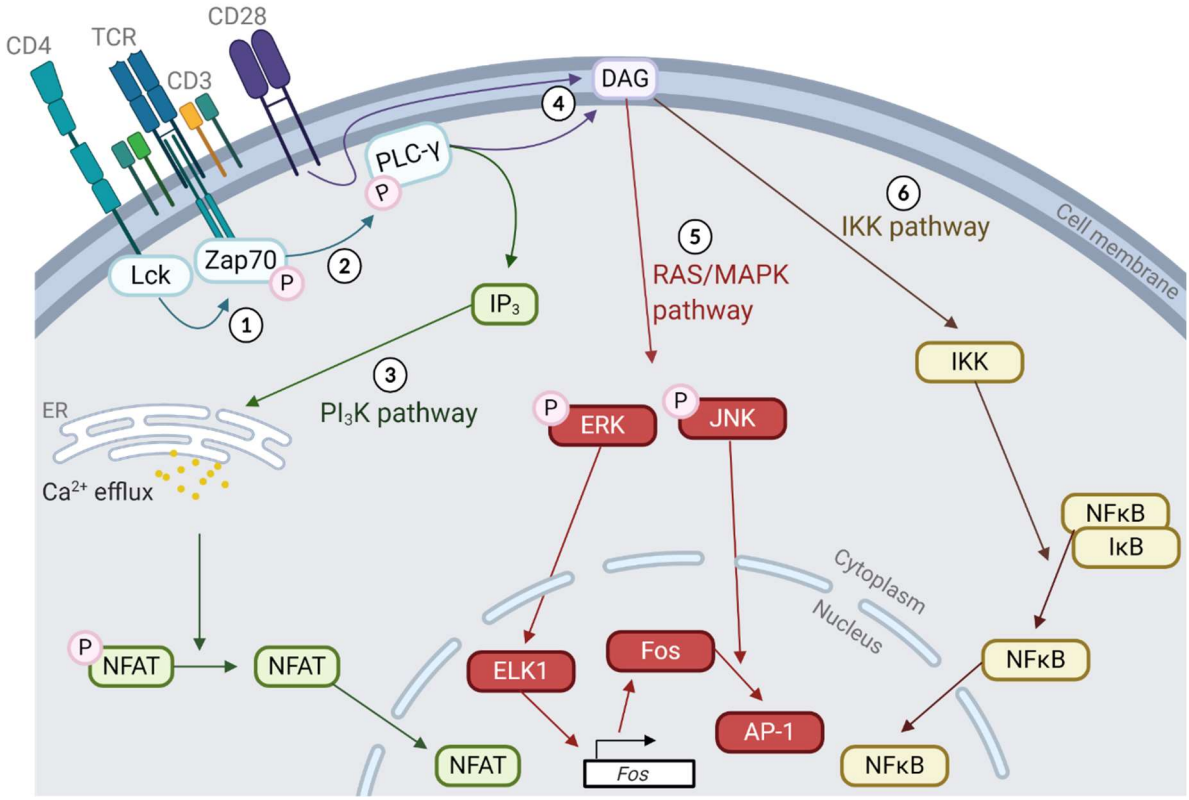


Figure 1.4: TCR signal transduction. (1) During TCR signalling, CD4 associates with the MHC-II molecule, causing a conformational change. The Lck protein is then able to recruit Zap70 from the cytoplasm to the cytoplasmic domain of the CD3 complex and phosphorylate (P) Zap70 into its active form. (2) Through a series of molecular interactions, Zap70 indirectly phosphorylates and thus activates PLC-γ. PLC-γ initiates a signalling cascade through three key pathways; the PI_3K pathway (3), the RAS/MAPK pathway (5) and the IKK pathway (6). In the PI_3K pathway, PLC-γ generates IP3, which binds a receptor on the Endoplasmic Reticulum (ER). This results in efflux of Ca^{2+} from the ER into the cytosol. Increased concentrations of Ca^{2+} result in the dephosphorylation of the NFAT transcription factor, allowing NFAT translocation to the cell nucleus. Immediate early genes of TCR signalling are subsequently transcribed. PLC-γ initiates the RAS/MAPK and IKK pathways through DAG. CD28 ligation by co-stimulatory molecules CD80/86 is also required for the generation of DAG (4). Within the RAS/MAPK pathway, ERK and JNK are phosphorylated within the cytosol. They are then able to translocate to the nucleus, where ERK activates the transcription factor Elk1, aiding transcription of *Fos*. Fos binds with JNK to form the transcription factor complex AP-1. Within the IKK pathway, IKK degrades IκB, releasing NFκB to translocate to the nucleus and act as a transcription factor.

1.3.1.1 Co-stimulatory and co-inhibitory receptors

Whilst ligation of CD28 is the best characterised co-stimulatory signal for T-cell activation, other co-modulatory receptors are also found on the T-cell surface. These receptors modulate TCR signalling negatively (co-inhibitory receptors) or positively (co-stimulatory receptors),

and thus play a key role in the regulation of T-cell activation and differentiation. Co-modulatory receptors mainly belong to two major families; the Immunoglobulin Superfamily (IgSF) or Tumour Necrosis Factor Receptor Superfamily (TNFRSF). Key IgSF members include CD28, Inducible T-cell co-stimulator (ICOS), Cytotoxic T-lymphocyte associated protein 4 (CTLA-4) and Programmed cell death-1 (PD-1). Key TNFRSF members include OX40 and Glucocorticoid-induced tumour necrosis factor receptor (GITR) (Chen and Flies, 2013).

Co-inhibitory IgSF members CTLA-4 and PD-1 are bound by their ligands CD80/86 and Programmed death ligand (PD-L)1/PD-L2 respectively. The CD80/86 ligands are shared between CTLA-4 and CD28, where CTLA-4 has a much higher affinity to bind these ligands. In this way, CTLA-4 acts as a co-inhibitory receptor by preventing co-stimulation through CD28 ligation (Krummel and Allison, 1995). PD-1 also acts to prevent efficient CD28 co-stimulation. Upon ligation by PD-L1 or PD-L2, the cytosolic tail of PD-1 becomes phosphorylated, allowing the recruitment of SH2-containing phosphatase 2 (SHP2) by its SH2 domain. The phosphatase activity of the enzyme proceeds to dephosphorylate CD28 and key TCR signalling molecules such as Zap70, preventing TCR signal transduction. Dephosphorylation of CD28 is most efficient, suggesting PD-1 ligation primarily acts to counteract CD28 co-stimulation (Hui et al., 2017; Walker, 2017).

OX40 and GITR are both TNFRSF co-stimulatory molecules, positively modulating TCR signalling upon ligation by their ligands, OX40 ligand (OX40L) and GITR ligand (GITRL) respectively. These receptors work through TNF receptor associated factors (TRAFs), a family of adaptor proteins. Through the recruitment of TRAFs, TNFRSF co-modulatory receptors are able to modulate TCR signal transduction through the RAS/MAPK pathway, the NFκB pathway and the non-canonical NFκB pathway (Ha et al., 2009).

1.3.1.2 IL-2 signalling

Upon T-cell activation, survival; proliferation; and differentiation is aided by intrinsic generation of both IL-2 and IL-2Rα (CD25), the distinguishing component of the high affinity IL-2 receptor. The IL-2 receptor is primarily found in two main forms. The moderate affinity receptor is comprised of the IL-2Rβ and IL-2Rγ chains, with an affinity of $K_d \sim 10^{-9}$ M. CD25 is upregulated upon T-cell activation and thus allows generation of the high affinity receptor, comprised of CD25, IL-2Rβ and IL-2Rγ chains. This high affinity receptor has an affinity of $K_d \sim 10^{-11}$ M (Kim et al., 2006; Liao et al., 2011). As such, the cell becomes more responsive to IL-2.

Binding of IL-2 to CD25 instigates formation of the high-affinity receptor complex, recruiting additional Janus Kinase (JAK)3 to the high affinity receptor and thus allowing JAK1 (associated with the IL-2Rβ chain) and JAK3 (associated with the IL-2Rγ chain) to activate each other through phosphorylation and proceed to phosphorylate the cytoplasmic tail of the IL-2Rβ chain. This phosphorylation allows recruitment of the adaptor protein Shc, which activates the PI_3K and the RAS/MAPK signalling pathways, amplifying these pathways which are also activated downstream of TCR signalling (Figure 1.5) (Gaffen, 2001). The transcription factor Signal Transducers and Activators of Transcription (STAT) 5 is also able to bind the phosphorylated cytoplasmic tail of the IL-2Rβ chain. Here, STAT5 is phosphorylated by JAK1 and JAK3, becoming activated. Once activated, the STAT5 homodimer translocates to the nucleus where it binds STAT5 response elements to induce transcription (Lin and Leonard, 2000). IL-2 signalling through STAT5 results in transcription of a range of genes involved in T-cell proliferation (Moriggl et al., 1999) and differentiation, including the IL-4Rα chain required for Th2 polarisation (Liao et al., 2008) and Foxp3 required for Treg (Burchill et al., 2007; Soper et al., 2007; Yao et al., 2007).

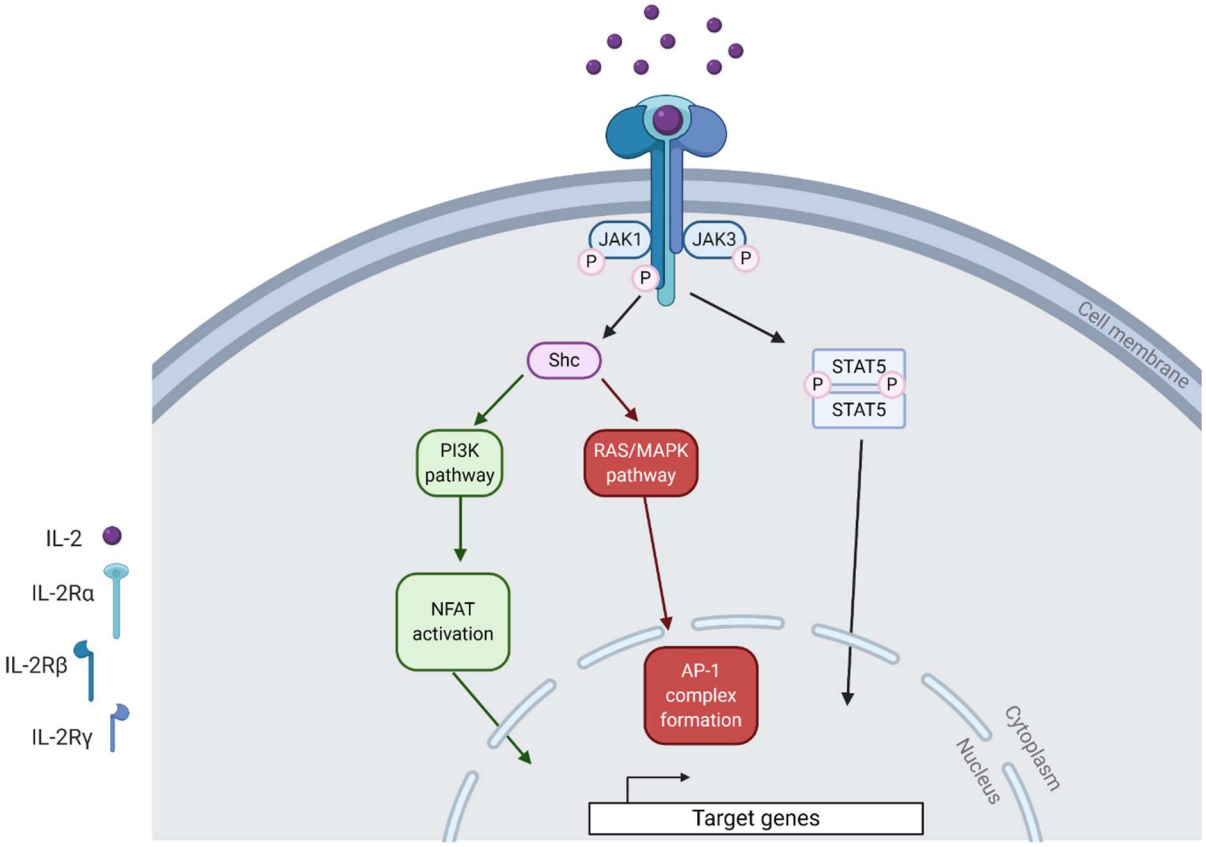


Figure 1.5: A diagram of IL-2 signalling transduction simplified. IL-2 binds initially to the IL-2Rα chain (CD25), which induces formation of the trimeric high affinity IL-2 receptor by recruiting IL-2Rβ and IL-2Rγ chains. Additional JAK3 is recruited to the cytoplasmic domain of the IL-2 receptor, allowing JAK1 and JAK3 to phosphorylate (P) one another and accordingly become activated. These activated JAK molecules phosphorylate the IL-2Rβ cytoplasmic tail, which allows recruitment and docking of the adaptor protein Shc. The PI3K and RAS/MAPK pathways become activated through the Shc adaptor, thus amplifying the TCR signal. The transcription factor STAT5 is also phosphorylated and activated through JAK1 and JAK3. Activated STAT5 translocates to the nucleus to exert its effects.

1.3.1.3 Reporting TCR signalling

Nuclear receptors are transcription factors that may be activated by steroid hormones or lipid-soluble signalling molecules, including Retinoic Acid (introduced in Chapter 1.1.2). Once bound, the activated nuclear receptor translocates to the nucleus to regulate gene transcription. The nuclear receptor subfamily 4 group A member (Nr4a) 1 is an immediate early gene of TCR signalling and orphan receptor that has traditionally been used to report TCR signalling (Moran et al., 2011; Osborne et al., 1994). However, the Ono Lab has identified

that TCR signalling has a more distinct correlation with Nr4a3 (Bending et al., 2018a). The correlation was determined by canonical correspondence analysis and demonstrates that Nr4a3 is a more appropriate reporter of TCR signalling, increasing the reliability of TCR signal reporting in the thymus and periphery. It has since been proposed that Nr4a1 and Nr4a3 may be a consequence of different TCR signalling downstream pathways. Nr4a3 expression appears to result from the PI_3K pathway and the NFAT transcription factor, whereas inhibition of these does not appear to affect transcription of Nr4a1 (Jennings et al., 2019). It is therefore prudent to note that Nr4a1 and Nr4a3 may differ in their response to TCR signalling.

Nr4a3 reports strong TCR signalling, regardless of co-stimulation or whether the TCR signal activates the T-cell (Bending et al., 2018a; Jennings et al., 2019). Here, strong TCR signalling occurs by recognition of cognate antigen, rather than weaker signalling that occurs from cross-reactivity during peptide mis-match (Jennings et al., 2019). Interestingly, high expression of Nr4a receptors has been associated with driving Treg development within the thymus by promoting Foxp3 expression (Bandukwala and Rao, 2013). Consequently, during development, a high affinity for self-antigen leads to Treg differentiation, preventing autoimmunity (Jordan et al., 2001).

1.4 Foxp3 and regulatory T-cells

Foxp3 was identified in 2003 as the master transcription factor for Treg by three groups; those of Rudensky, Sakaguchi and Ramsdell (Fontenot et al., 2003; Hori et al., 2003; Khattri et al., 2003). Thus, Foxp3 is necessary for Treg suppressive activity and conveys the Treg phenotype, forming a specific marker of Treg. For the Treg suppressive phenotype, *Foxp3* is constitutively expressed. Mutations in the *Foxp3* gene cause Immunodysregulation, polyendocrinopathy,

enteropathy, X-linked (IPEX) syndrome in humans and Scurfy in mice. These diseases result in Treg deficiency, and subsequent autoimmune diseases.

1.4.1 Regulatory T-cell suppressive mechanisms

Foxp3 augments and amplifies the suppressive mechanisms conveyed by TCR and cytokine signalling, such as increased CD25 and CTLA-4 expression (Gavin et al., 2007). The resulting Treg suppressive mechanisms (Figure 1.6) can be grouped into three categories; cell-cell, soluble suppressive factors and competition type mechanisms. One mechanism of cell-cell contact suppression is through CTLA-4. CTLA-4 is highly expressed on Treg and can modify DC activity to become tolerogenic. For instance, CTLA-4 ligation stimulates the DC to up-regulate indoleamine 2,3-dioxygenase (IDO), an enzyme that catabolizes tryptophan, creating a tryptophan deprived environment and thus inhibiting T-cell function. In addition, CTLA-4 induces the down-regulation of co-stimulatory molecules (Oderup et al., 2006; Walker and Sansom, 2011). Further, CTLA-4 can capture co-stimulatory molecules CD80/CD86 from APCs and degrade them via trans-endocytosis, thus inhibiting the co-stimulatory signal transduced by CD28 in T-cells and reducing the opportunity for T-cell activation (Qureshi et al., 2011).

Soluble suppressive factors include cytokines such as IL-10. IL-10 may suppress T-cell activation by inhibiting the CD28 co-stimulatory pathway. IL-10 further prevents pro-inflammatory cytokine release from mast cells and reduces MHC-II expression on DCs (Taylor et al., 2006). Whilst IL-10 can be secreted by Treg, it is more commonly associated with Tr1 cells, a suppressive T-cell subset that does not express Foxp3.

Finally, competition-based mechanisms include CD25 expression. CD25 is expressed upon T-cell activation. Treg consequently up-regulate CD25 as a method of limiting IL-2 in the local environment, thus limiting T-cell proliferation (Busse et al., 2010). CTLA-4 additionally

acts in a competitive based manner, as CTLA-4 binds CD80/86 with a higher affinity than CD28, reducing co-stimulation (Krummel and Allison, 1995).

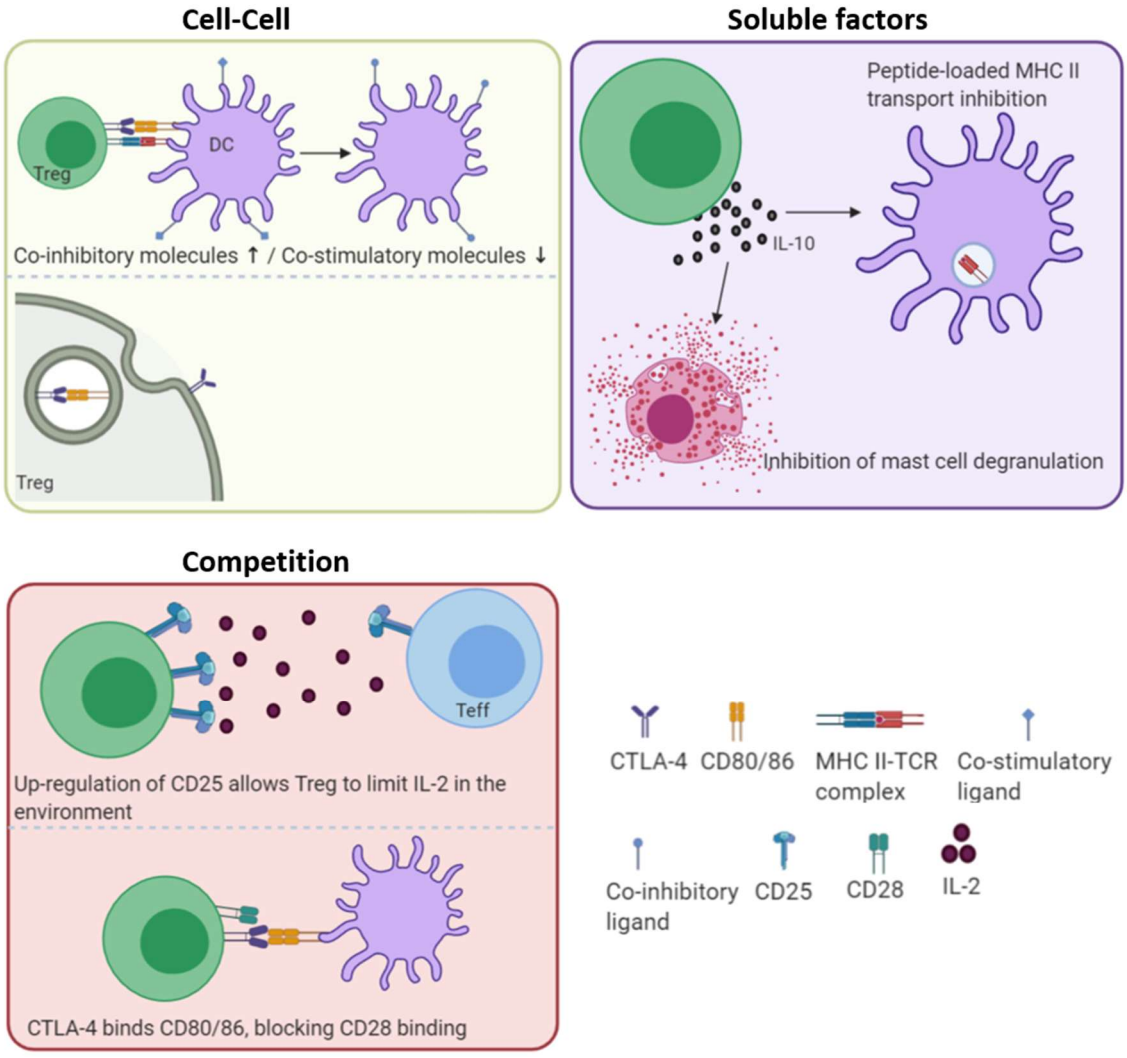


Figure 1.6: Regulatory T-cell suppressive mechanisms. Treg can exert their suppressive phenotype by cell-cell contact (CTLA-4), soluble factors (IL-10) or competition type mechanisms (CD25 and CTLA-4). Cell-cell mechanisms refer to instances where the Treg directly interacts with another cell to exert its effect. Soluble factors refer to cytokines and other secreted factors that are released by the Treg into the local environment, thus modifying the local microenvironment. Finally, competition-based mechanisms refer to instances where the Treg competes with APCs to prevent T-cell activation. These may also be cell-cell contact mechanisms, such as CTLA-4.

1.4.2 Regulatory T-cell differentiation

Treg work to suppress inappropriate T-cell activation against self or harmless foreign antigen. Treg recognising self-antigen typically arise within the thymus (tTreg), whilst Treg recognising foreign antigen arise within the periphery (pTreg) (Shevach and Thornton, 2014). Within the thymus, T-cells that strongly recognise self-antigen undergo negative selection via apoptosis, known as clonal deletion. However, some self-reactive T-cells escape clonal deletion and become tTreg. These tTreg precursors have received a strong TCR signal within the thymus and subsequently express CD25 and Foxp3 (Hsieh et al., 2012). Foxp3 expression occurs downstream of Nr4a family member expression as described in Chapter 1.3.1.3.

tTreg differentiation requires co-stimulation in addition to TCR signalling; CD28 deficient and CD80/86 deficient mice have a notable reduction in Treg frequency (Tai et al., 2005). During Treg differentiation, a c-Rel dependent pathway distinct from T-cell activation is associated with CD28 ligation (Vang et al., 2010). c-Rel is able to bind the *Foxp3* enhancer region to promote transcription (Long et al., 2009). Downstream transcription factors from TCR/CD28 signalling, including NFAT and AP-1, also promote *Foxp3* transcription required for the Treg phenotype (Figure 1.7). As such, NFAT and AP-1 directly bind the *Foxp3* promoter (Mantel et al., 2006). Consequently, Foxp3, co-inhibitory CTLA-4 and co-stimulatory TNFRSF members are upregulated (Tai et al., 2005).

After CD28 co-stimulation, further co-stimulation from TNFRSF members is required for Treg differentiation. The TNFRSF members involved include GITR, OX40 and TNFRII. These co-stimulatory molecules are found on Treg and their precursors; their expression is directly correlated with TCR signal strength (Mahmud et al., 2014). Tai *et al*. propose that TNFRSF members translate TCR signalling into a “molecular program” for Treg differentiation. Indeed, upon agonist ligation, the tTreg precursors exhibit increased sensitivity to IL-2 via increased

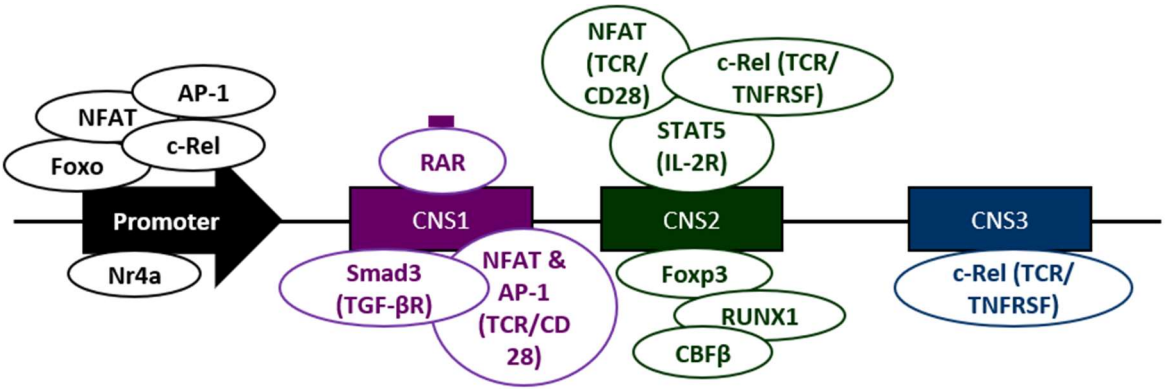


Figure 1.7: Transcriptional control of the Foxp3 gene. Key transcription factors downstream of TCR signalling bind to the *Foxp3* gene promoter, including NFAT, AP-1, c-Rel and the Nr4a transcription factors. In addition to the promoter, the *Foxp3* gene contains three key enhancer regions; CNS1, CNS2 and CNS3. CNS1 is required for pTreg differentiation. Transcription factors of particular note that bind CNS1 are NFAT and AP-1, a downstream consequence of TCR signalling and amplified by CD28 signalling, and Smad3. Smad3 is transcribed as a result of the TGF-βR signalling pathway. The Retinoic Acid Receptor (RAR) can also be found at the CNS1 region, where binding of Retinoic Acid is not necessary for pTreg differentiation but rather increases transcriptional activity when present. The CNS2 region, when demethylated, conveys stability to the Treg. Foxp3 is associated with demethylation of the CNS2 region as part of a positive feedback loop. CNS3 is required for tTreg differentiation, requiring c-Rel binding. c-Rel is part of the NFκB family transcribed downstream of TCR and TNFRSF member signalling.

responsiveness of the IL-2 receptor and transcription factor STAT5 (Mahmud et al., 2014).

Upon exit from the thymus, tTreg may further differentiate within the periphery; here they acquire an activated effector phenotype (eTreg). eTreg have increased suppressive capacity and hence can be identified by upregulation of molecules such as CTLA-4, ICOS and TIGIT (reviewed by Cretney *et al*. (Cretney et al., 2013)). Bending *et al.* reported that eTreg can be identified by their Persistent transcription of the *Foxp3* gene using *Foxp3*-Tocky reporter mice (Bending et al., 2018b).

Alternatively, naïve CD4 T-cells in the periphery may be polarised to pTreg in response to foreign antigen under non-inflammatory conditions (Chen et al., 2003). These pTreg are considered distinct and less stable than tTreg, due to their capacity to down-regulate *Foxp3*

expression in response to cognate antigen immunisation (Floess et al., 2007; Miyao et al., 2012). However, Goldstein *et al.* note that such activity is reported only within an IL-2 deficient environment (Goldstein et al., 2013). Upon exogenous administration of IL-2, loss of the regulatory phenotype may be prevented (Duarte et al., 2009; Tang et al., 2008).

pTreg differentiation was further believed to differ from tTreg differentiation by the requirement of TGF-β signalling (Yamazaki et al., 2007). TGF-β binds to the Conserved Non-coding Sequence (CNS) 1 region of the *Foxp3* gene in order to promote *Foxp3* expression. Indeed, the CNS1 region is required for pTreg differentiation but not tTreg differentiation (Zheng et al., 2010). In TGF-β deficient mice, pTreg are diminished *in vivo* (Marie et al., 2005), similar to that seen in CNS1 deficient mice, but no evidence was reported of a decreased tTreg output. Later evidence found that TGF-β may also be required for tTreg differentiation, but likely through a different mechanism (Chen and Konkel, 2015; Liu et al., 2008).

Alongside TGF-β, pTreg polarisation also requires the presence of IL-2. In an environment deficient in IL-2 but enriched with IL-6, TGF-β rather polarises naïve T-cells into a pro-inflammatory Th17 phenotype. The Th17 / Treg axis appears to be controlled through the opposing actions of STAT3 and STAT5. STAT3 is activated by IL-6 signalling and binds to the IL-17 gene locus to induce IL-17 expression and Th17 polarisation. Activation of STAT5 by IL-2 signalling leads to STAT5 binding of these binding sites, preventing STAT3 binding, thus preventing IL-17 transcription (Yang et al., 2011).

The concept of Treg as a distinct lineage of T-cell has been largely based on reports from neonatal thymectomy resulting in autoimmunity. More recently, these findings have been disputed. Ono and Tanaka (2015) propose an alternative negative feedback model to the lineage theory. They suggest that Foxp3 results from typical T-cell activation as one of three fates. After inflammation, T-cells either die, become Tmem or Treg. Thus, a Tmem /

Treg axis is described (Ono and Tanaka, 2015). The negative feedback model has gained increasing support, including from Zhang *et al.* (Zhang et al., 2016), where this model best fits the published data.

1.5 *Heligmosomoides polygyrus* infection promotes Foxp3 expression

Finney *et al*. published in 2007 that Foxp3 expression can be found in the mLN of mice infected with *H. polygyrus*. This response occurs by day-28 of infection, where a strong immune modulatory response is reported (Finney et al., 2007). Numerous reports account that *H. polygyrus* infection can induce Treg capable of suppressing the T-cell response to bystander antigens, preventing various inflammatory conditions (McSorley and Maizels, 2012). This would suggest that *H. polygyrus* are able to induce *Foxp3* expression in a non-specific manner. Indeed, Grainger *et al.* subsequently identified that Treg are directly induced by a component of *H. polygyrus* secreted HES through a pathway analogous to that of TGF-β (Grainger et al., 2010). Interestingly, in an ovalbumin sensitisation model, administration of exogenous mammalian TGF-β failed to exert the immunomodulatory effects seen upon administration of HES (McSorley et al., 2012).

In 2017, the Maizels group identified the TGF-β-like molecule in HES as Hp-TGM (Johnston et al., 2017). Hp-TGM is structurally distinct to TGF-β and requires no further processing to become activated. Despite their lack of structural similarity, Hp-TGM signals through TGF-β receptors to activate the TGF-β pathway and subsequently induce *Foxp3* expression. Interestingly, the maximum TGF-β signal from receptor binding was significantly higher from purified Hp-TGM than from exogenous TGF-β. Further, *in vitro* naïve CD4 T-cells were converted to Treg more efficiently with the addition of Hp-TGM than exogenous TGF-β; also exhibiting higher mean fluorescence intensity of Foxp3. Importantly, under Th17

polarising conditions (IL-6), TGF-β and Hp-TGM induced similar proportions of Th17 cells, where Hp-TGM induced Treg in addition to Th17 that did not occur by TGF-β (Johnston et al., 2017). These data demonstrate how HES from *H. polygyrus* promotes tolerance.

It is clear, however, that Hp-TGM does not account for the entirety of the immunomodulation derived from HES. HES appears to differentially affect the innate and adaptive immune responses. This was observed by McSorely *et al.* (2012) when heat inactivating HES in an ovalbumin-induced allergic asthma model. Heat-inactivated HES had no apparent effect on the induction of tolerance at sensitisation to ovalbumin. However, heat-inactivation of HES did impede immunomodulation when administered post-sensitisation at challenge. (McSorley et al., 2012).

Investigating Foxp3 expressing T-cells *in vivo*, Smith *et al.* reported rapid expansion of the $Foxp3^{+}Helios^{+}$CD4 T-cell population (tTreg) during *H. polygyrus* infection, with a delayed expansion of $Foxp3^{+}Helios^{-}$CD4 T-cells (pTreg) (Smith et al., 2016). Considering the expression of Helios, a marker of tTreg, the authors concluded that *H. polygyrus* infection preferentially expands the tTreg population. Helios is, however, a controversial marker of tTreg. Akimova *et al.* found that Helios expression correlates with T-cell activation (Akimova et al., 2011). Considering Helios as a marker of T-cell activation would alternatively suggest that activated, or eTreg rapidly increase, whilst naïve or previously naïve Treg show a delayed response. Smith *et al.* further administered IL-2 in a structurally stable complex, increasing the $Foxp3^{+}Helios^{+}$CD4 T-cell population. Consequently, *H. polygyrus* worm burden increased and the Th2 response was suppressed (Smith et al., 2016). These findings are consistent with expanding the eTreg population.

Whilst increasing the proportion of Treg during infection was associated with an expected increase in worm burden, Treg depletion using a mouse model with a diphtheria toxin conjugated *Foxp3* gene (Foxp3-DTR mice) unexpectedly also increased the *H. polygyrus* worm burden. The authors proposed that this was due to uncontrolled excessive T-cell activity (Smith et al., 2016). The same effect was found by Rausch *et al.* who also identified that Foxp3-DTR mediated Treg depletion did not decrease worm burden but rather worsened intestinal pathology, despite reporting a stronger Th2 response (Rausch et al., 2009). Whilst Treg depleted by Foxp3-DTR were unsuccessful in parasite clearance, Smith *et al.* found that T-cell depletion using anti-CD25 early during infection was associated with increased worm clearance (Smith et al., 2016). However, targeting of CD25 expressing cells is unlikely to have depleted Treg alone. It therefore remains unclear if a specific T-cell population upregulates expression of *Foxp3* and whether such induced Treg primarily prevent the anti-parasite response or host inflammation.

1.6 Thesis Aims

H. polygyrus are known to modulate the murine host immune response in order to establish chronic infection. One such strategy employed is through the induction of Treg by the promotion of *Foxp3* expression. However, the Treg population is highly heterogenous and it is therefore difficult to identify infection-reactive cells *in vivo*. The question remains as to whether a specific subset of T-cell expresses *Foxp3* in response to *H. polygyrus* infection *in vivo*, and whether these Treg primarily function to prevent tissue pathology or the anti-parasite T-cell response. Further, due to a lack of *in vivo* tools, it was previously difficult to analyse the expression of *Foxp3* throughout infection, and thus determine whether *Foxp3*

transcription is differentially regulated at different stages of infection. The Tocky system will aid such investigations.

The fact that mice are typically resistant to re-infection with *H. polygyrus* after parasite clearance suggests that immunomodulatory mechanisms are insufficient against the host memory response. It is therefore of interest to dissect the relationship between the effective anti-parasite T-cell response and negative regulatory mechanisms.

This thesis aims to:

(1) Further understand the mechanisms of T-cell suppression *in vivo*, by analysing T-cell responses and *Foxp3* dynamics at different stages of primary *H. polygyrus* infection.
(2) Understand the relationship between the memory T-cell response and mechanisms of T-cell suppression *in vivo*, by analysing TCR signalling and *Foxp3* dynamics in both primary and secondary *H. polygyrus* infection.

2 Chapter Two: Materials and Methods

2.1 Timer Of Cell Kinetics and Activity

The Timer of Cell Kinetics and Activity (Tocky) system was developed by the Ono Lab (Bending et al., 2018a) and utilises Fluorescent Timer protein (Subach et al., 2009) to report whether a gene is actively transcribed. Fluorescent Timer, here called Timer protein, is an mCherry derivative. The mCherry fluorophore has an initial phase of blue fluorescence before spontaneously maturing to red fluorescence. Subach *et al.* identified six key mutations (M18V, E34K, K69R, L84W, S149T and A224S) in the mCherry amino acid sequence that delay fluorescence maturation. Therefore, in Timer protein the blue fluorescent form is detectable (here named Timer-Blue) with a half-life reported by Subach *et al.* of 7.5 hours, later found by the Ono lab to be approximately 4 hours in the context of murine T-cells. The red fluorescent form of Timer protein (here named Timer-Red) was found to have a half-life of approximately 120 hours (Bending et al., 2018a).

The Ono lab report Treg dynamics and TCR signalling *in vivo* using *Foxp3*-Tocky and *Nr4a3*-Tocky respectively. Transcription of *Foxp3* and *Nr4a3* are reported independently of the gene itself. For this to occur, the Timer protein sequence is located on a Bacterial Artificial Chromosome (BAC), along with the gene (*Foxp3* or *Nr4a3*) promoter and all associated regulatory regions. Upon gene transcription, the gene of interest and the Timer gene are transcribed in parallel. Parallel reporting allows transcription to be reported without affecting the resulting protein. After translation, the fluorophore maturation is temporal and

irreversible. In this way, active transcription is reported by Timer-Blue fluorescence, whilst Timer-Red fluorescence reports a history of gene transcription.

Cells expressing Timer protein will have different ratios of Timer-Blue protein to Timer-Red protein depending on the dynamics of gene transcription. Upon gene transcription for the first time, the Timer-Blue protein is found without Timer-Red fluorescence (Timer-Blue^{+}Timer-Red^{-}). As transcription continues, Timer-Blue protein matures to Timer-Red protein and thus both fluorescent forms are found within the cell (Timer-Blue^{+}Timer-Red^{+}), unless transcription terminated, in which case all of the Timer-Blue fluorescence matures to Timer-Red (Timer-Blue^{-}Timer-Red^{+})(Figure 2.1A). The dynamics of gene transcription influence the level of fluorescence and ratio of Timer-Blue to Timer-Red protein, and thus the data is classed as continuous.

Due to the data being continuous, trigonometric transformation is required for effective analysis. First, each cell is assigned a Timer Angle. The Timer Angle is a value between 0 and 90 and represents the position of the cell between the Timer-Blue axis and the Timer-Red axis. A Timer Angle of 0 represents Timer-Blue^{+}Timer-Red^{-} fluorescence, whilst a Timer Angle of 90 denotes Timer-Blue^{-}Timer-Red^{+} fluorescence (Figure 2.1B). The Timer Angle therefore reports transcriptional activity.

The Timer Angle can be subsequently divided into biologically relevant loci regarding transcriptional dynamics (Timer Locus). A Timer Angle of 0 is classified as New transcription, whilst a Timer Angle above 0 and below 30 is categorised as New to Persistent transitioning (NPt) transcription. Considering the half-life of Timer-Red protein is much longer than the half-life of Timer-Blue, cells up to a Timer Angle of 45 are unable to decrease in Timer Angle value. We can therefore consider all cells classified as New or NPt as having newly-initiated

transcription. Cells with a Timer Angle between 30 and 60 are classified as having Persistent transcription. This is due to the ratio of Timer-Blue to Timer-Red indicating active transcription. Cells with a Timer Angle above 60 and below 90 are classified as Persistent to Arrested transitioning (PAt), whilst cells with a Timer Angle of 90 are considered Arrested transcription. Cells with PAt and Arrested transcription can decrease in Timer Angle value, becoming either PAt or Persistent upon the upregulation of transcription and thus a higher ratio of Timer-Blue protein (Figure 2.1C).

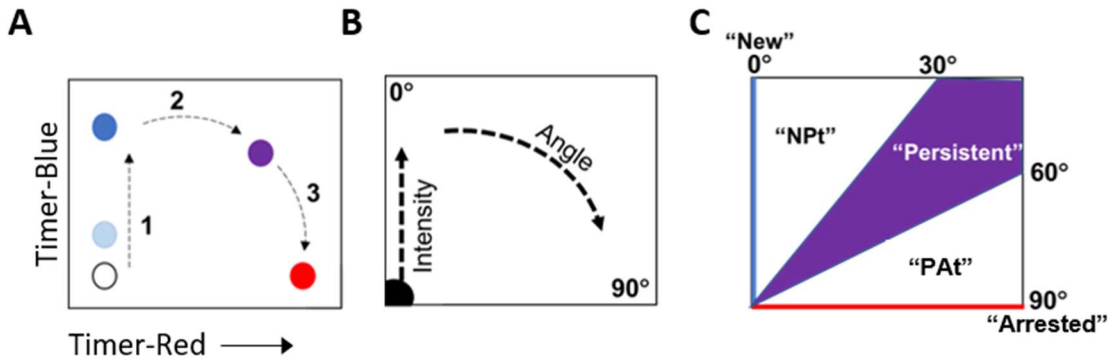


Figure 2.1: Timer-Blue and Timer-Red analysis. Upon translation, the Timer protein has a Blue fluorescent form (Timer-Blue) with a half-life of approximately 7 hours, before spontaneously maturing to the Red fluorescent form (Timer-Red). (A) Upon transcription of the Timer gene for the first time in Timer memory, Timer-Blue is observed without Timer-Red fluorescence (1). As transcription continues, Timer-Blue matures to the Timer-Red form of the protein (2), and thus both Timer-Blue and Timer-Red proteins are present. Upon termination of transcription, all of the Timer-Blue fluorescence matures to Timer-Red (3), and the cell moves down the Timer-Blue axis of the flow cytometry plot. (B) Each cell has a Timer Angle and Timer Intensity value based on its position within the flow cytometry plot between the Timer-Blue and Timer-Red axis. (C) The Timer Angle can be categorised as one of five biologically relevant transcription states, known as Timer-loci. These are New (a Timer Angle of 0), New to Persistent transitioning (NPt, a Timer Angle above 0 and below 30), Persistent (a Timer Angle between 30 and 60), Persistent to Arrested transitioning (PAt, a Timer Angle above 60 and below 90) and Arrested (a Timer Angle of 90).

2.2 Mice

The *Nr4a3*-Tocky, OT-II-*Nr4a3*-Tocky and *Foxp3*-Tocky reporter strains (Table 2.1) were used as described in Bending *et al.* (Bending et al., 2018a). In brief, these strains have a C57BL/6 background, and wild type (WT) C57BL/6 mice were used alongside transgenic reporter strains for flow cytometric analysis. *Nr4a3*-Tocky mice possess Nr4a3-Timer Foxp3-IRES-GFP, using an Nr4a3 BAC construct to report TCR signalling and a Foxp3 internal ribosomal entry site (IRES) linked GFP construct to report *Foxp3* transcription. *Nr4a3*-Tocky mice were previously crossed with OT-II mice expressing an ovalbumin specific transgenic TCR. This mating resulted in OT-II *Nr4a3*-Timer Foxp3-IRES-GFP; OT-II-*Nr4a3*-Tocky mice. *Foxp3*-Tocky mice report *Foxp3* transcription via a Foxp3-Timer BAC construct. Maintenance and breeding were undertaken at Charles River UK, and later at Imperial College London Central Biomedical Service. All live experimental work was undertaken in accordance with the UK Animals (Scientific Procedures) Act, 1986, and in accordance with the local Animal Welfare and Ethical Review Body at Imperial College London.

Table 2.1: Mouse strains. A table of mouse strains used in this thesis.

Mouse strain	Background	Description	Source
***Nr4a3*-Tocky** (*Nr4a3*-Tocky:*Foxp3*$^{IRES-GFP}$)	C57BL/6J	**Tg(RP23-122N18-ΔNr4a3Timer)[1]** x **B6.Cg-Foxp3tm1Mal/J[2]**. [1] BAC reporter transgenic with the first coding exon of *Nr4a3* replaced by *Timer (Fast-FT)*. [2] IRES-GFP cassette reporter within the exon 11 of the *Foxp3* gene (Wang et al. 2008)	Masahiro Ono
OT-II *Nr4a3*-Tocky	C57BL/6J	*Nr4a3*-Tocky x **B6.Cg-Tg(TcraTcrb)425Cbn/J[1]** [1] Alpha-chain and beta-chain TCR specific for chicken ovalbumin peptide residues 323-339	Masahiro Ono
***Foxp3*-Tocky**	C57BL/6J	**Tg(RP23-330D17-ΔFoxp3Timer)** BAC reporter transgenic with the first coding exon of *Foxp3* replaced by *Timer* (*Fast-FT*).	Masahiro Ono

2.3 *Heligmosomoides polygyrus* infection

2.3.1 Culturing *H. polygyrus*

WT mice were infected with 200 L3 stage *H. polygyrus* larvae in 200 µl water by oral gavage. From 14-days post infection, faeces were collected from the mice to isolate *H. polygyrus* eggs. Faeces were crushed in Milli-Q water to form a paste in a 50 ml conical tube. The tube was topped up with Milli-Q water and centrifuged at 600 x g for 2 minutes. The supernatant was discarded, and the faecal paste was washed twice more with Milli-Q water. After the last supernatant was discarded, the faecal paste was spread onto damp filter paper (Whatman) inside Petri dishes. These dishes were then kept in a dark place at room temperature for 10-days, with Milli-Q water moistening the edges of the filter paper every second day. On day-7 and day-10, Milli-Q water was pipetted around the edge of the filter paper to retrieve L3 *H. polygyrus* larvae. Larvae were collected into a 50 ml conical tube and subsequently filtered using a Baermann set up, whereby layers of lens cleaning tissue (Whatman) were sandwiched between muslin cloth (unbleached, John Lewis) and the Baermann filled with Milli-Q water. L3 larvae were applied to the top of the muslin cloth, and live larvae were able to traverse through the filter paper and collect at the bottom of a 15 ml conical tube. Larvae were then washed thrice with Milli-Q water, centrifuging at 300 x g for 10 minutes, and stored at 4^{o}C for up to 6 months. Before use, larvae were washed 3 x with Milli-Q water, centrifuging at 300 x g for 10 minutes, and counted on a McMaster chamber.

2.3.2 Time Course

Foxp3-Tocky or *Nr4a3*-Tocky Mice were infected with 200 L3 stage *H. polygyrus* larvae in 200 µl water by oral gavage. Naïve mice were gavaged with 200 µl water. Mice were culled at 7-, 10-, 14-, or 28- days post infection in *Foxp3*-Tocky mice and 7-, 10- and 28-days post-infection in *Nr4a3*-Tocky mice.

2.3.3 Primary vs secondary infection

Foxp3-Tocky or *Nr4a3*-Tocky Mice were infected with 200 L3 stage *H. polygyrus* larvae in 200 µl water by oral gavage. At 14-days post infection, infected mice were treated with 1 µg / ml Ivermectin (Sigma) in drinking water for 5 days. 23 days later, mice were re-infected with 200 L3 stage *H. polygyrus* larvae in 200 µl water by oral gavage and analysed at day-7 for secondary infection. Mice with primary infection were infected for the first time with 200 L3 stage *H. polygyrus* larvae in 200 µl water by oral gavage 7-days prior to analysis; concurrent to Naïve mice receiving water by oral gavage.

2.4 Ovalbumin

1 % Ovalbumin protein (Sigma) was administered in drinking water to OT-II-*Nr4a3*-Tocky mice for 72 hours. Mice were culled for analysis at the end of the 72 hours.

2.5 Flow cytometry

mLN were isolated into cold cPBS (PBS supplemented with 2 % foetal calf serum and 1 mM EDTA (Sigma)) and processed into single cell suspensions by manual dissociation through a 70

µm cell strainer. Cells were washed with PBS before staining in a V-bottom 96 well plate. In brief, a fixable eFluor 780 viability dye (eBiosciences) diluted in PBS was applied to all samples for 30 minutes on ice. Cells were washed with cPBS and centrifuged at 500 x g for 3 minutes. Anti-mouse CD16/32 antibody (BioLegend) was then applied for 20 minutes on ice before washing with cPBS and centrifuging. When biotin-conjugated antibodies were used, these were added in cPBS for 30 minutes on ice before washing with cPBS and centrifuging. Markers were then identified using the following directly conjugated antibodies (Table 2.2): CD4 BUV395 or BUV496 (clone GK1.5 BD Biosciences), CD4 APC (clone RM4-5, eBiosciences), TCRβ BUV737 (clone H57-597, BD Biosciences), TCRβ Alexa Fluor 700 (clone H57-597, BioLegend), CD25 PerCPcy5.5 (PC61.5, eBiosciences), CD44 Alexa Fluor 700 (clone IM7, BioLegend), OX40 PE-Cy7 (clone OX86, BioLegend), GITR FITC (clone DTA-1, BioLegend), GITR BUV395 (clone DTA-1, BD Bioscience), PD-1 APC (clone RMP1-30, BioLegend), CXCR5 PE-Cy7 (clone SPRCL5, Invitrogen), CD11b Biotin (clone M1/70, Invitrogen), CD11b Pe-Cy7 (clone M1/70, BioLegend), CD11c Biotin (clone N418, Invitrogen), CD11c AF700 (clone N418, BioLegend), CD19 BUV395 (clone 1D3, BD Biosciences), CD19 Biotin (clone 1D3, eBiosciences), CD45.2 BUV737 (clone 104, BD Biosciences), CD103 BV421 (clone 2E7, BioLegend), NK1.1 Biotin (clone PK136, Invitrogen), PD-L1 PE-Dazzle 594 (clone 10F.962, BioLegend), PD-L2 PE-Dazzle 594 (clone TY25, BioLegend), gdTCR Biotin (clone GL3, Invitrogen), I-Ab PercP-Cy5.5 (clone AF6-120.1, BioLegend), F4/80 APC (clone Bm8, BioLegend), TER-119 Biotin (clone TER-119, Invitrogen), Gr1 Biotin (clone RB6-8C5, eBiosciences), Streptavidin FITC (BioLegend). These were diluted in cPBS and applied on ice for 30 minutes. Data was collected on a BD LSRFortessa or cells sorted on a BD Aria. The blue form of *Foxp3*-Timer protein was detected in the blue (450/40 nm) channel excited off the 405 nm laser. The red form was detected in the mCherry (610/20) channel excited off the 561 nm laser.

Table 2.2: Table of antibodies. A Table of markers/antibodies with the fluorophores used to detect them and in which experiments these antibodies were used.

Detecting	Fluorophore	Experiment
CD4	BUV395, BUV496	All Time Course, Primary vs Secondary infection, Ova
CD4	APC	RNA-seq
TCRβ	BUV737	All Time Course, Primary vs Secondary infection, Ova
TCRβ	AF700	RNA-seq
CD25	PerCP-Cy5.5	All
CD44	AF700	All Time Course, Primary vs Secondary infection, Ova
OX40	Pe-Cy7	Time Course
GITR	FITC	Foxp3-Timer Time Course
GITR	BUV395	Foxp3-Timer Primary vs Secondary infection
PD-1	APC	Primary vs Secondary infection
CXCR5	Pe-Cy7	Primary vs Secondary infection
Lineage markers (CD11b, CD11c, CD103, I-Ab, NK1.1, TER-119, CD19, CD45.2, gdTCR, F4/80, Gr1)	Biotin Streptavidin-FITC	Foxp3-Timer Time Course confirmation experiment (refer to figure), Foxp3-Timer Primary vs Secondary infection
I-Ab	PercP-Cy5.5	Primary vs Secondary infection (WT mice for Antigen Presenting Cell experiment)
CD103	BV421	Primary vs Secondary infection (WT mice for Antigen Presenting Cell experiment)
F4/80	APC	Primary vs Secondary infection (WT mice for Antigen Presenting Cell experiment)
CD19	BUV395	Primary vs Secondary infection (WT mice for Antigen Presenting Cell experiment)
CD45.2	BUV737	Primary vs Secondary infection (WT mice for Antigen Presenting Cell experiment)
CD11c	AF700	Primary vs Secondary infection (WT mice for Antigen Presenting Cell experiment)
CD11b	PE-Cy7	Primary vs Secondary infection (WT mice for Antigen Presenting Cell experiment)
PD-L1	PE-Dazzle	Primary vs Secondary infection (WT mice for Antigen Presenting Cell experiment)
PD-L2	PE-Dazzle	Primary vs Secondary infection (WT mice for Antigen Presenting Cell experiment)

2.5.1 Gating strategy

First, manual compensation was applied to all samples on the FlowJo software using cells from WT mice for single-stains and un-stained Tocky cells to compensate for Timer Blue and Timer Red. To identify CD4 T-cells, a standard gating strategy was applied. This standard gating strategy within the FlowJo software first identified lymphocytes by their size (reported by FSC-A) and complexity (SSC-A), (Figure 2.2A). Within this population, single cells were gated on by their height (FSC-H) to area (FSC-A) ratio (Figure 2.2B). Live cells were then determined within the single cell population, identified by the exclusion of Viability Dye (Figure 2.2C). Finally, CD4 T-cells were identified by CD4-BUV395, CD4-BUV496 or CD4-APC expression and TCRβ-BUV737 or TCRβ-AF700 (Figure 2.2D). In the *Foxp3*-Timer primary vs secondary experiments and the Day 7 vs Day 28 experiment in Chapter 3 looking at day effect (section 3.2.1), an additional step was incorporated to exclude other cell lineages, whereby lineage defining markers were stained with antibody conjugated-FITC and these cells excluded from analysis.

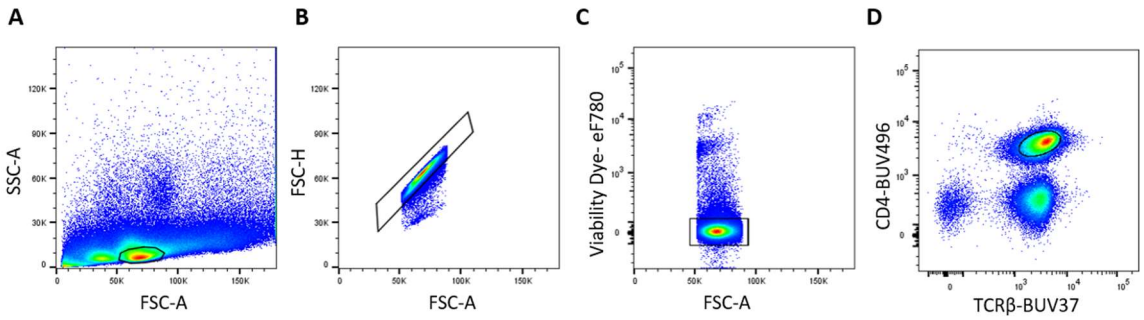


Figure 2.2: Standard gating strategy. FCS files were imported into FlowJo software for analysis and compensated. (A) Lymphocytes were gated on by their size (FSC-A) and complexity (SSC-A). (B) Single cells within this population were gated on by their height (FSC-H) to area ratio. (C) Of these cells, viable cells were identified by the exclusion of viability dye. (D) Finally, CD4 T-cells were gated on for from their CD4 and TCRβ expression.

2.5.2 Tocky analysis

After compensation and gating, the csv files for the cell population to be investigated were exported. Csv files were also exported for WT cells where Timer protein fluorescence was not present to allow for fluorescence normalisation of Timer and FSC-A. Using R, files underwent data normalisation and trigonometric transformation to give a Timer Angle value for each cell as seen in section 2.1, using R codes written by Dr Masahiro Ono (codes available upon request), as described previously (Bending et al., 2018a). The success of the normalisation and trigonometric transformation was confirmed by assessment of quality control output files.

2.5.3 t-SNE analysis

t-SNE analysis used the CRAN package *Rtsne*. $CD4^{+}GITR^{high}$ T-cell data was exported from FlowJo in csv format and day-7 infected samples concatenated. A threshold value was determined for each marker to distinguish negative and positive populations. The CRAN package *EMCluster* was used to identify clusters in the t-SNE plot.

2.6 RNA extraction

Cells were sorted by Fluorescence Activated Cell Sorting (FACS) using a BD Aria machine into 100 µl of Extraction Buffer from the PicoPure RNA isolation kit (Applied Biosystems). Samples were heated to 42^{o}C for 30 minutes and vortexed before storage at -80^{o}C. RNA extraction occurred according to the PicoPure RNA isolation kit manufacturer's instructions, including the optional DNase (Qiagen) treatment step.

2.7 RNA-seq and analysis

RNA-seq library preparation followed the Smart-seq2 protocol (Picelli et al., 2014) to create libraries from RNA extracted in section 2.6. Library quality was assessed by Bioanalyzer (Agilent) and quantified by Qubit (Life Technologies). Library concentrations were subsequently normalised and pooled. Sequencing was undertaken by the Imperial Genomics Facility on an Illumina HiSeq2500 sequencer, returning .fastq files. QC was assessed by *fastQC*. The *HISAT2* program was used to align files to the mm10 mouse genome. Sample files were then processed ready for analysis using *samtools*, resulting in .bam files. Next, the *Salmon* analysis pipeline was used (Patro et al., 2017) for quantification, producing gene count data. The gene count data was subsequently imported into *DESeq2* (Love et al., 2014) for analysis of differentially expressed genes (DEGs). DEGs were identified as genes with > 1 log fold change when compared to any other group. Principle Component Analysis (PCA) was performed within the *DESeq2* package and the heatmap created using *gplots*.

2.8 Statistics

All graphs were created in R and statistics performed in R using the following CRAN packages: ggplot2; gplots; Rmisc; R2HTML; ade4; ggbeeswarm; dunn.test. Data was tested for a normal distribution using a Shapiro-Wilk test, whereby a *p* value below 0.05 indicated that data was not normally distributed, whilst a *p* value above 0.05 indicated that data was normally distributed. The statistical test applied to data depended on the Shapiro-Wilk test outcome and the data type. Where more than two groups were compared, either a one way ANOVA followed by a Tukey's honestly significant difference post-hoc test was used for normally distributed data, or a Kruskal-Wallis followed by a Dunn's test for multiple comparisons post-

hoc test was performed for non-parametric data. For tests comparing two means, a t-test was used for normally distributed data and a Mann-Whitney U test for non-parametric data.

3 Chapter Three: Transcriptional dynamics of *Foxp3* during primary *Heligmosomoides polygyrus* infection

3.1 Background

A key immune receptor associated with both Treg and helminth infection is GITR. GITR is a co-stimulatory molecule that is highly upregulated on Treg, especially eTreg, reviewed by Ronchetti *et al.* (Ronchetti et al., 2015) and supported by *Foxp3*-Tocky data (Bending et al., 2018b). Indeed, GITR expression is initiated downstream of *Foxp3* transcription (Khattri et al., 2003). Ono *et al.* described that GITR expression is a more robust identifier of Treg than the commonly used IL-2Rα chain, CD25 (Ono et al., 2006). Depletion of $CD4^+GITR^+$ T-cells resulted in more severe autoimmunity than depletion of $CD4^+CD25^+$ T-cells, and a lower percentage of the remaining T-cells expressed *Foxp3*. Uraushihara *et al.* further identified that the $CD4^+GITR^+$ T-cell fraction is mainly $Foxp3^+$, whilst those cells $Foxp3^-$ are exclusively $CD45RB^{low}$ under physiological conditions, and thus classified as memory-phenotype T-cells (Uraushihara et al., 2003). Memory-phenotype T-cells have been demonstrated to more efficiently give rise to Treg (Curotto de Lafaille et al., 2004); with some classified as ex-Treg from previous *Foxp3* expression (Miyao et al., 2012), highlighted by Ono and Tanaka (Ono and Tanaka, 2015).

It was initially argued that GITR ligation on Treg by its ligand, GITRL, abrogates the suppressive capacity of Treg. GITR engagement appeared to remove the anergic state of Treg and re-instate responsiveness to IL-2. Treg were subsequently able to proliferate and their suppressive function diminished (Ji et al., 2004). Stephens *et al.* however, showed that $CD4^+CD25^-$ Treg and not $CD4^+CD25^+$ Treg lost their suppressive function in this context

(Stephens et al., 2004). The majority of Treg are $CD4^+CD25^+$, and therefore this loss of suppressive function is unlikely to have a large overall effect. Indeed, other groups also reported Treg proliferation after GITR ligation, however, they found that the suppressive capacity of Treg was instead augmented (Clouthier and Watts, 2014; Igarashi et al., 2008; Kanamaru et al., 2004; Liao et al., 2010; Zhou et al., 2007). This was especially evident in an experimental mouse model over-expressing GITRL, where Treg numbers were found to have expanded compared to WT mice whilst also retaining their suppressive capacity (van Olffen et al., 2009).

Mahmud *et al.* investigated the role of GITR in tTreg differentiation. They identified that tTreg precursors expressed high levels of GITR, which directly correlated with the strength of TCR signalling. Like previous studies, the authors identified that GITR ligation augmented the T-cells responsiveness to IL-2. However, in the context of tTreg progenitor cells, this enhanced the differentiation into tTreg in the thymus (Mahmud et al., 2014). Considering the memory-phenotype of $CD4^+GITR^+Foxp3^-$ T-cells, and the potential plasticity of such memory-phenotype T-cells (Miyao et al., 2012), it is likely that GITR continues to play a role in Treg differentiation within the periphery.

GITR may also be expressed by activated T-cells, albeit to a lower extent. In the downstream of TCR signalling, NFκB positively regulates and NFAT negatively regulates GITR expression. In this context, GITR is thought to protect against Activation Induced Cell Death (AICD)(Zhan et al., 2008). GITR promotes the upregulation of CD25 and IL-2 expression, enhancing the T-cell activation state (Igarashi et al., 2008; Kanamaru et al., 2004; Ronchetti et al., 2004). The ability to enhance the T-cell response, whilst simultaneously inhibiting T-cell

suppressive mechanisms made an attractive target in the treatment of helminth infection. These have been largely unsuccessful, likely due to the persisting suppressive capacity of Treg.

It was reported in *Trichinella spiralis* infection that anti-GITR therapy (using a GITR agonist, DTA-1) resulted in increased anti-parasite IgG and IgM antibodies but no effect was seen on the level of parasite infection (Furze et al., 2006). This data is consistent with T-cell activation being enhanced, alongside Treg suppressive function being augmented. It is important to note that in this study, approximately 80 % of CD4 T-cells expressed GITR by day-7 of infection. This would suggest that GITR was upregulated non-selectively in response to *Trichinella spiralis* larvae. Anti-GITR therapy in the context of *Litomosoides sigmodontis* infection yielded similar results, where an initially enhanced Th2 response was observed without any additional parasite clearance. Further, the authors also reported drastically increased GITR expression on CD4 T-cells during infection (Taylor et al., 2005).

Alternatively, some helminth studies have found GITR agonists to be effective in parasite clearance. D'Elia *et al.* also used the agonistic anti-GITR antibody DTA-1 for treating *Trichuris muris* infection of C57BL/6 mice, showing that the worm burden was significantly decreased. However, this appears to have primarily been due to enhanced T-cell activation as opposed to decreased Treg suppressive capacity. The percentage of $Foxp3^+$ T-cells did not change, and IL-10 expression was unaltered. In addition, significant gut pathology occurred as a result of anti-GITR treatment (D'Elia et al., 2009). Haque *et al.* also demonstrated successful parasite clearance using DTA-1 in the treatment of *Leishmania donovan*. Here, the authors identified that anti-GITR therapy in this context relied on T-cell activation and did not affect Treg function (Haque et al., 2010).

Within *H. polygyrus* infection of BALB/c mice, Finney *et al.* report a subtle increase in the proportion of CD4 T-cells expressing GITR by day-28 of infection, where 8.5 % of CD4 T-cells in Naïve mice expressed GITR compared to 13.8 % at day-28 of infection. The data further suggests that GITR expression may begin to increase as early as day-7 of infection (Finney et al., 2007). $CD4^+CD25^+$ T-cells are often considered to be Treg, whilst $CD4^+CD25^-$ T-cells are considered conventional T-cells. Here, Finney *et al.* found that the $CD4^+CD25^-$ T-cell population upregulated GITR expression to a greater extent than the $CD4^+CD25^+$ T-cell population. Further, GITR upregulation seen within the $CD4^+CD25^+$ T-cell population was restricted to $Foxp3^-$ T-cells. Thus, this study identified GITR expression in response to *H. polygyrus* infection is associated with Teff and not Treg, suggesting GITR as a potential marker of an anti-parasite T-cell response.

Such GITR expression has been associated with the latter chronic phase of *H. polygyrus* infection but is not described during the early phase. It is likely that the anti-parasite immune response and parasite mediated immune suppression vary during infection. Throughout both infection phases (residence within the submucosa, followed by the lumen), *H. polygyrus* release HES. HES has been implicated in the immune-modulatory capabilities of *H. polygyrus* to allow chronic infection to persist. From the adult parasite, a total of 374 proteins were identified within these secretions (Hewitson et al., 2011b), compared to 214 within HES from the L4 larvae (Hewitson et al., 2013). Of these proteins, 135 were found in both, and 72 uniquely found in L4 larvae HES. Considering that the protein composition of HES changes, it is possible that HES mediated immune modulation also differs between the two stages of infection.

This chapter aims to explore whether *Foxp3* transcription is differentially regulated at different stages of infection. Further, this chapter aims to investigate the relationship between infection-induced Treg and infection-reactive GITR^{+}*Foxp3*$^{-}$ CD4 T-cells.

3.2 Results

3.2.1 *Foxp3* transcription dynamics change during the course of infection

The visibility of *H. polygyrus* to the immune system likely changes throughout infection according to parasite location. It is therefore logical that the immune response and regulation varies accordingly. Further, these may be affected by the proximity of the parasite and subsequent exposure to HES. To investigate corresponding T-cell regulation, *Foxp3*-Tocky mice were gavaged with 200 L3 stage *H. polygyrus* larvae. The mLN were then analysed by flow cytometry at 7-, 10-, 14- and 28-days post infection.

At 7- and 10-days post infection, the raw data (shown by representative flow cytometry plots, Figure 3.1A) suggests that *Foxp3*-Timer transcriptional dynamics are altered by infection. This is based on the visually expanded *Foxp3*-Timer-Blue^{+}Red^{+} population. However, quantification of the percentage of CD4 T-cells expressing *Foxp3*-Timer during infection (Figure 3.1B) showed no significant difference between Naïve and Infected mice. This suggests that any infection-induced *Foxp3* expression is likely occurring within individual T-cells as opposed to within the wider Treg population.

Upon data normalisation and trigonometric transformation, transcriptional dynamics of *Foxp3*-Timer within individual T-cells was identified in terms of Timer Locus (Figure 3.1C). These loci were categorised as “New”, “NPt”, “Persistent”, “PAt” and “Arrested” transcription, as described in Chapter 2.1. Accordingly, New and NPt are both considered as newly-initiated *Foxp3* transcription. Newly-initiated *Foxp3*-Timer transcription occurred at day-7 of infection (NPt increasing from 0.005 % of CD4 T-cells in Naïve mice to 0.05 % of CD4 T-cells at day-7, p=0.03). The proportion of CD4 T-cells cells with Persistent *Foxp3*-Timer transcription also increased at day-7 of infection (Persistent increasing from 0.02 % of CD4 T-

cells in Naïve mice to 0.3 % at day-7, *p*=0.03). Considering both appear to increase by a factor of 10, I suggest that newly-initiated *Foxp3*-Tocky transcription occurs within T-cells without recent *Foxp3* expression, and this *Foxp3* expression is likely sustained during early infection, becoming eTreg.

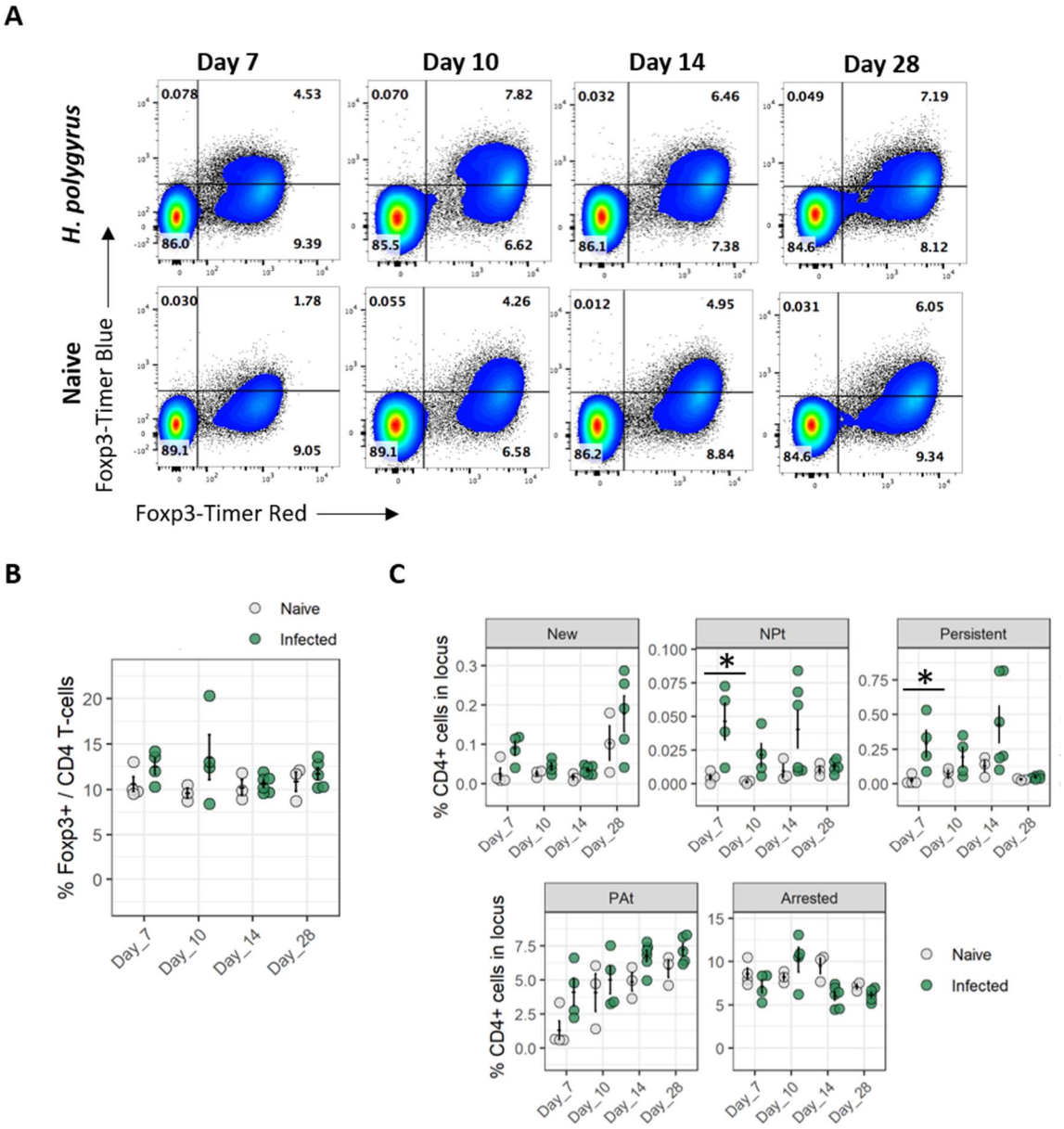


Figure 3.1: Foxp3 transcription dynamics change during the course of infection. *Foxp3*-Tocky mice were gavaged with 200 L3 *H. polygyrus* larvae (Infected) or H_2O (Naïve) and analysed at 7-, 10-, 14- or 28-days post infection. (A) Representative plots of *Foxp3*-Timer fluorescence throughout infection. (B) Total % of CD4 T-cells expressing *Foxp3*-Timer. (C) The % of CD4 T-cells in each Timer loci post normalisation and trigonometric analysis. Naive n = 3-4, infected n = 4-6. Each time point was collected as two independent experiments. A Mann Whitney U test was undertaken for statistical analysis. * denotes a p value < 0.05. Error bars show standard error of the mean.

By day-28, *Foxp3*-Timer transcriptional activity appears to have returned to the base-line level. There is little evidence of increased newly-initiated or Persistent *Foxp3* transcribing cells. I therefore identify that the *Foxp3* response likely changes according to the infection cycle of *H. polygyrus*. Indeed, at day-28 of infection, *H. polygyrus* reside within the small intestinal lumen as opposed to the submucosa seen in earlier infection.

Due to experimental constraints, block design was difficult for the time course experiment. It was therefore important to determine that between-day variations did not contribute to the differences observed between early and late infection. To address this, mice were infected either 7- or 28-days prior to analysis and were analysed on the same day (Figure 3.2A, B). Consistent with previous observations, newly-initiated and Persistent transcription was likely found at 7- but not 28-days post infection (Figure 3.2 C). This data supports that day-effect was not responsible for the differences observed during the time course.

Considering that *Foxp3* transcriptional activity is increased at day-7 of infection, expression of CD25 and CD44 (where CD44 is a marker of antigen experience) were analysed by Median Fluorescence Intensity (MFI) within the different Timer Loci as markers of T-cell activation (Figure 3.3A, B). Expression of CD25 was increased within the PAt locus compared to the New locus (p=0.01). Whilst not statistically significant, CD25 expression appears to also be increased in the NPt and Persistent loci compared to New. A larger sample size would be required to confirm or deny this trend due to large between-experiment variations. Increased CD25 expression within the PAt and potentially NPt and Persistent loci would indicate that CD25 is increased with *Foxp3* transcriptional activity. There is also some evidence that expression of CD44 may be increased in the NPt and Persistent *Foxp3*-Timer loci compared to New and Arrested loci. This would indicate that antigen experience is associated with *Foxp3*

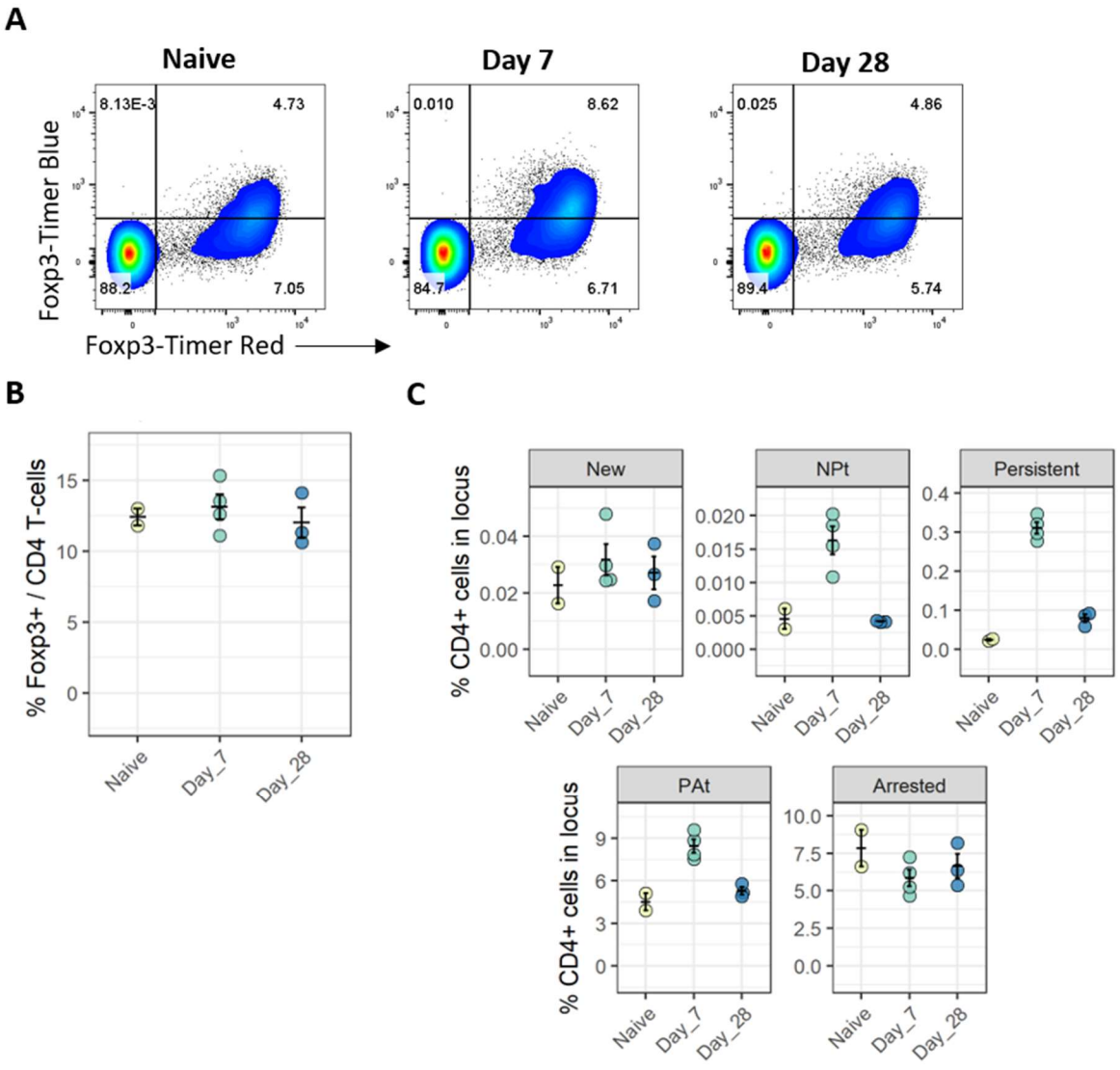


Figure 3.2: Day effect is unlikely to be responsible for the differences in Foxp3 transcriptional dynamics. *Foxp3*-Tocky mice were gavaged with 200 L3 *H. polygyrus* larvae (Infected) or H_2O (Naïve) and analysed at 7- and 28-days post infection. (A) Representative plots of *Foxp3*-Timer fluorescence throughout infection. (B) Total % of CD4 T-cells expressing *Foxp3*-Timer. (C) The % of CD4 T-cells in each Timer loci post normalisation and trigonometric analysis. Naive n = 2, Infected n = 3-4. This data constitutes one experiment. Error bars show standard error of the mean.

transcription, which would be expected. These data are not statistically significant, a larger sample size would be required considering the high variation within the data.

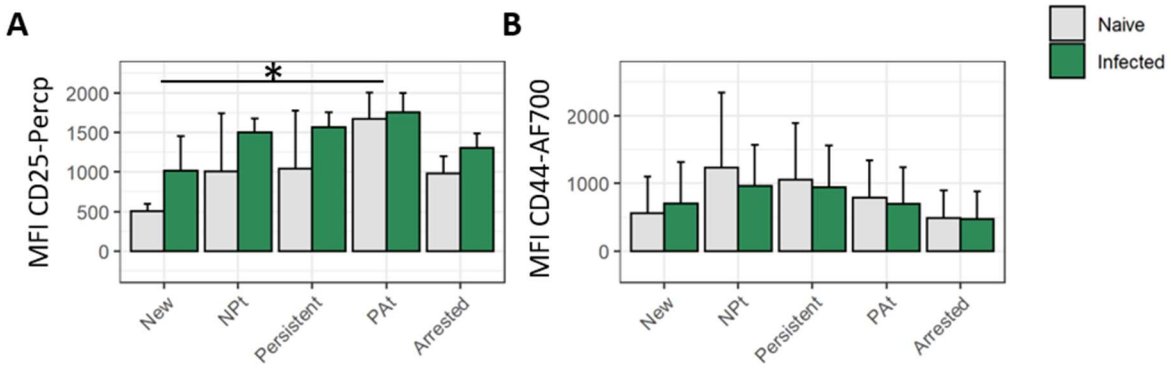


Figure 3.3: Expression of T-cell activation markers by Foxp3-Timer Locus. (A) Median Fluorescence Intensity (MFI) of CD25-Percp by *Foxp3*-Timer Locus at day-7 of infection. (B) MFI of CD44-AF700 by *Foxp3*-Timer Locus at day-7 of infection. n = 4. Data from two independent experiments. Error bars show standard deviation of the mean.

3.2.2 GITR is associated with *Foxp3* transcription and early parasite infection

Upregulated GITR expression appears to be primarily associated with Teff during *H. polygyrus* infection (Finney et al., 2007). However, GITR is highly associated with Treg, where the vast majority of Treg are GITR$^+$. Indeed, considering that the GITR$^+$Foxp3$^-$ T-cell population are considered memory-phenotype T-cells under physiological conditions and may contain ex-Treg, exploring the GITR$^+$ population may give insight into the origins of the newly-initiated *Foxp3* transcribing T-cells. It is first important to establish that GITR expression is induced within *Foxp3*-Tocky mice, which have a C57BL/6 background, whereas the referenced study was undertaken on BALB/c mice. The proportion of CD4 T-cells expressing GITR (Figure 3.4A, B) expanded at 7-days post-infection by 53 % (increasing from 12.0 % of CD4 T-cells in Naïve mice to 18.3 % at day-7 of infection, p=0.05), and by 70 % at day-10 of infection (increasing from 12.0 % of CD4 T-cells in Naïve mice to 20.4 % at day-10 of infection, p=0.05). This expansion was lost by 28-days post infection. This data indicates that some T-cells up-regulate GITR expression in response to early infection, which is not found in the latter phase in C57BL/6 mice.

OX40 is a TNFRSF member and co-stimulatory molecule associated with enhancing an ongoing T-cell response and preventing Treg suppressive activities (Croft et al., 2009). OX40, like GITR, is upregulated downstream of *Foxp3* expression in Treg and agonistic OX40 ligation *in vivo* has been reported to deplete immune-reactive Treg during inflammation (Bending et al., 2018b). Thus, increased OX40 expression would likely be associated with increased effector T-cell mechanisms. The proportion of CD4 T-cells expressing OX40 or co-expressing OX40 and GITR did not appear to largely increase over the course of infection (Figure 3.4A, C), except a potential increase may have been found at day-10 of infection with increased statistical power. Day-10 is approximately the time of parasite migration through the tissue. Interestingly, there was an increase in the proportion of CD4 T-cells that expressed GITR without OX40 at day-7 and -10 of infection. This could indicate a sub-optimal anti-parasite T-cell response during early infection.

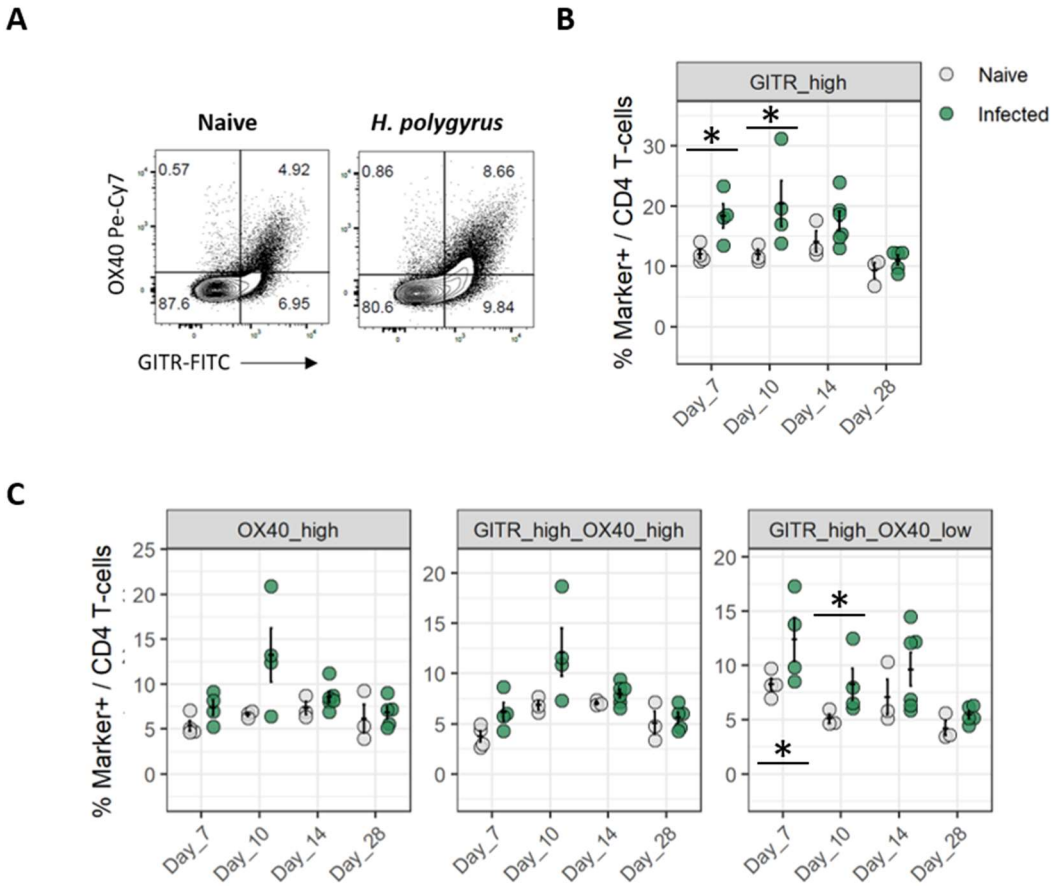


Figure 3.4: GITR expression is associated with early parasite infection. (A) Representative plot of CD4 T-cells for GITR and OX40 expression within Infected and Naïve mice. (B) The % of CD4 T-cells expressing GITR at 7-, 10-, 14- or 28-days post infection. (C) % of CD4 T-cells expressing OX40, OX40 and GITR or GITR but not OX40. Naive n = 3-4, infected n = 4-6. Each time point was collected as two independent experiments. A Mann Whitney U test was undertaken for statistical analysis. * denotes a p value < 0.05. Error bars show standard error of the mean.

Based on the findings by Finney *et al.*, I hypothesised that the increased proportion of GITR expressing CD4 T-cells found at day-7 of infection compared to Naïve mice was likely from the *Foxp3*$^{-}$ T-cell population. I further explored whether a GITR response may be observed in Treg when divided into subsets depending on their *Foxp3*-Timer fluorescence and thus *Foxp3* transcriptional state. To explore this, expression of GITR and OX40 were analysed (Figure 3.5) within T-cells with *Foxp3*-TimerBlue^{+}Red^{+} fluorescence, *Foxp3*-TimerBlue^{-}Red^{+} fluorescence or *Foxp3*-Timer^{-} T-cells (referred to here as *Foxp3*$^{-}$) (Figure 3.5A).

The data shows a potential trend for an increased proportion of *Foxp3*$^{-}$ T-cells that expressed GITR (Figure 3.5B) during early infection (day-7, potentially increasing from 4.0 % of *Foxp3*$^{-}$ T-cells in Naïve mice to 6.7 % in infected mice, p=0.3; day-10, potentially increasing from 3.2 % of *Foxp3*$^{-}$ T-cells in Naïve mice to 10.9 % in infected mice, p=0.06), and an increased proportion was found at day-14 of infection (increasing from 4.0 % of *Foxp3*$^{-}$ T-cells in Naïve mice to 6.7 % in infected mice, p=0.03). No increase in the proportion of *Foxp3*-TimerBlue^{+}Red^{+} or *Foxp3*-TimerBlue^{-}Red^{+} cells expressing GITR was observed. GITR is highly associated with Treg, and thus these cells predominantly already expressed GITR.

Upon analysis of T-cells that co-expressed GITR and OX40 (Figure 3.5C), co-expression was found to increase in *Foxp3*$^{-}$ T-cells at day-10 (increasing from 0.7 % in Naïve mice to 2.7 % in Infected mice, p=0.05). Day-10 of infection coincides roughly with the time the parasites migrate through the intestinal tissue, and thus an increase in OX40 likely correlates with an

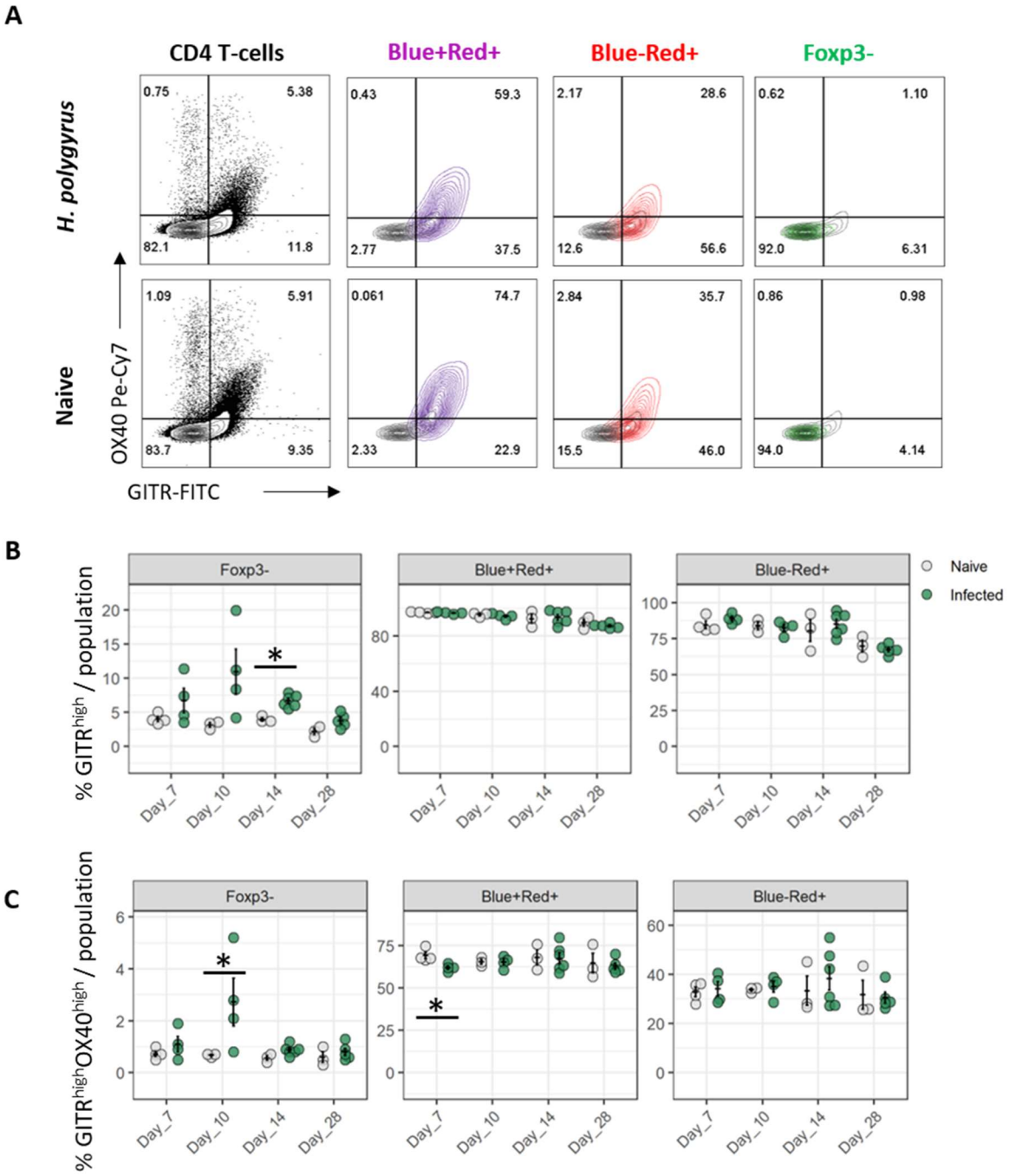


Figure 3.5: GITR expression appears to be increased in the Foxp3$^-$ T-cell population. (A) Representative plots of GITR and OX40 expression within overall CD4 T-cells, *Foxp3*-Timer Blue+Red+ (Blue+Red+) CD4 T-cells, *Foxp3*-Timer Blue-Red+ (Blue-Red+) CD4 T-cells and Foxp3$^-$ CD4 T-cells. (B) The percentage of the T-cell subsets in A expressing GITR at 7-, 10-, 14- and 28-days post infection. (C) % of each T-cell subset expressing both GITR and OX40 at 7-, 10-, 14- and 28-days post infection. Naive n = 3-4, infected n = 4-6. Each time point was collected as two independent experiments. A Mann Whitney U test was undertaken for statistical analysis. * denotes a p value < 0.05. Error bars show standard error of the mean.

increase in inflammation and thus effector T-cell mechanisms. A decreased proportion of *Foxp3*-TimerBlue^{+}Red^{+} cells co-expressing GITR and OX40 was found at day-7 of infection (decreasing from 69 % in naïve mice to 62 % in infected mice, p=0.03). This suggests that during early infection, reactive Treg may become less susceptible to inhibition.

3.2.3 The GITR^{high}CD44^{high} population is enriched with infection-reactive T-cells

During physiological conditions, the GITR^{high} T-cell population consists of Treg and memory-phenotype T-cells. However, during *H. polygyrus* infection, evidence suggests that GITR is exclusively upregulated on non-regulatory activated T-cells in response to the infection (Finney et al., 2007). Here we used CD44, a marker of antigen experience, to investigate the relationship between GITR^{high}*Foxp3*-Timer^{+} and GITR^{high}*Foxp3*-Timer^{-} T-cells during *H. polygyrus* infection.

There is some evidence that the GITR^{high}CD44^{high} and GITR^{low}CD44^{high} populations (Figure 3.6A, B) expanded during early infection, despite no statistical significance, based on the change in contour shape (Figure 3.6A). Indeed, the inconclusive statistics may be attributed to a lack of statistical power. For 80 % power, a sample size of 13 mice would be required. Confirmation of this finding would suggest that GITR^{high}CD44^{high} and GITR^{low}CD44^{high} populations include antigen-experienced T-cells that are specific to either parasite antigen or to self-antigen from tissue damage during infection.

Upon interrogation of these subsets (Figure 3.7A, B), it is apparent that *Foxp3* transcription is associated with GITR expression but not CD44 expression, based on the *Foxp3*-Timer expression within the GITR^{high}CD44^{high} and GITR^{high}CD44^{low} T-cell subsets compared to the GITR^{low}CD44^{high} and GITR^{low}CD44^{low} subsets. However, the proportion of GITR^{high} cells

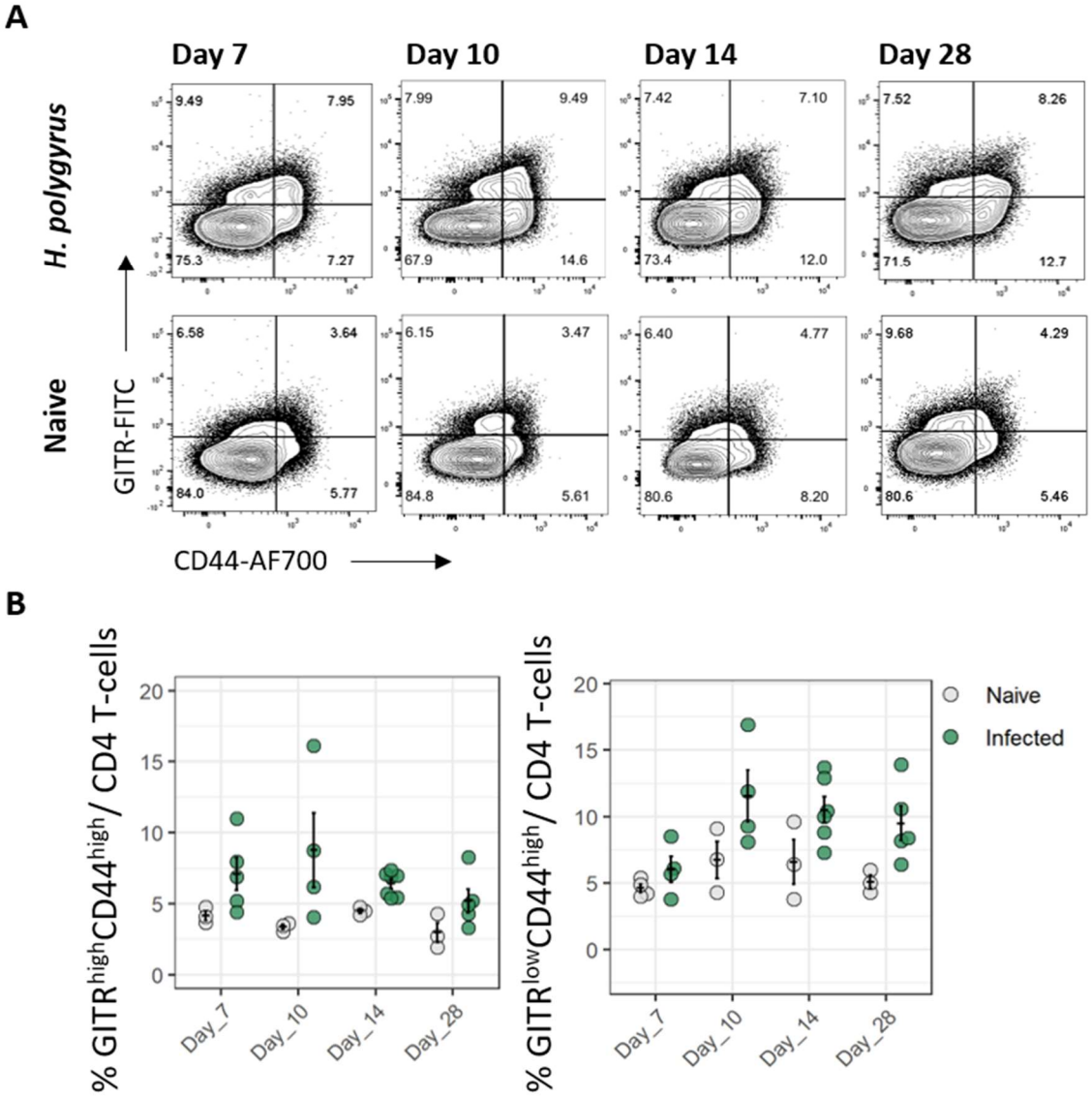


Figure 3.6 The GITR^{high}CD44^{high} T-cell population likely expands. (**A**) Representative plots of GITR and CD44 expression in CD4 T-cells at 7-, 10-, 14- and 28-days post infection. (**B**) % of CD4 T-cells GITR^{high}CD44^{high} or GITR^{low}CD44^{high}. Naive n = 3-4, infected n = 4-6. Each time point was collected as two independent experiments. A Mann Whitney U test was undertaken for statistical analysis. * denotes a p value < 0.05. Error bars show standard error of the mean.

transcribing *Foxp3* was not increased as a consequence of infection. Whilst consistent with the literature, this is surprising based on the change in *Foxp3*-Timer expression seen in Figure 3.7A. Indeed, *Foxp3*-Timer expression around the 45-degree angle in the Timer-Blue-Red space seems to increase, particularly in the GITR^{high}CD44^{high} population of infected mice.

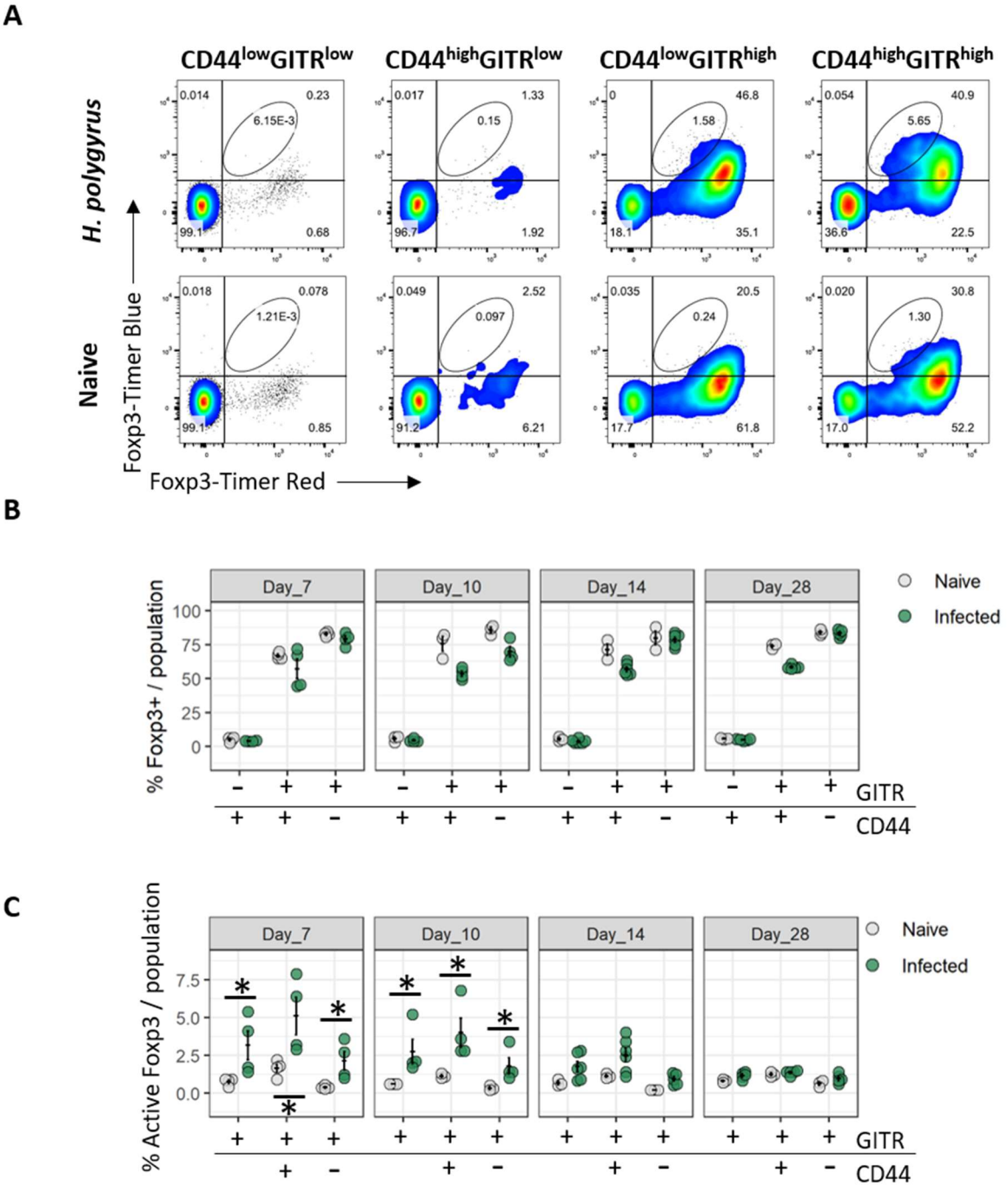


Figure 3.7: GITR^{high}CD44^{high} T-cells are enriched with Persistent Foxp3 transcribing cells. (A) Representative flow cytometry plots of *Foxp3*-Timer expression in different CD44 and GITR T-cell subsets. (B) % of the T-cell subset expressing *Foxp3*-Timer at 7-, 10-, 14- and 28-days post infection. (C) % of the T-cell subset within the oval gate in A. Naive n = 3-4, infected n = 4-6. Each time point was collected as two independent experiments. A Mann Whitney U test was undertaken for statistical analysis. * denotes a p value < 0.05. Error bars show standard error of the mean.

Persistent *Foxp3* transcription (classified here as cells within the 45-degree angle gate of Figure 3.7A) was quantified within GITR^{high} populations (Figure 3.7C). Early during infection, Persistent *Foxp3* increased in the GITR^{high} population (4.3 × and 4.7 × increase at day 7- and 10- of infection respectively, increasing from 0.75 % of GITR^{high} T-cells in Naïve mice to 3.2 % at day-7 and from 0.6 % in Naïve mice to 2.8 % at day-10, both showing p=0.03) despite total *Foxp3* expression not increasing. Analysis of the CD44^{high} and CD44^{low} subsets within the GITR^{high} population revealed that a larger proportion of GITR^{high}CD44^{high} T-cells upregulated *Foxp3* transcription during infection than GITR^{high}CD44^{low} cells at 7-days post infection (5.1 % of GITR^{high}CD44^{high} T-cells compared to 2.1 % of GITR^{high}CD44^{low} T-cells, p=0.04).

Considering this evidence of increased *Foxp3* transcription early during infection, Timer Locus analysis was applied to further analyse the dynamics of *Foxp3*-Timer transcription in the GITR^{high}CD44^{high} T-cell population (Figure 3.8). Timer Locus analysis identified that newly-initiated *Foxp3*-Timer transcription occurred at 7-days post infection (NPt: increasing from 0.07 % of GITR^{high}CD44^{high} T-cells in Naïve mice to 0.4 % in infected mice, an increase of 414 %, p=0.03) before reducing to baseline by day-28. Persistent *Foxp3*-Timer transcription appeared to be maintained in this subset throughout early infection (day-7: increasing from 0.4 % in Naïve mice to 2.0 % in infected mice, p=0.03; day-10: potentially increasing from 0.7 % in Naïve mice to 3.3 % in infected mice, p=0.06) before reducing to baseline at day 28.

The apparent response of the GITR^{high}CD44^{high} population during early infection when the parasite is within the intestinal tissue and subsequent resolution later in infection suggests that the GITR^{high}CD44^{high} population includes T-cells that are reactive to either or both parasite antigen and self-antigen released by tissue damage. Either way, these cells are likely to be reactive to inflammation seen during the early infection phase.

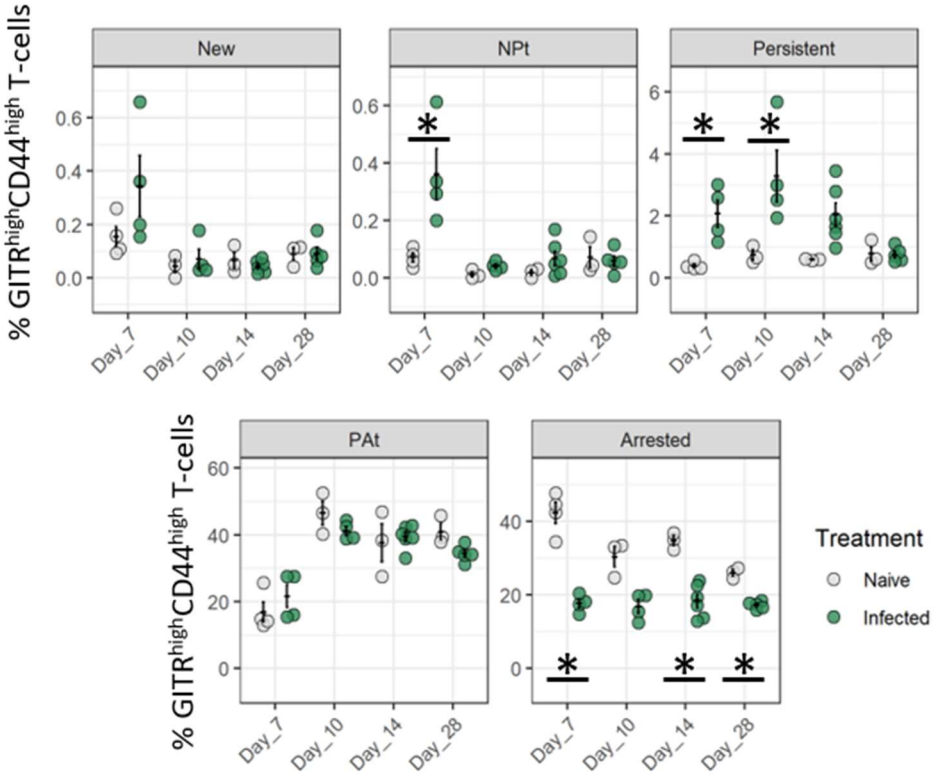


Figure 3.8: Timer Locus analysis of the GITR^{high}CD44^{high} T-cell subset. The proportion of GITR^{high}CD44^{high} T-cells expressing Foxp3-Timer within each Timer Locus was quantified across the time course of H. polygyrus infection. Naive n = 3-4, infected n = 4-6. Each time point was collected as two independent experiments. A Mann Whitney U test was undertaken for statistical analysis. * denotes a p value < 0.05. Error bars show standard error of the mean.

3.2.4 New *Foxp3* transcription appears to originate within activated T-cells

Whilst it is known that the GITR^{high} population is comprised of Treg and memory-phenotype T-cells (and in the case of infection, activated T-cells), the relationship between GITR^{high} Treg and non-regulatory GITR^{high} T-cells (here combining the memory-phenotype T-cells and activated T-cells) remains unclear. t-SNE analysis was therefore undertaken on the GITR^{high} T-cell population. t-SNE analysis is a method for visualising high dimensionality data in a single plot, where cells with similar expression of the chosen parameters cluster together, and away from cells with dissimilar expression, thus allowing determination of whether cell populations are similar or different based on the given parameters. The time point of 7-days post infection

was selected for t-SNE analysis due to the *Foxp3* transcriptional activity previously observed. Flow cytometry data from three *H. polygyrus* infected mice was combined for analysis. The t-SNE plot showed two distinct clusters of T-cells (Figure 3.9A).

Importantly, Cluster 1 comprises the non-regulatory T-cell population, based on the lack of *Foxp3*-TimerRed fluorescence (Figure 3.9B). Cluster 2 contains Treg, as identified by *Foxp3*-TimerBlue^{+}Red^{+} and *Foxp3*-TimerBlue^{-}Red^{+} fluorescence. It is of interest that *Foxp3*-TimerBlue^{+}Red^{-} cells, which have newly-initiated *Foxp3* transcription, can be found primarily within the non-regulatory cluster (Cluster 1). Considering that *Foxp3*-TimerBlue^{+}Red^{-} cells must become either *Foxp3*-TimerBlue^{+}Red^{+} or *Foxp3*-TimerBlue^{-}Red^{+}, it appears that newly-initiated *Foxp3* transcription arises within the non-regulatory population, where these cells go on to become Treg. The location of the *Foxp3*-TimerBlue^{+}Red^{-} cells appears to largely coincide with CD44 and CD25 expression, suggesting activated T-cells as a potential source of newly-initiated *Foxp3* transcribing cells. This finding was robust, as it was reproducible using multiple datasets of day-7 *H. polygyrus* infected mice (data not shown).

3.2.5 Transcriptomic features of infection-reactive Treg and activated T-cells during early infection

t-SNE analysis supports the hypothesis that infection-reactive *Foxp3* transcription is initiated in activated T-cells. To further address this hypothesis, the transcriptional signature of New *Foxp3* transcribing cells (*Foxp3*-TimerBlue^{+}Red^{-}, here referred to as “New Treg”) and Persistent Treg (*Foxp3*-TimerBlue^{high}Red^{high}) were compared to PAt/Arrested Treg (*Foxp3*-TimerBlue^{low}Red^{high}) and activated T-cells (*Foxp3*-TimerBlue^{-}Red^{-}CD25^{high}) (Figure 3.10A).

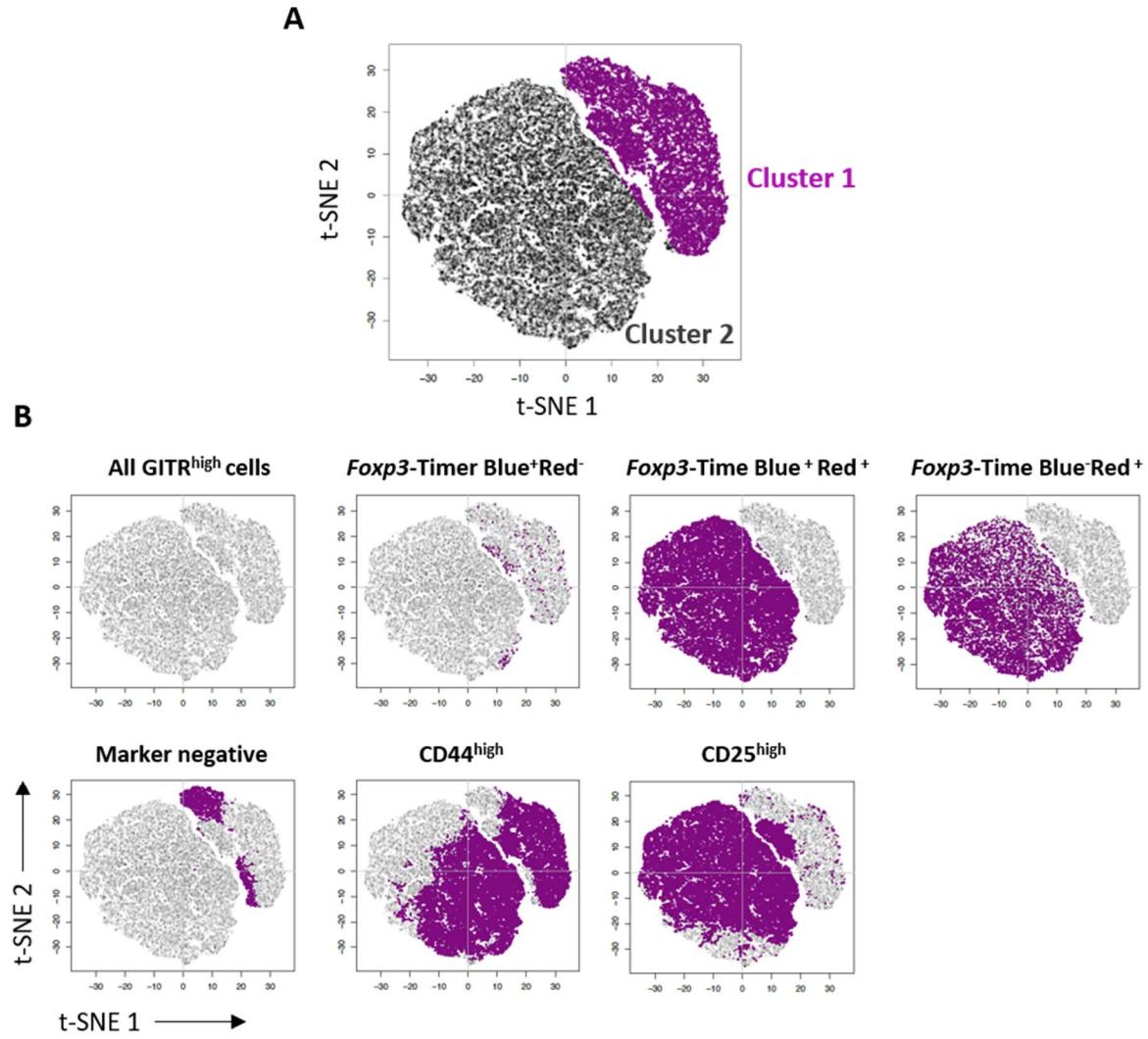
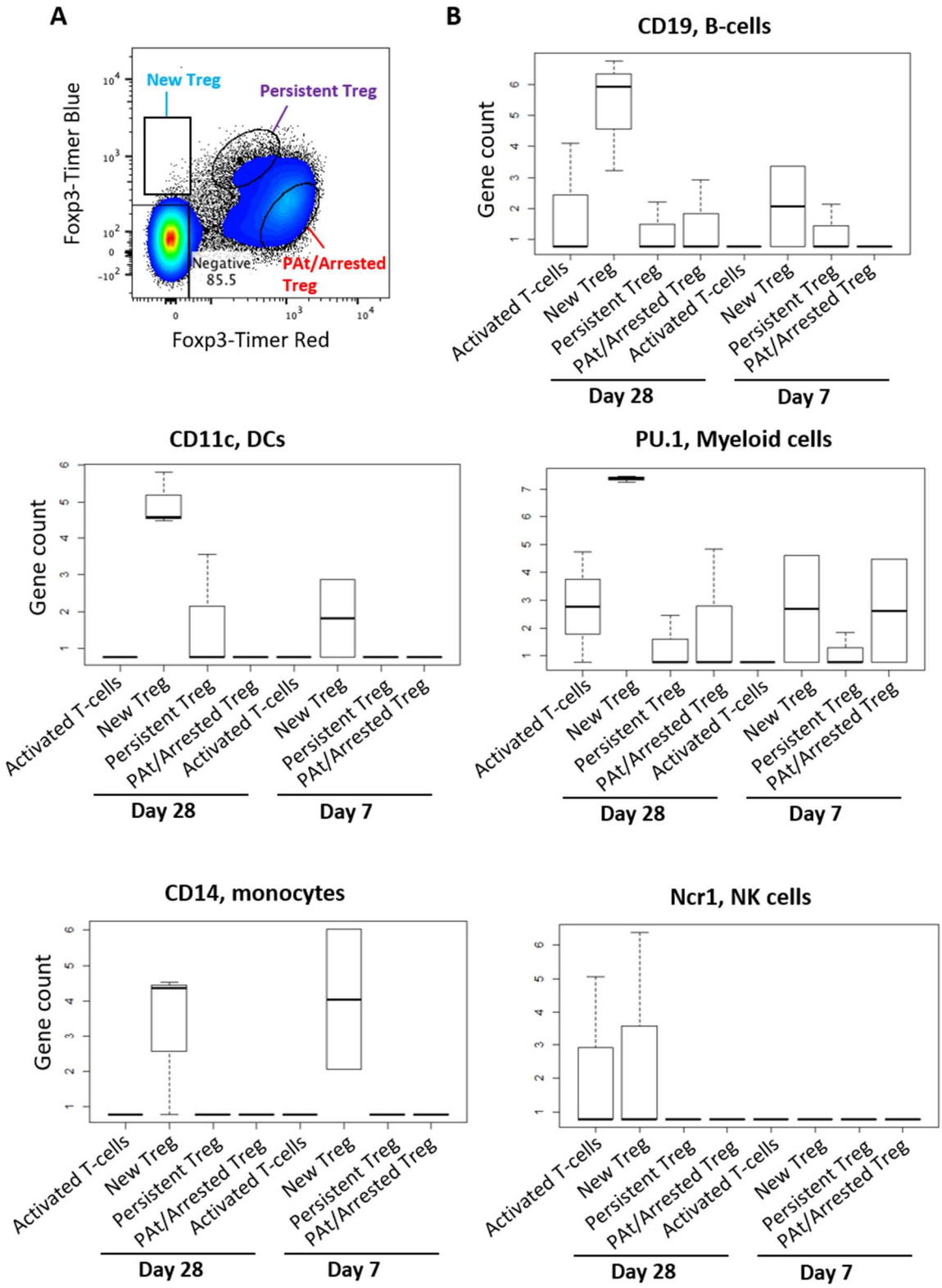


Figure 3.9: t-SNE analysis of GITR^{high} CD4 T-cells. (A) Upon t-SNE analysis, the GITR^{high} CD4 T-cell population can be split into two distinct clusters, Cluster 1 (purple) and Cluster 2 (grey). (B) Expression of each marker (purple dot indicates a cell expressing this marker) within the GITR^{high} CD4 T-cell population. Data from n=3 at 7-days post infection from one experiment.

Samples were collected at 7- and 28-days post infection for n=3 (n=2 for day-7 PAt/Arrested Treg and day-28 New Treg due to technical difficulties). Samples were sorted by FACS for the above populations. The Smart-seq2 protocol was followed to produce RNA libraries for sequencing.

A quality control check was performed on the RNA-seq data produced from the libraries. This aimed to assess the quality of the samples and to determine whether any sample contamination occurred during sample collection. Analysis by *fastQC* revealed that while the libraries were not of good quality, they were of adequate quality, however, the reads were not deep. Conclusions from this data must therefore be made with caution. The presence of key lineage-specific RNA not associated with T-cells was then assessed within each sample to look for sample contamination. The potential contaminants investigated included B-cells (*Cd19* [CD19]), DC cells (*Itgax* [CD11c]), monocytes (*Cd14* [CD14]), NK cells (*Ncr1*) and myeloid cells (*SPI1* [PU.1]) (Figure 3. 10B).

Upon plotting *Cd19* expression for each sample (Figure 3. 10C), it became clear that B-cell contamination affected some samples more than others. Samples which showed expression of *Cd19* were therefore excluded from analysis, in addition to samples expressing high levels of other lineage markers from Figure 3. 10 B. Further samples were excluded from analysis if the sample number for that group dropped below n=2. The samples excluded were all samples from day-28 (D28-), D7N1, D7N2, D7P1. The remaining samples were all from day-7 (D7-), D7P2 and D7P3 (Day-7, Persistent Treg biological replicates 2 and 3), D7Q1 and D7Q3 (Day-7 PAt/Arrested Treg biological replicates 1 and 3), D7E1, D7E2 and D7E3 (Day-7 activated T-cells, biological replicates 1-3). Expression of genes related to different cell lineages within the remaining samples were assessed, and these samples were found to show very little to no contamination. To combat the remaining (although distinctly lower) possibility of contamination, only T-cell related genes were analysed in terms of differentially expressed genes. Finally, the initial sorting of samples into the *Foxp3* subpopulations was confirmed by analysing *Foxp3* expression (Figure 3.10D). Both Persistent and PAt/Arrested Treg were found to highly express *Foxp3,* as expected. Some, albeit lower, *Foxp3* expression was identified


A
New Treg
Persistent Treg
PAt/Arrested Treg
Negative
85.5
Foxp3-Timer Blue
Foxp3-Timer Red
B
CD19, B-cells
Gene count
CD11c, DCs
PU.1, Myeloid cells
CD14, monocytes
Ncr1, NK cells
Activated T-cells
New Treg
Persistent Treg
PAt/Arrested Treg
Day 28
Day 7

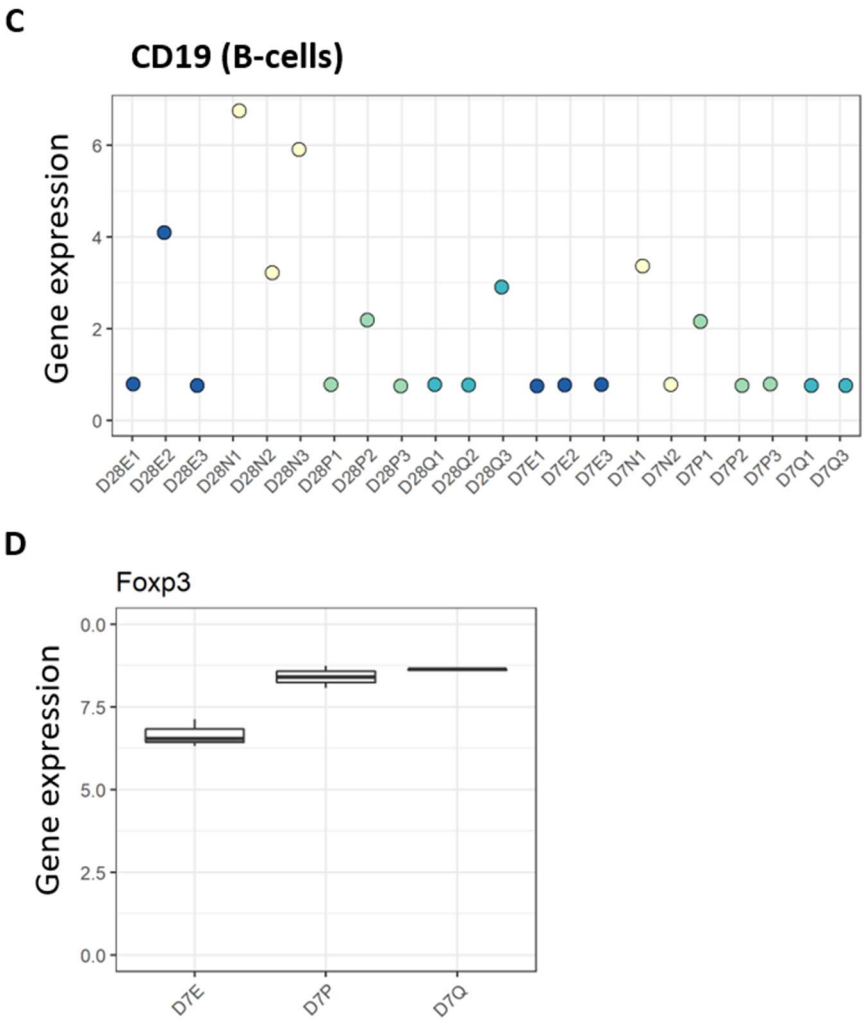


Figure 3.10: Contamination of non-T-cells within some RNA-seq samples. (A) 1000 cells were sorted by FACS as New Treg, Persistent Treg, PAt/Arrested Treg, or Activated T-cells (*Foxp3*-Timer^{-} CD25^{high}) at 7- and 28-days post *H. polygyrus* infection. (B) Normalised gene count data was plotted for each sample regarding 5 genes relating to different non-T-cell lineages. (C) CD19 expression within individual samples. New Treg (N), Persistent Treg (P), PAt/Arrested Treg (Q) and Activated T-cells (E) at day 7 (D7) or day 28 (D28) or infection. (D) Normalised gene count expression of Foxp3 within the non-excluded samples. Data from n=2-3. Error bars show standard deviation of the mean.

within the activated T-cell population. High expression was expected within the Treg populations, but not within the activated T-cell samples. Such expression suggests that these T-cells may be in the process of becoming Treg. Analysis of activated T-cell genes, particularly

those pertaining to the expected Th2 response, was required to confirm an anti-parasite T-cell nature of these cells.

Principle Component Analysis (PCA) is a linear technique of dimensionality reduction to visualise high-dimensionality data. Similar samples are expected to cluster together, whilst samples with large differences are expected to separate in the plot. Prior to PCA, T-cell related genes were selected, using the Gene Ontology T-cell gene list, accessed using the term GO:0042110. PCA was then performed using normalised gene count data of these T-cell related genes, where normalised gene count data refers to the amount of mRNA present. Interestingly, the axis with the largest variance (PC1) appears to possibly separate PAt/Arrested Treg somewhat from the other samples (Figure 3.11A), suggesting that Persistent Treg and activated T-cells may be more similar to each other than to PAt/Arrested Treg. Unfortunately, variation is high within the PAt/Arrested Treg samples across PC1, although both samples can be found to the right of the other samples. This finding must therefore be treated with caution.

A heatmap with hierarchical clustering was then produced of selected effector T-cell and Treg genes (Figure 3.11B). These genes were chosen for their role in Treg suppressive mechanisms or the anti-parasite response. Hierarchical clustering indicated that based on these genes, Persistent Treg are more similar to activated T-cells than to PAt/Arrested Treg. This supports the separation of samples along the PC1 axis seen in the PCA result. The heatmap shows that activated T-cells expressed the Th2 genes IL-4 and GATA3. These cells also highly expressed immune checkpoint molecules OX40, Icos and Lag3 to an intermediate level compared to the Treg populations.

The expression of individual effector T-cell and Treg genes was further assessed within these samples (Figure 3.11C). It appears that IL-4, a cytokine secreted by Th2 cells and highly implicated in the anti-helminth T-cell response, was highly expressed by activated T-cells and to a lower extent by Persistent Treg. Such expression within Treg was surprising. If such expression were true, this may potentially indicate an activated T-cell past. However, we are unable to rule out contamination with the ILC2 lineage due to the identification of these cells relying on the exclusion of T-cell markers.

In addition to IL-4, activated T-cells appeared to express IL-13, another effector T-cell related gene. Expression of these genes suggests an effector phenotype to the activated T-cells. It is also apparent that the activated T-cell population expressed genes traditionally associated with Treg, including *Tnfrsf18* (GITR)*, Icos* (Icos) and *Ctla4* (CTLA-4). These genes are highly expressed on Treg and only upregulated on T-cells upon activation. Whilst this gene expression could be indicative of such T-cell activation in the activated T-cell population, the level of gene expression is comparable to that of the Treg populations. These factors, combined with the *Foxp3* transcription within this population, suggest that these activated T-cells may potentially be in the process of becoming Treg. This data supports the data from the t-SNE analysis suggesting that parasite-reactive Treg originate from the activated T-cell population.

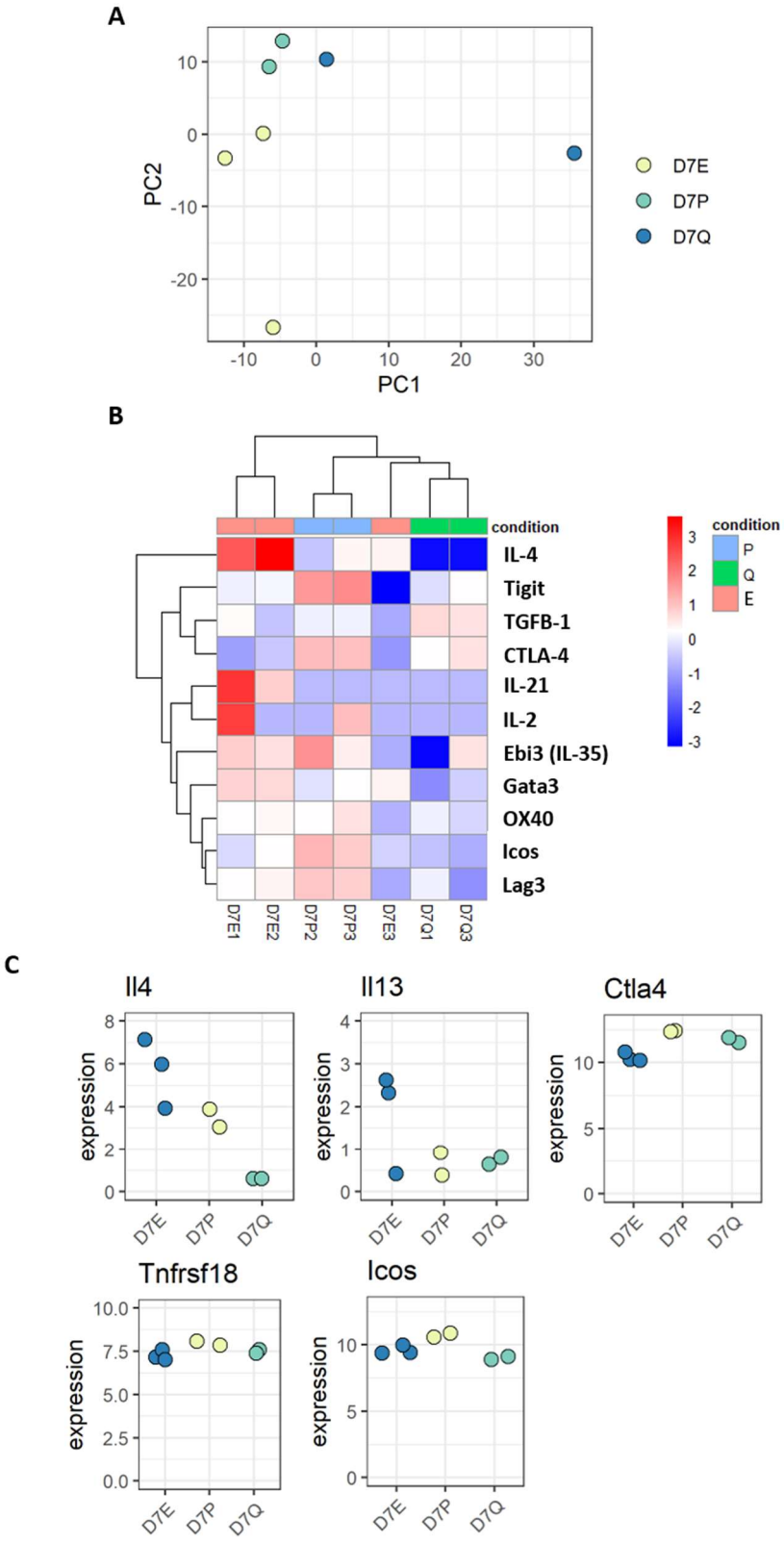


Figure 3.11: RNAseq analysis. P= Persistent Treg, Q= PAt/Arrested Treg, E= Activated T-cells. (A) PCA of the analysed samples. (B) Heat map including hierarchical clustering of selected effector T-cell and Treg genes. (C) Normalised gene count expression for selected effector T-cell and Treg genes. Data from samples not contaminated by other cell lineages. n= 2-3. Data from day 7 of infection.

3.3 Discussion

This chapter aimed to investigate whether *Foxp3* transcription is dynamically induced in non-Treg and Treg populations in response to *H. polygyrus* infection. My data suggests that during the first phase of infection, when *H. polygyrus* are located within the submucosa, *Foxp3* transcription is actively induced and maintained, before returning to baseline by day-28. I go on to show that the source of these new *Foxp3* transcribing cells is likely within the GITR^{high}CD44^{high} T-cell population. Finally, using t-SNE analysis I identify a close relationship between infection-reactive Treg and CD25^{high}*Foxp3*$^{-}$ activated T-cells, a relationship supported by transcriptomic data. Together, these results suggest that *Foxp3* transcription is likely arising in the infection-reactive activated T-cell population. Further, *Foxp3* transcription is dynamically regulated throughout *H. polygyrus* infection and is likely directly affected by the infection phase.

While my data showed little evidence for a generally expanded *Foxp3*$^{+}$ Treg population in line with that observed by Rausch *et al.* (Rausch et al., 2008), Smith *et al.* (2016) reported an increased proportion of CD4 T-cells expressing Foxp3 in BALB/c mice at day-28 of infection (Smith et al., 2016). Further, modest expansion of the Foxp3^{+}CD25^{+} population as a proportion of CD4 T-cells was reported at day-28 of *H. polygyrus* infection in BALB/c mice (Finney et al., 2007; Wilson et al., 2005). In contrast, my experiments used mice from a C57BL/6 background, and thus the lack of a Foxp3 response at day-28 can be accounted to the mouse strain (Smith et al., 2016). Using *Foxp3*-Tocky mice on a C57BL/6 background allowed the investigation of *Foxp3* dynamics on an individual cell basis. Indeed, I found an increased proportion of CD4 T-cells displayed Persistent *Foxp3* transcription (Persistent Treg)

at day-7 but not day-28 of infection. Such changes in *Foxp3* transcription, on the single cell level and not the population level, have previously been difficult to identify.

In this study, I did not assess the suppressive capacity of these Treg. However, Persistent *Foxp3* transcription is strongly linked to a more suppressive Treg phenotype *in vivo* (Bending et al., 2018b). $CD25^+$ CD4 T-cells isolated at day-28 of infection were reported to exhibit an increased suppressive capacity over those isolated from Naïve mice (Finney et al., 2007). The suppressive capacity of Treg at day-7 of infection was not reported. However, Maizels *et al.* imply that the suppressive capacity of Treg at day-28 is greater than that at day-7 of infection (Maizels et al., 2012). If increased suppressive activity were confirmed, such a finding would be surprising in the context of my data; in my hands, *Foxp3*$^+$ T-cells at day-28 show reduced *Foxp3* transcription compared to those at day-7. The suppressive activity of Treg as assessed by *in vitro* Treg suppression assays is now considered largely unreliable, and thus an *in vivo* comparison would be required. If such an *in vivo* comparison identified increased suppressive activity of Treg at day-28 of infection over day-7, it would be of interest to compare the *in vivo* suppressive capacity of *Foxp3*$^+$ Treg isolated from mice at the end of an unrelated acute infection to the suppressive capacity of *Foxp3*$^+$ Treg isolated at day-28 of *H. polygyrus* infection. This would be in order to establish whether the activated state of the Treg was responsible for any increased suppressive capacity.

Whilst a small subset of CD4 T-cells are Persistent Treg at day-7, these are far outnumbered by *Foxp3*-TimerBlue$^-$Red$^+$ Treg (Arrested Treg). Any enhanced suppressive capacity of the Persistent Treg would likely be masked by the Arrested Treg. Adoptive transfer of Persistent Treg and Arrested Treg separately *in vivo* in a model of inflammation could be

used to compare the suppressive capacity of Persistent Treg and Arrested Treg during infection. Unfortunately, the low proportion of Persistent Treg makes such studies difficult.

Evidence of newly-initiated *Foxp3* transcription suggests that *Foxp3* was induced in a new subset of T-cells for the first time. However, *Foxp3*-TimerRed protein has a half-life of approximately 122 hours (Bending et al., 2018b), and so it is possible that *Foxp3* transcription could have been re-instated within ex-Treg that terminated *Foxp3* transcription more than 122 hours before. To determine whether this was the case, a fate-mapping experiment could be undertaken.

A trend was identified whereby a potential reduction in Arrested Treg was observed during early infection (Figure 3.1 and 3.2). These cells could have undergone apoptosis, become ex-Treg, or upregulated *Foxp3* transcription to become either Persistent Treg, or Treg within the PAt *Foxp3*-Timer locus. A trend towards an increase in the proportion of Treg within the PAt locus was also observed, suggesting that cells within the *Foxp3*-Timer Arrested locus increased their frequency of *Foxp3* transcription to that of the *Foxp3*-Timer PAt locus. Such a potential finding aligns with reports that tTreg respond to *H. polygyrus* infection (Smith et al., 2016). This second mechanism does not invalidate the presence of newly-initiated *Foxp3* in a non-Treg subset.

To explore the origin of the T-cells with newly-initiated *Foxp3* transcription, we considered the GITR^{high}*Foxp3*$^{-}$ population. The GITR^{high}*Foxp3*$^{-}$ population was considered based on previous studies that identified upregulation of GITR primarily on Teff within *H. polygyrus* infection (Finney et al., 2007), thus suggesting that they are likely to be infection-reactive. Therefore, expansion of the GITR^{high} T-cell population in my early infection data

suggests a parasite related T-cell response. Expansion of the GITR^{high} T-cell population is lost by day-28 of infection, coinciding with reduced frequency of *Foxp3* transcription.

I further identified that the GITR^{high}CD44^{high} T-cell population likely expands during early infection, subject to increased statistical power. This suggests that the expanded GITR^{high} population is enriched with parasite-reactive T-cells. I find that this population appears to transcribe *Foxp3* for the first time, and these cells sustain *Foxp3* transcription, becoming eTreg. This suggests that parasite-reactive T-cells may be the source of parasite-reactive Treg.

To further explore this relationship, t-SNE analysis was performed on data from three mice at day-7 of infection. Here, t-SNE analysis considered the flow cytometry markers to plot each cell in a location dependent on its similarities and differences in marker expression (CD25-Percp, CD44-AF700, *Foxp3*-TimerBlue, *Foxp3*-TimerRed) compared with other cells. I performed t-SNE analysis on the GITR^{high} T-cell population, identifying that T-cells with New *Foxp3*-Timer transcription were close and thus similar to both the GITR^{high}CD44^{high}*Foxp3*$^{-}$ T-cell population and the GITR^{high}CD25^{high}*Foxp3*$^{-}$ T-cell population, suggesting that *Foxp3* transcription arises within activated, and likely antigen-experienced T-cells. It is important to note that t-SNE clustering is based on the parameters provided, here the flow cytometry markers, and thus may only suggest a potential relationship. Further evidence is therefore required to draw conclusions from this data.

To provide this evidence, RNA-seq analysis was undertaken. RNA-seq revealed that activated T-cells and Persistent Treg are transcriptionally similar, based on PCA analysis and hierarchical clustering. Indeed, activated T-cells appear to transcribe *Foxp3* mRNA not reported by *Foxp3*-Timer. This may suggest that these cells, or some of these cells, are in the process of converting to Treg. Alternatively, some of the cells could be pre-existing Treg but

with *Foxp3*-Timer expression below the level of detection of the flow cytometer. To explore these scenarios, it would be of great interest to perform single cell RNA-seq, followed by RNA velocity analysis. RNA velocity analysis uses the splice state of mRNA to "predict the future state of individual cells" (La Manno et al., 2018).

The RNA-seq data does need to be treated with caution, due to the recognised discrepancy between mRNA and subsequent protein levels (Liu et al., 2016), and the cell lineage contamination within some samples. However, samples showing contamination were excluded from analysis and only genes primarily associated with T-cells were assessed, further focussing our observations around *Foxp3*. The presence of two biological replicates for reactive and non-reactive Treg made statistical analysis redundant and so I may only observe trends within this data. However, the RNA-seq data combined with the t-SNE analysis and newly-initiated *Foxp3* transcription within the $GITR^{high}CD44^{high}$ T-cell population all indicate that *Foxp3* transcription is initiated within activated T-cells. I am therefore justified in suggesting that activated T-cells are likely one source of Treg during *H. polygyrus* infection.

In conclusion, my data suggests that the frequency of *Foxp3* transcription may be increased within Arrested Treg upon *H. polygyrus* infection, where these Treg are likely to be tTreg. Further, I identify that *Foxp3* transcription is also initiated and sustained within the $GITR^{high}CD44^{high}$ T-cell population enriched with infection-reactive T-cells. Therefore, it appears that during *H. polygyrus* infection, *Foxp3* transcription is induced in both pTreg and tTreg. I hypothesise that induction of helminth-reactive pTreg may be a mechanism employed by the helminth to prevent or reduce their own anti-helminth T-cell activity.

4 Chapter Four: A comparison of primary and secondary *Heligmosomoides polygyrus* infection

4.1 Background

Primary (1^o) infection with *H. polygyrus* larvae largely results in chronic infection, whereas re-infection, also known as secondary (2^o) infection, typically results in rapid parasite clearance and chronic infection is not established. Such resistance to re-infection appears more effective when the 1^o infection was drug cured (Behnke and Wakelin, 1977; Finkelman et al., 1997) or when HES was administered with alum adjuvant (Hewitson et al., 2011a). This suggests that an appropriate memory response was able to be formed, aiding parasite clearance upon re-infection. It has been observed that upon parasite clearance in 1^o infection, $CD4^+IL\text{-}4^+$ T-cells survive to become memory T-cells (Mohrs et al., 2005). Indeed, upon 2^o infection, a CD4 and IL-4 dependent Tmem response is recognised to reduce parasite maturation and egg production (Finkelman et al., 1997).

IL-4 is a Th2 related cytokine that can function to promote the differentiation of naïve T-cells into Th2, repressing Th1 differentiation. Such immune polarisation is typically necessary in an anti-parasite response. In addition, IL-4 is associated with the stimulation of B-cells (Howard et al., 1982; Vitetta et al., 1985) and class-switching to IgG1 and IgE antibodies (Mohrs et al., 2001) traditionally associated with an anti-parasite response. Subsequently, IL-4 has been identified as an essential component required for *H. polygyrus* clearance in both 1^o and 2^o infection (Reynolds et al., 2012; Urban et al., 1995). It is important to note that CD4 T-cells constitute the primary source of IL-4 during *H. polygyrus* infection (Gause et al., 1996;

Svetic et al., 1993). King *et al.* identified that IL-4 producing Th2 cells are found almost exclusively within the B-cell compartment of mLN during *H. polygyrus* infection, and are classified as Tfh (King and Mohrs, 2009).

B-cells are necessary for *H. polygyrus* clearance in 2^{o} infection, but involved to a lesser extent in 1^{o} clearance (McCoy et al., 2008; Wojciechowski et al., 2009). An initial polyclonal antibody response is identified in 1^{o} infection, which limits egg production but does not appear to promote parasite clearance. Parasite-specific antibodies are generated later, aiding resistance to 2^{o} infection. The importance of parasite-specific antibodies in 2^{o} infection resistance is demonstrated by the inability to clear 2^{o} infection in $J_H^{-/-}$ mice lacking the Immunoglobulin heavy chain (IgH), and thus unable to undergo antibody class switching (McCoy et al., 2008). The same is apparent within μMT mice (Wojciechowski et al., 2009) which lack the IgM heavy chain and thus are deficient for mature B-cells. This study demonstrates an additional antibody-independent role of B-cells. Here, the authors show that cytokine-producing effector B-cells promote the proliferation and differentiation of anti-parasite effector Th2 and memory Th2 cells (Wojciechowski et al., 2009).

Whilst B-cell and T-cell zones are both found within lymph nodes, Tfh cells explicitly localise to the B-cell germinal centre and aid the B-cell response to infection. Bcl6 is classified as the lineage-defining transcription factor of Tfh, and its identification was instrumental in the classification of Tfh as a distinct lineage. Differentiation from naïve T-cells is dependent upon IL-6 and ICOSL signalling (Crotty, 2014; Vinuesa et al., 2016).

Unsurprisingly considering the key role of B-cells, Tfh are central for the anti-parasite response in *H. polygyrus* 2^{o} infection. Whilst not all Tfh cells exhibit a Th2 phenotype, those secreting IL-4 were determined to be required for B-cell activity during infection. King *et al.*

go on to suggest that such IL-4 expressing cells may not be terminally differentiated as Tfh (King and Mohrs, 2009). This is in conflict with the theory that Tfh are a unique lineage of T-cell, differentiating from naïve cells independently of a Th1, Th2 or Th17 background (Nurieva et al., 2008). The authors proceed to note that other studies (Bauquet et al., 2009) and (Vogelzang et al., 2008) find Tfh cells with an effector T-cell phenotype, thus supporting their conclusion. The findings of King *et al.* were supported by those of Zaretsky *et al.*. Here the authors identified that Tfh cells during *S. mansoni* infection display both Tfh markers and markers of a Th2 phenotype, including IL-4 and GATA3 (Glatman Zaretsky et al., 2009). The authors here suggest that Tfh may be a stage of differentiation as opposed to a distinct cell lineage.

The idea of T-cell differentiation states, as opposed to rigid distinct cell lineages, has gained traction. For instance, Waysbort *et al.* demonstrate that high CD25 expression is a stage of T-cell activation. They identify that upon TCR signalling, a low level of CD25 is expressed, whilst IL-2 expression is highly upregulated. IL-2 is secreted, aiding in T-cell proliferation. As IL-2 levels drop, proliferation is reduced and CD25 becomes upregulated (Waysbort et al., 2013). High CD25 expression has traditionally been associated with Treg, indeed CD25 was previously used as the main Treg identifier before the identification of Foxp3. Ono *et al.* later theorised that rather than a distinct lineage of T-cell, Treg are instead a stage of T-cell activation (Ono et al., 2006).

Ono *et al.* go on to propose the feedback control model. They hypothesise that upon antigen recognition and T-cell activation, naïve T-cells become $CD4^{+}CD25^{+}$ T-cells. After a delay, these cells either up-regulate Foxp3 expression, becoming Treg; persist without Foxp3 expression as Tmem; or undergo apoptosis in the resolution of inflammation. The surviving

Tmem and Treg compete for binding to APCs loaded with the cognate antigen, protecting against activation of naïve T-cells with a lower affinity TCR for the antigen. In this way, upon administration of novel antigen, Foxp3 acts as a delayed negative regulator and promotes resolution of infection. Upon subsequent administration of the same antigen, both Tmem and Treg are able to immediately respond, allowing for a much quicker and shorter T-cell response (Ono and Tanaka, 2015).

As such, both pTreg and Tmem are thought to differentiate from effector T-cells after infection resolution, and therefore have the same TCR as the effector T-cell. Stimulation of this TCR with antigen upon re-infection does not require co-stimulation for T-cell activation, thus allowing a more rapid response. CD44 is a marker of antigen experience, and thus under physiological conditions, CD44 expressing cells are considered memory-phenotype T-cells. However, CD44 is also upregulated on Teff during infection, and therefore CD44 expressing cells during inflammatory conditions may be Teff, memory-like T-cells or Tmem, where Tmem and Teff are infection-reactive. Considering the $CD44^{high}$ population may contain all of these subsets, here we call the $CD44^{high}$*Foxp3*-$Timer^{-}$ subset discussed in Chapter 3 “non-regulatory T-cells” as opposed to explicitly Tmem or Teff.

Considering *H. polygyrus* are initially able to establish chronic infection, but subsequent infections are rapidly cleared, *H. polygyrus* infection provides a useful model to explore non-regulatory T-cell and Treg dynamics within the periphery. This chapter aims to dissect the relationship between Treg and non-regulatory T-cells in such an inflammatory environment.

4.2 Results

4.2.1 *Foxp3* is actively transcribed in T-cells upon secondary infection.

The *Foxp3* response to *H. polygyrus* infection was assessed within 1^{o} and 2^{o} infected *Foxp3*-Tocky mice to compare the primary response and the non-regulatory T-cell responses. For this, mice were infected with 200 L3 stage *H. polygyrus* and treated at day-14 of infection with the anthelmintic drug Ivermectin in drinking water for 5 days. Three weeks later, mice were challenged with 200 L3 stage *H. polygyrus* and analysed at day-7 post-challenge (2^{o} infection). Alternatively, mice were untreated until challenge date and received 200 L3 stage *H. polygyrus* (1^{o} infection) or water (Naïve) at the same time as 2^{o} infected mice were challenged (Figure 4.1).

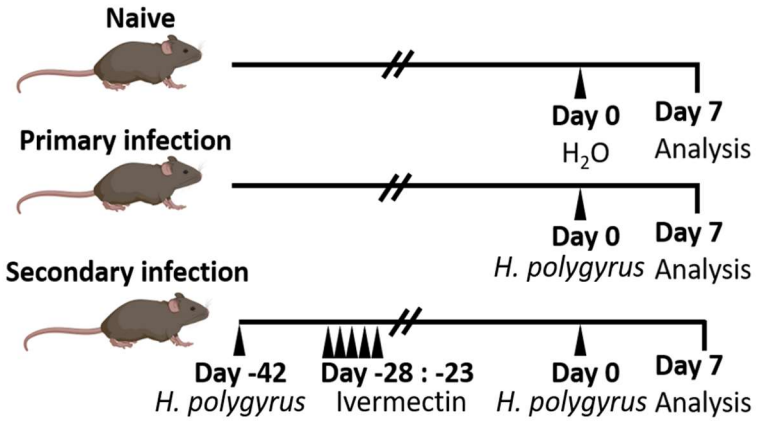


Figure 4.1: Infection schematic. Naïve mice received H_2O by oral gavage 7-days before analysis. Primary infected mice received 200 L3 stage *H. polygyrus* larvae 7-days before analysis. Secondary infected mice were gavaged with 200 L3 stage *H. polygyrus* larvae and drug cured with Ivermectin in drinking water 14 days later for 5 days. 23 days later, mice were re-infected for secondary infection with 200 L3 stage *H. polygyrus* larvae.

Expression of *Foxp3*-Timer was assessed within CD4 T-cells (Figure 4.2A, B). No significant change in the proportion of CD4 T-cells expressing *Foxp3*-Timer was observed in either 1^o or 2^o infection. However, upon analysis of *Foxp3*-Timer Locus (Figure 4.2C), *Foxp3*-Timer showed that the proportion of CD4 T-cells newly-initiating *Foxp3*-Timer transcription increased by 6.5-fold in 1^o infection (NPt increased from 0.002 % in Naïve mice to 0.013 % in 1^o infection, p=0.05) and 4-fold in 2^o infection to 0.008 % (p=0.05). The proportion of cells identified with Persistent *Foxp3*-Timer transcription also increased in both 1^o and 2^o infection, from 0.026 % in Naïve mice to 0.25 % in 1^o infection (p=0.03) and 0.26 % in 2^o infection (p=0.05), a 10-fold increase. This data suggests that *Foxp3*-Timer transcription was actively occurring in 2^o infection in addition to 1^o infection, indeed there was no statistical difference found in Persistent Treg between 1^o and 2^o infection (p=0.45). An increase in PAt cells was also observed within 2^o infection, from 4.6 % in Naïve mice to 6.5 % in 1^o infection (p=0.06) and 7.5 % in 2^o infection (p=0.003), appearing to correlate with a decrease in Arrested Treg, from 8.1 % in Naïve mice to 6.0 % in 1^o infection (p=0.07), and 5.6 % in 2^o infection (p=0.05). This data suggests that CD4 T-cells expressed *Foxp3*-Timer and therefore *Foxp3* for the first time at an increased rate due to both 1^o and 2^o *H. polygyrus* infection, which is maintained in Persistent transcription. There is evidence that Arrested cells may also be upregulating *Foxp3*-Timer, particularly in 2^o infection.

4.2.2 The T-cell subset enriched with parasite-reactive non-regulatory T-cells and Treg expands during secondary infection

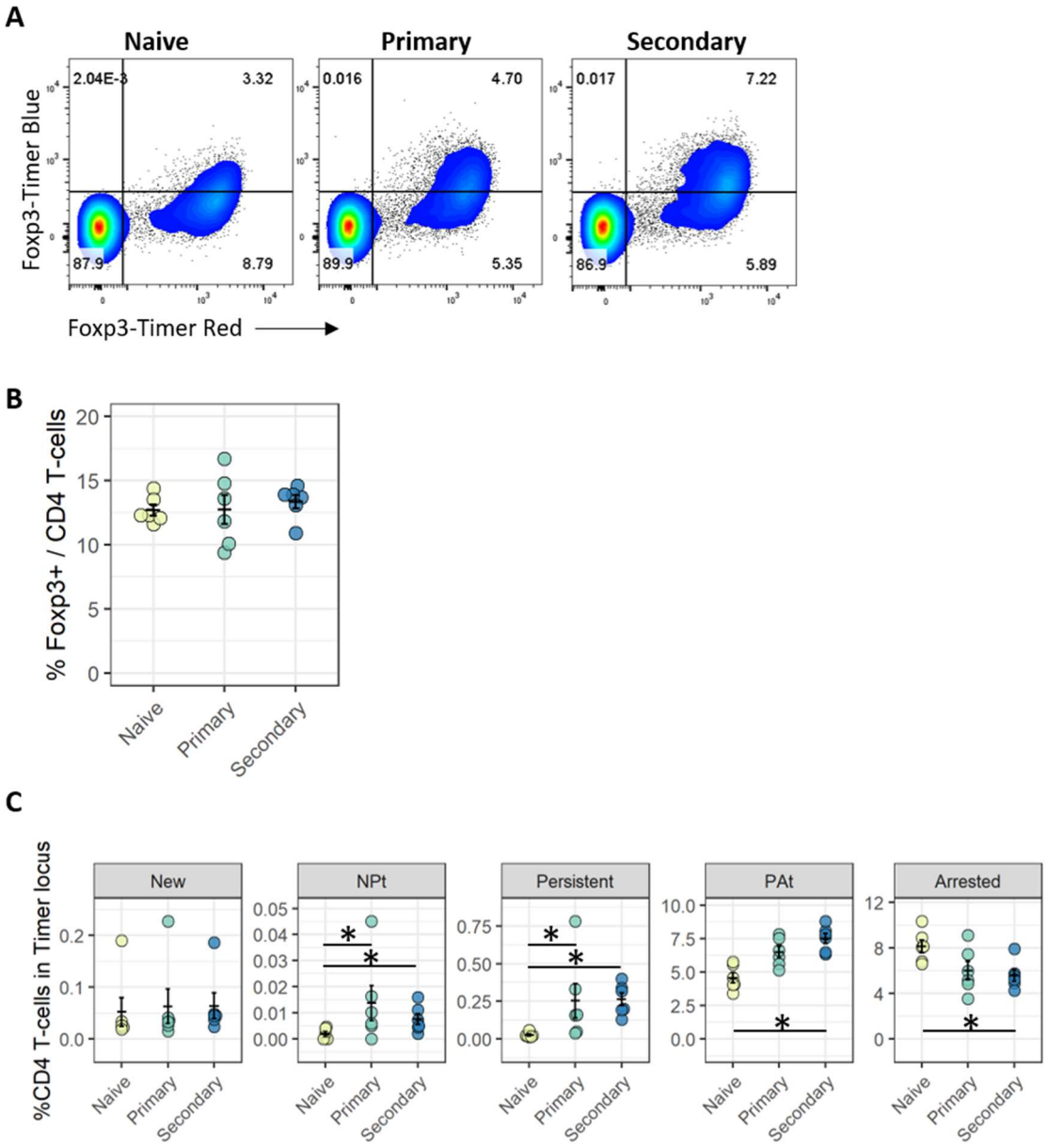


Figure 4.2: Foxp3 transcription is activated and sustained in CD4 T-cells and Foxp3-Timer$^+$ pre-existing Treg in secondary infection. For secondary infection, *Foxp3*-Timer mice were gavaged with 200 L3 *H. polygyrus* larvae. At day-14 of infection, infected mice were treated with 1 µg/ml Ivermectin in drinking water for five days. At 42 days post-infection, mice were challenged with 200 L3 *H. polygyrus* larvae. For primary infection, *Foxp3*-Timer mice were gavaged with 200 L3 *H. polygyrus* larvae on the same day as secondary mice were challenged. Naïve mice received water by oral gavage. Seven days later, mice were euthanised and analysed. (A) Representative plots of *Foxp3*-Timer fluorescence in Naive, primary and secondary infected mice. (B) Percentage of CD4 T-cells expressing *Foxp3*-Timer. (C) Timer Locus analysis showing percentage of CD4 T-cells expressing *Foxp3*-Timer in each locus. Data from two independent experiments. n=6. Data was tested for a normal distribution using a Shapiro test. (B) displayed a normal distribution, resulting in a One way ANOVA. (C) did not have a normal distribution, resulting in a Kruskal-Wallis test followed by a Dunn Test for multiple comparisons if Kruskal Wallis test was significant. * signifies p≤ 0.05. Error bars show standard error of the mean.

In Chapter 3, I demonstrated that the GITR^{high}CD44^{high} population likely contains parasite-reactive T-cells and is particularly enriched with *Foxp3*-Timer transcribing cells. *Foxp3*-Timer^{+} cells within this population are likely arising from GITR^{high}CD44^{high}*Foxp3*-Timer^{-} activated T-cells during 1^{o} *H. polygyrus* infection. Here, the proportion of CD4 T-cells expressing GITR and CD44 (Figure 4.3A), and thus believed to be enriched with parasite-reactive T-cells, was enumerated (Figure 4.3B). GITR^{high}CD44^{high} T-cells were significantly increased in 2^{o} infection (14.9 % in 2^{o} infection, p=0.0009, an increase of 2-fold from the 7.6 % found in Naïve mice), whilst an increase of ~20 % was found in 1^{o} infection, although not statistically significant (9.4 % in 1^{o} infection, p=0.08). This 1^{o} infection data reflects that seen in the previous chapter. Indeed, when this data is combined with the day-7 data from Chapter 3.2.3, there is a statistically significant increase from 6.4 % to 8.4 %, (p=0.05) in GITR^{high}CD44^{high} T-cells (Naïve n=9, day-7 primary infection n=11). The marked increase in GITR^{high}CD44^{high} T-cells within 2^{o} infection supports that a memory T-cell response is occurring in this fraction.

Expression of *Foxp3*-Timer was then assessed specifically within GITR^{high}CD44^{high} T-cells (Figure 4.4). Objectively, expression of *Foxp3*-Timer Blue and Red fluorescence indicates that *Foxp3*-Timer may be more dynamically expressed in 2^{o} infection than in 1^{o} infected or Naïve mice (Figure 4.4A). However, the total proportion of GITR^{high}CD44^{high} T-cells transcribing *Foxp3*-Timer (Figure 4.4B) was significantly decreased in 2^{o} infection, from 81.2 % in Naïve mice to 52.1 % in 2^{o} infection, p*2=0.004; where the p value was multiplied by 2 to account for the GITR^{high}CD44^{high} population being split into two groups. Accordingly, the percentage of GITR^{high}CD44^{high}*Foxp3*-Timer^{-} T-cells (Figure 4.4C) correspondingly increased (from 18.9 % in Naïve mice to 47.9 % in 2^{o} infection, p*2=0.004). These results suggest that GITR^{high}CD44^{high}*Foxp3*-Timer^{-} T-cells disproportionately expand in response to infection.

Indeed, quantifying the percentage of GITR^{high}CD44^{high}*Foxp3*-Timer^{+} cells (Figure 4.4D) as a proportion of CD4 T-cells indicates that this population has expanded in 2^{o} infection compared to Naïve mice (an increase from 6.1 % in Naïve mice to 7.7 % in 2^{o} infection, p=0.03). This data suggests that within 2^{o} infection, both GITR^{high}CD44^{high} non-regulatory T-cells and Treg have proliferated in response to infection.

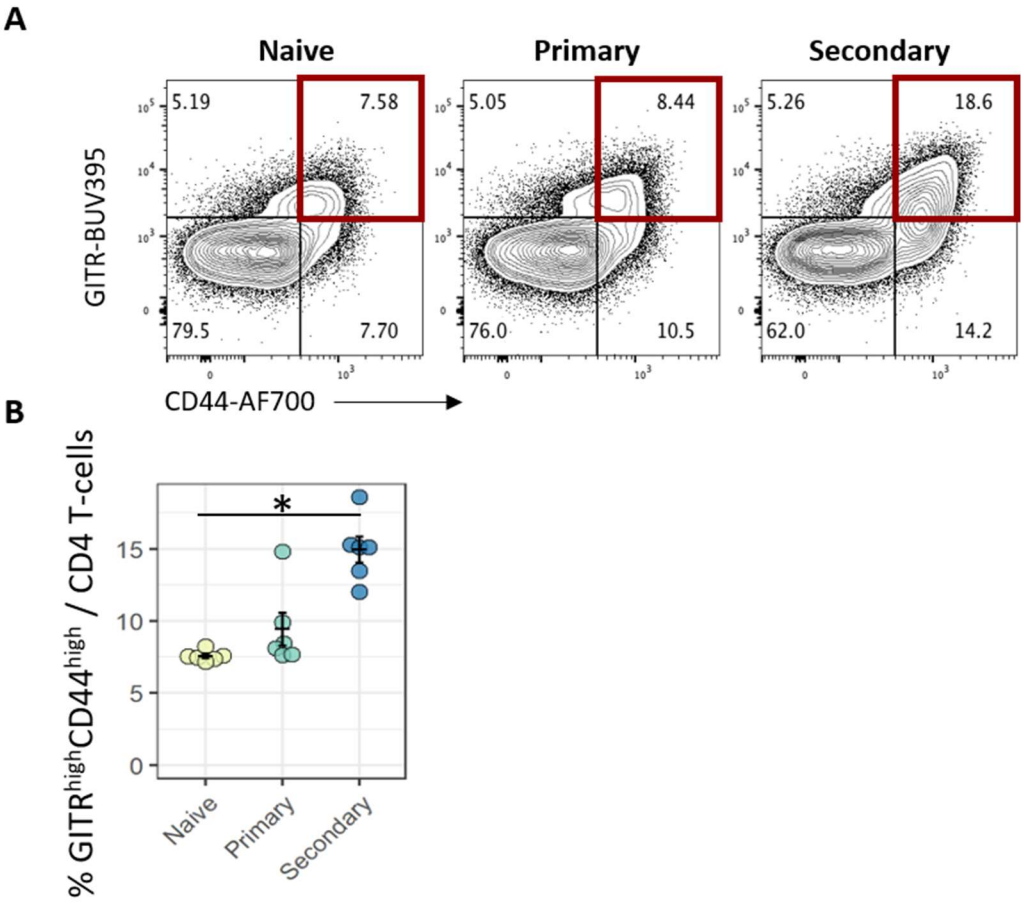


Figure 4.3: The GITR^{high}CD44^{high} population expands in 2^{o} infection. (A) Representative plots of GITR-BUV395 and CD44-AF700 expression in CD4 T-cells of primary and secondary *H. polygyrus* infected mice, alongside Naïve. (B) Percentage of CD4 T-cells GITR^{high}CD44^{high}. For statistics, a Kruskal Wallis test was performed followed by a Dunn test for multiple comparisons, * signifies p≤ 0.05. Error bars show standard error of the mean.

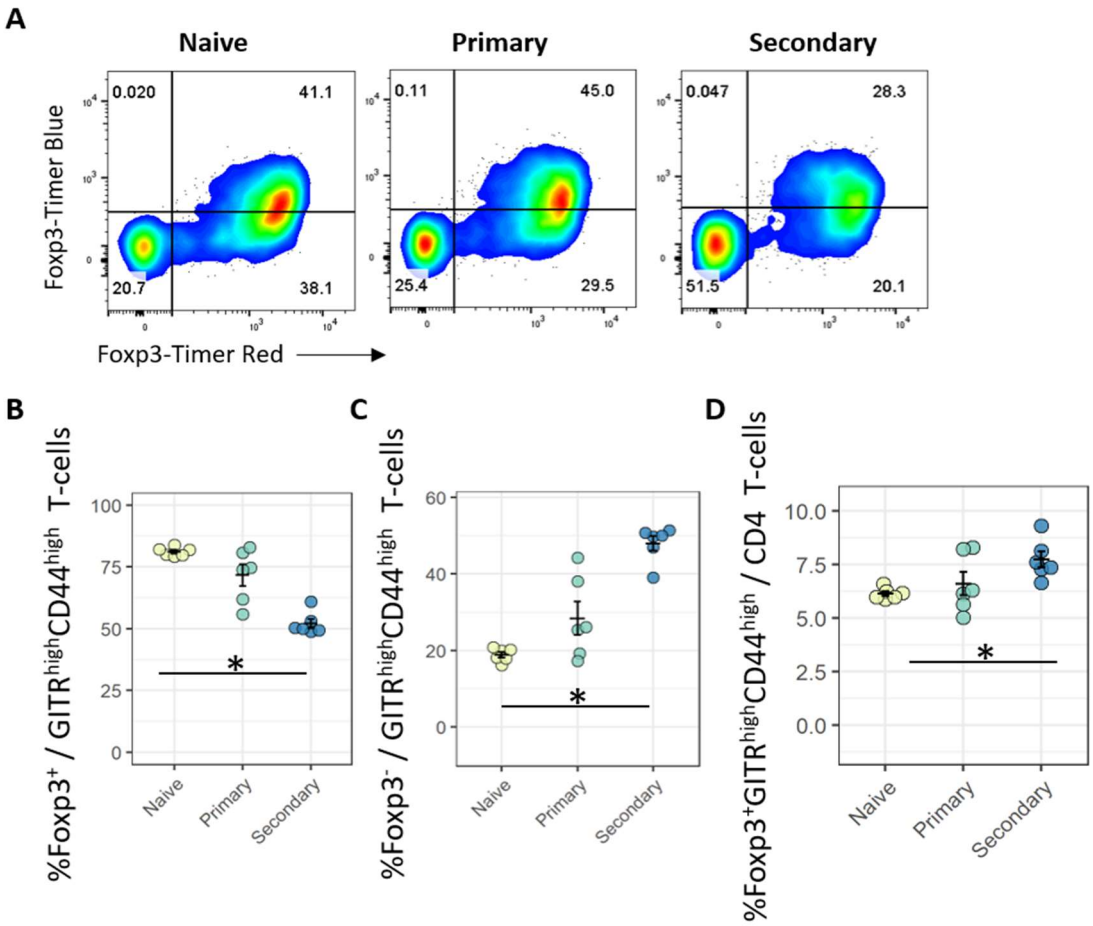


Figure 4.4: The proportion of infection-reactive Foxp3-Timer$^-$ T-cells expands disproportionately compared to infection-reactive Foxp3-Timer$^+$ T-cells in 2^o infection. (A) Representative flow cytometry plots of *Foxp3*-Timer expression in GITR^{high}CD44^{high} T-cells. (B) Proportion of GITR^{high}CD44^{high} T-cells expressing *Foxp3*-Timer. (C) Proportion of GITR^{high}CD44^{high} T-cells *Foxp3*-Timer$^-$. (D) The proportion of GITR^{high}CD44^{high} T-cells expressing *Foxp3*-Timer as a proportion of CD4 T-cells. Data in (B) and (C) were not normally distributed by Shapiro test, so a Kruskal Wallis test was performed followed by a Dunn Test of multiple comparisons. The p value was multiplied by 2 due to the GITR^{high}CD44^{high} T-cell population being split into two groups for (B) and (C). In (D), data was normally distributed, and a one-way ANOVA was performed, followed by a Tukey's honestly significant difference post-hoc test. * signifies p≤ 0.05. Error bars show standard error of the mean.

4.2.3 *Foxp3*-Timer transcription is active in the GITR^{high}CD44^{high} T-cell population in secondary infection

Foxp3-Timer expression was analysed within GITR^{high}CD44^{high} T-cells to assess whether active *Foxp3* expression occurs as a result of 2^o infection within the T-cell subset enriched with

infection-reactive T-cells. Of those expressing *Foxp3*-Timer (Figure 4.5A), a much larger proportion of GITR^{high}CD44^{high} T-cells in 1^{o} and 2^{o} infection appeared to have a *Foxp3*-Timer angle value below 90 than in Naïve mice. This indicates that a higher proportion of GITR^{high}CD44^{high}*Foxp3*-Timer^{+} T-cells exhibited active *Foxp3* transcription during both 1^{o} and 2^{o} *H. polygyrus* infection than in Naïve mice. This was investigated by analysis of the mean *Foxp3*-Timer Angle value (Figure 4.5B). The mean *Foxp3*-Timer Angle value decreased significantly from 86.4 in Naïve mice to 82.8 in 1^{o} infection (p= 0.006), and to 81.8 in 2^{o} infection (p=0.0008).

The transcription dynamics of *Foxp3*-Timer were further investigated using Timer Locus analysis (Figure 4.5C). Here, again only GITR^{high}CD44^{high}*Foxp3*-Timer^{+} cells were analysed due to the disproportionate expansion of GITR^{high}CD44^{high} *Foxp3*-Timer^{-} cells. A higher proportion of GITR^{high}CD44^{high}*Foxp3*-Timer^{+} cells have newly-initiated *Foxp3*-Timer transcription in both 1^{o} and 2^{o} infection compared to Naïve mice (NPt increasing from 0.01 % to 0.17 % in 1^{o} infection, p=0.02; and to 0.08 % in 2^{o} infection, p=0.04). These cells appeared to maintain expression of *Foxp3*-Timer (Persistent increasing from 0.45 % in Naïve mice to 3.6 % in 1^{o} infection, p=0.02; and 3.7 % in 2^{o} infection, p=0.009; an increase of 8-fold). Further, the proportion of cells exhibiting PAt transcription increased in 2^{o} infection (PAt increasing from 46.8 % in Naïve mice to 65.0 % in 2^{o} infection, p=0.002; and potentially increased to 59.4 % in 1^{o} infection, p=0.06). The proportion of Arrested Treg decreased from 43.1 % in Naïve mice to 26.8 % in 1^{o} infection (p=0.02) and to 16.5 % in 2^{o} infection (p=0.002). Considering that only cells expressing *Foxp3*-Timer were analysed, a decrease in Arrested Treg demonstrates that more active *Foxp3*-Timer transcription occurred in both 1^{o} and 2^{o} infection within this T-cell subset. Such active *Foxp3*-Timer transcription in 2^{o} infection was unexpected considering the reduced susceptibility to *H. polygyrus* infection and clear inflammatory

environment. The presence of newly-initiated *Foxp3*-Timer transcription suggests that infection-reactive Treg are developing in addition to the Treg that arose within 1° infection.

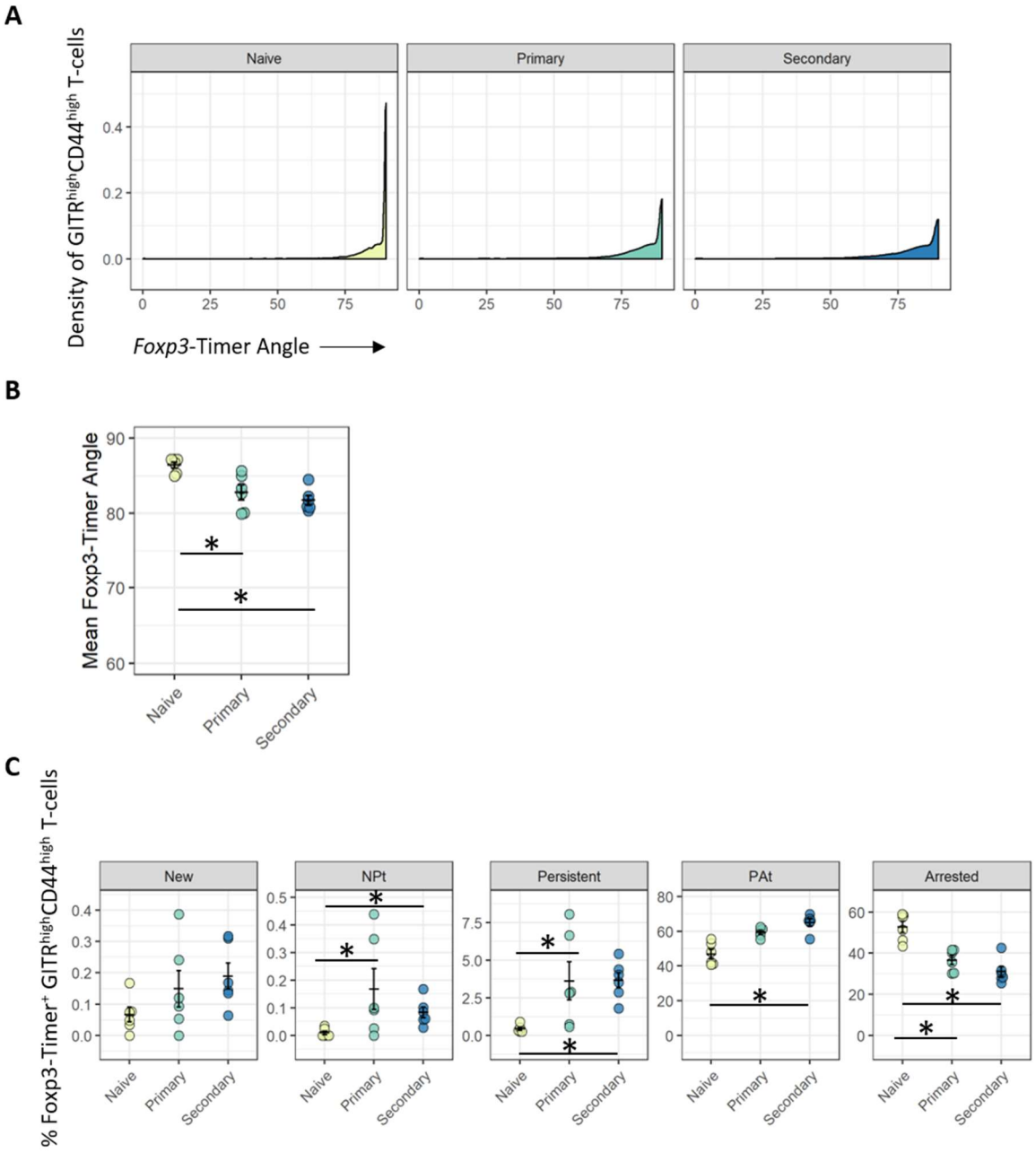


Figure 4.5: The GITR^{high}CD44^{high} T-cell subset enriched with parasite-reactive T-cells exhibit active Foxp3 transcription. (A) *Foxp3*-Timer Angle distribution of GITR^{high}CD44^{high}*Foxp3*-Timer^{+} T-cells. Angle distribution data combined for n=3, representative plots. (B) Mean *Foxp3*-Timer Angle value of GITR^{high}CD44^{high}*Foxp3*-Timer^{+} T-cells. (C) Timer Locus analysis of GITR^{high}CD44^{high}*Foxp3*-Timer^{+} T-cells. Data from two independent experiments for (B) and (C), n=6. Data was normally distributed, so a one-way ANOVA was performed, followed by Tukey's honestly significant difference post-hoc test analysis. * signifies p≤ 0.05. Error bars show standard error of the mean.

Whilst there is evidence of newly-initiated *Foxp3*-Timer transcription in 2^{o} infection, the disproportionate increase in GITR^{high}CD44^{high}*Foxp3*-Timer^{-} T-cells may suggest that Treg differentiation is somewhat delayed or inhibited. Upon analysis of CD25 expression (Figure 4.6), a decreased proportion of GITR^{high}CD44^{high}*Foxp3*-Timer^{-} T-cells (Figure 4.6A) are found to express CD25 (6.0 %) compared to Naïve mice (14.4 %, p=0.003) and 1^{o} infection (14.1 %, p=0.005). Considering that the GITR^{high}CD44^{high}*Foxp3*-Timer^{-} T-cell population expanded, the decreased proportion of CD25 expressing cells is likely accounted for within these new cells to the subset as opposed to down-regulation of CD25 on pre-existing GITR^{high}CD44^{high}*Foxp3*-Timer^{-} T-cells. This would suggest that a potential three-step Treg differentiation pathway may occur in this instance; initial upregulation of GITR, followed by CD25 upregulation to allow increased responsiveness to IL-2 signalling, eventually followed by New *Foxp3* transcription. As such, *Foxp3* transcription would be delayed whilst an effective anti-parasite T-cell response occurs.

In support of such a proposal, the proportion of GITR^{high}CD44^{high}*Foxp3*-Timer^{+} T-cells (Figure 4.6B) expressing CD25 increased in both 1^{o} and 2^{o} infection. Further, of those cells expressing CD25, the level of such expression as measured by MFI (Figure 4.6C) was not decreased in GITR^{high}CD44^{high} non-regulatory T-cells and was found to increase in GITR^{high}CD44^{high} Treg in 1^{o} infection (an increase from 192 MFI in Naïve mice to 239 MFI in 1^{o} infection, p=0.03). These data support an initial GITR^{high}CD25^{low}*Foxp3*-Timer^{-} activation stage and an eventual GITR^{high}CD25^{high}*Foxp3*-Timer^{+} stage.

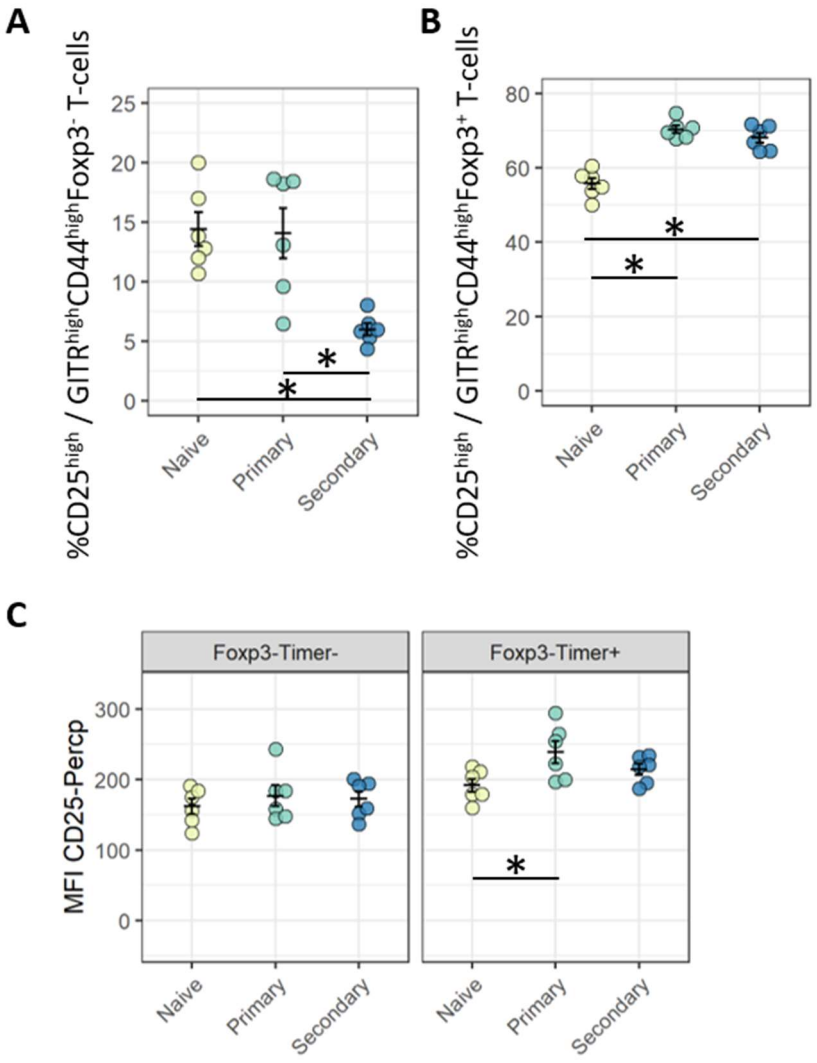


Figure 4.6: A reduced proportion of non-regulatory T-cells show CD25 expression in 2^o infection. (A) Proportion of GITR^{high}CD44^{high}*Foxp3*-Timer$^-$ T-cells expressing CD25. (B) Proportion of GITR^{high}CD44^{high}*Foxp3*-Timer$^+$ T-cells expressing CD25. (C) Median Fluorescence Intensity (MFI) of CD25-PercpCy5.5 in CD25^{high}GITR^{high}CD44^{high} T-cells with or without *Foxp3*-Timer transcription. Data was normally distributed, so a one-way ANOVA was performed, followed by Tukey's honestly significant difference post hoc analysis. * signifies p≤ 0.05. Error bars show standard error of the mean.

4.2.4 Investigation of peripheral TCR signalling dynamics within *H. polygyrus* infection

Foxp3 expression is associated with T-cell activation and is a gene transcribed downstream of TCR signalling. To determine whether *Foxp3* expression observed within 1^o and 2^o infection arose in such a manner, *Nr4a3*-Tocky mice were used to assess TCR signalling, through the

expression of *Nr4a3*, reported by *Nr4a3*-Timer. *Nr4a3*-Timer is expressed *in vivo* upon TCR signalling from cognate antigen on an APC. T-cell activation is associated with active TCR signalling, and so an increase in the proportion of T-cells with Persistent TCR signalling (Bending et al., 2018a) would imply an increase in the proportion of activated T-cells.

4.2.4.1 Validation of *Nr4a3*-Tocky for investigating peripheral TCR signalling

To further validate that *Nr4a3*-Tocky can be used *in vivo* to identify activated T-cells in the periphery, here I use OT-II-*Nr4a3*-Tocky mice. Instead of the usual diverse repertoire of TCRs, the T-cells of these mice are restricted to recognise a short peptide sequence of chicken ovalbumin; signalling through this TCR is reported by *Nr4a3*-Timer. The cognate antigen, ovalbumin, was administered in drinking water for three days. Objective analysis of *Nr4a3*-Timer fluorescence (Figure 4.7) suggests that *Nr4a3*-Timer expression is more active within ovalbumin treated mice. This supports that *Nr4a3*-Timer reports TCR signalling *in vivo*.

4.2.4.2 An increased antigen niche is likely observed in secondary infection

To investigate whether *Foxp3*-Timer expression in 2^{o} *H. polygyrus* infection may be a downstream consequence of T-cell activation, TCR signalling in 1^{o} and 2^{o} infection was observed (Figure 4.8). The same experimental procedure was followed as in Chapter 4.2.1, except using *Nr4a3*-Tocky mice in place of *Foxp3*-Tocky. Here, cells were gated for $CD44^{high}$ to enrich for antigen-experienced T-cells; consequently, *Nr4a3*-Timer was analysed within *Foxp3*-$GFP^{+}CD44^{high}$ T-cells (Figure 4.8A). The proportion of *Foxp3*-$GFP^{+}CD44^{high}$ cells having received a TCR signal and therefore *Nr4a3*-$Timer^{+}$ (Figure 4.8B) decreased in 1^{o} infection, from

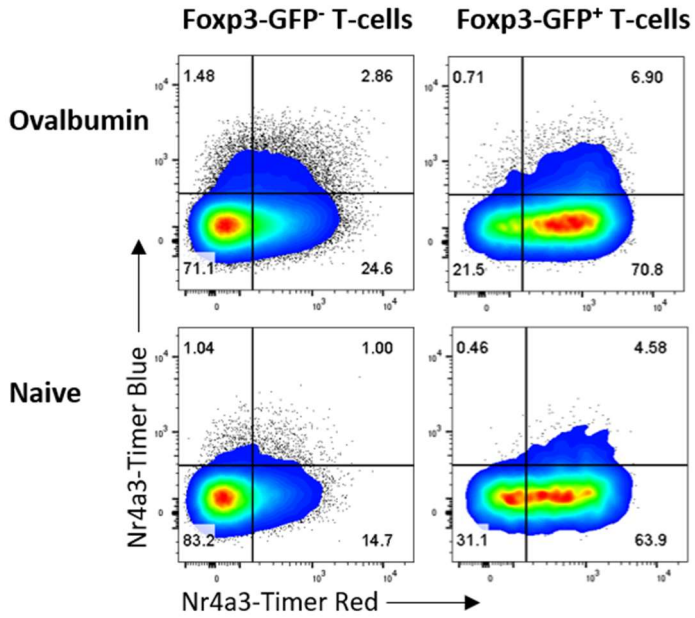


Figure 4.7: Ovalbumin administration in OT-II Nr4a3-Tocky mice increases TCR signalling. *Nr4a3*-Timer fluorescence of *Foxp3*-GFP$^-$ and *Foxp3*-GFP$^+$ CD4 T-cells after 72 hours of ovalbumin administration to OT-II *Nr4a3*-Tocky mice. Error bars show standard error of the mean.

62.8 % in Naïve mice to 54.4 % in 1^o infection (p= 0.05), before being restored in 2^o infection to 61.7 %. This data was from a single experiment, and therefore must be repeated to ensure the data is reproducible.

Upon analysis of *Nr4a3*-Timer dynamics (Figure 4.8C), a larger proportion of *Foxp3*-GFP$^+$CD44^{high} cells received New TCR signalling in 2^o infection, increasing from 1.6 % in Naïve mice to 2.8 % in 2^o infection, p= 0.05. If this result were reproducible, it would suggest that the *Foxp3*-GFP$^+$CD44^{high} cells (which should be enriched with antigen-experienced Treg) in 2^o infection are likely to have experienced a larger antigen niche than those in 1^o infection. The likely source of an increased antigen niche would be self-antigen.

Upon analysis of *Foxp3*-GFP$^-$CD44^{high} T-cells, a similar relationship is observed between Naïve, 1^o and 2^o infected mice (Figure 4.9A, B) as is seen in *Foxp3*-GFP$^+$CD44^{high} cells.

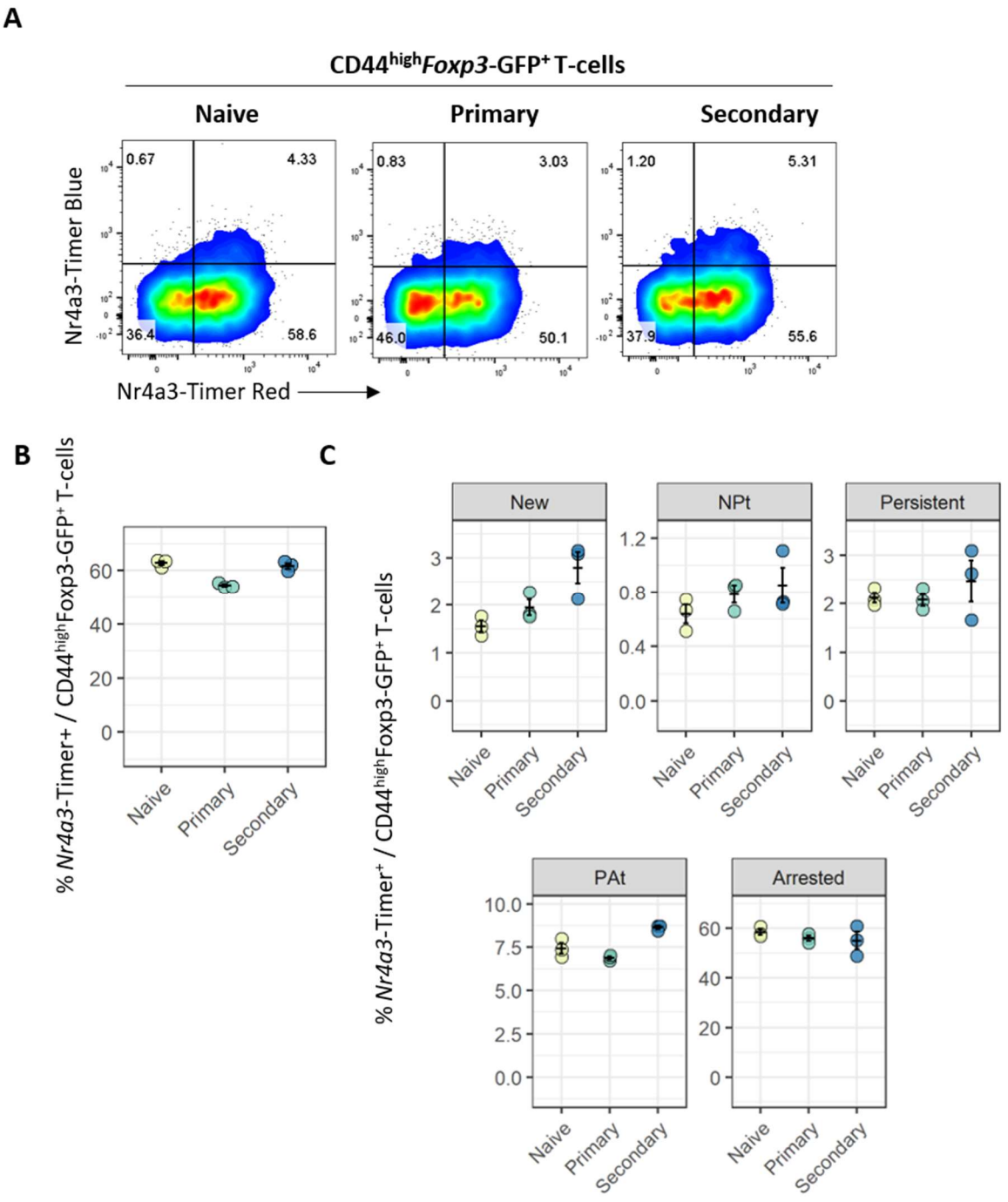


Figure 4.8: CD44^{high}Foxp3-GFP^{+} T-cell TCR signalling appears to differ between 1^{o} and 2^{o} H. polygyrus infection. (A) Representative flow cytometry plots of *Nr4a3*-Timer expression in CD44^{high}*Foxp3*-GFP^{+} T-cells during infection. (B) Percentage of CD44^{high}*Foxp3*-GFP^{+} T-cells transcribing *Nr4a3*-Timer. (C) Timer Locus analysis of CD44^{high}*Foxp3*-GFP^{+} T-cells for *Nr4a3*-Timer. Data from one experiment, n=3. A Kruskal-Wallis test followed by a Dunn Test for multiple comparisons was performed for statistics. * signifies p≤ 0.05. Error bars show standard error of the mean.

Again, there is a potential decrease in the proportion of these cells having undergone TCR signalling in 1^{o} infection, which is not seen in 2^{o} infection. Newly initiated and Persistent TCR signalling is also potentially increased in 2^{o} infection (Figure 4.9C). It is interesting that a similar increase in TCR signalling is seen between *Foxp3*-GFP^{-}CD44^{high} and *Foxp3*-GFP^{+}CD44^{high} cells, potentially suggesting a close relationship between these two subsets. A statistically significant difference would likely be found in the Timer Locus if the statistical power was increased.

A decrease in TCR signalling would be surprising considering the active expression of *Foxp3*-Timer previously identified in 1^{o} infection. If this finding were reproducible, this would suggest that *Foxp3*-Timer expression in 1^{o} infection would likely be due to an alternative mechanism other than a downstream consequence of TCR signalling, such as soluble factors. Indeed, a mechanism may be occurring to inhibit TCR signalling during 1^{o} infection. The likely restoration of TCR signalling in 2^{o} infection could suggest that such a mechanism is over-come, and *Foxp3* expression could be a consequence of TCR signalling in this context.

4.2.5 TCR signalling is inhibited in CD44^{high}*Foxp3*-GFP^{-} T-cells but not CD44^{high}*Foxp3*-GFP^{+} T-cells

TCR signalling was then assessed within the key time points of 1^{o} *H. polygyrus* infection identified within Chapter 3; 7- and 28-days post infection (Figure 4.10). Expansion of parasite-specific T-cell clones would be identifiable by an increased proportion of cells receiving TCR signalling of their cognate antigen and thus actively transcribing *Nr4a3*-Timer. At 7-days post infection, a lower proportion of CD44^{high}*Foxp3*-GFP^{-} T-cells (Figure 4.10A) exhibited Persistent TCR signalling than in Naïve mice, decreasing from 2.3 % in Naïve mice to 1.5 % at day-7 of

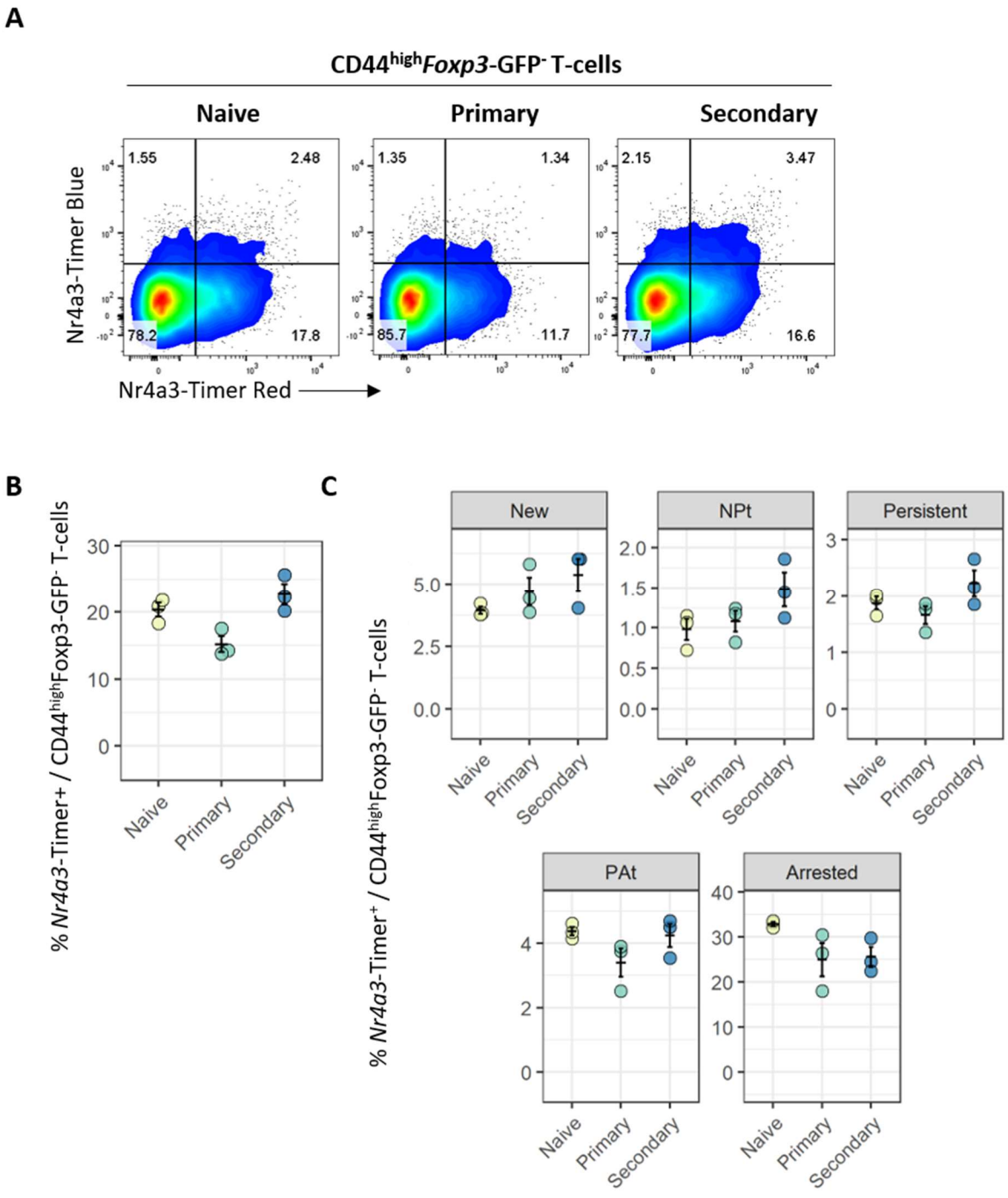


Figure 4.9: CD44^{high}Foxp3-GFP^{-} T-cell TCR signalling appears to differ between 1º and 2º H. polygyrus infection. (A) Representative flow cytometry plots of *Nr4a3*-Timer expression in CD44^{high}*Foxp3*-GFP^{-} T-cells during infection. (B) Percentage of CD44^{high}*Foxp3*-GFP^{-} T-cells expressing *Nr4a3*-Timer. (C) Timer Locus analysis of CD44^{high}*Foxp3*-GFP^{-} T-cells for *Nr4a3*-Timer. Data from one experiment, n=3. Error bars show standard error of the mean.

infection (p=0.05). By day-28 of infection, the difference in Persistent *Nr4a3*-Timer transcription between Infected and Naïve mice appeared to be reduced and not statistically significant (p=0.3). This data would suggest that during early infection, a decreased proportion of antigen-experienced T-cells are receiving repeated TCR signalling. In the context of infection, the absence of increased TCR signalling suggests that T-cell activation and TCR signalling are likely inhibited. This appears to lessen in the latter stages of *H. polygyrus* infection, suggesting that any such mechanisms are at least in part overcome. Alternatively, during early infection, infection-reactive T-cells receiving TCR signalling could be more prone to apoptosis.

Any inhibition of TCR signalling is less apparent within $CD44^{high}$*Foxp3*-GFP^{+} T-cells (Figure 4.10B). A decrease in Persistent TCR signalling is not found at either day-7 or day-28 of infection. This finding may suggest that T-cells receiving Persistent TCR signalling are more likely to become Treg in *H. polygyrus* infection, which would not be unexpected. This may still occur whilst TCR signalling inhibition is occurring; it is possible that T-cell activation is limited and the limited T-cells that are activated become Treg. Expression of the T-cell activation marker CD25 and marker of antigen experience, CD44, was assessed at day-7 of infection within $CD4^{+}$*Foxp3*-GFP^{+} T-cells by *Nr4a3*-Timer Locus (Figure 4.10C). CD25 expression may be somewhat increased in the NPt, Persistent and PAt loci compared to the New locus, although this is not statistically significant. This could suggest that CD25 expression is enhanced in Treg receiving repeated TCR signalling, implying a more activated state. CD44 expression is not found to increase by Timer Locus. This would imply that CD44 has predominantly been expressed by $CD4^{+}$*Foxp3*-GFP^{+} T-cells prior to their receiving TCR signalling.

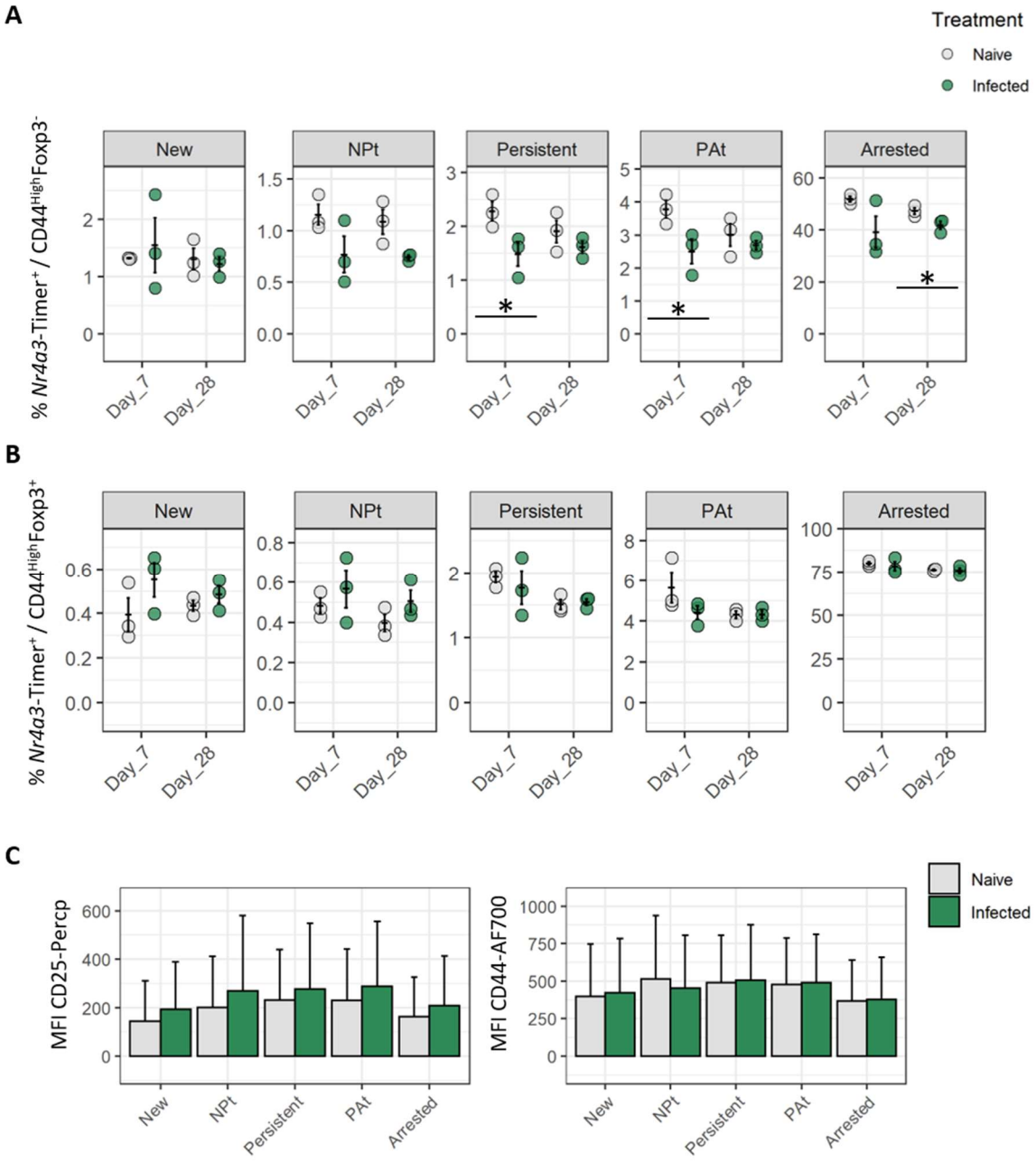


Figure 4.10: TCR signalling is inhibited in CD44^{high}Foxp3-GFP^{-} T-cells but not CD44^{high}Foxp3-GFP^{+} T-cells. (A) Timer Locus analysis of the proportion of CD44^{high}*Foxp3*-GFP^{-} T-cells expressing *Nr4a3*-Timer at day-7 and -28 of *H. polygyrus* infection. (B) Timer Locus analysis of the proportion of CD44^{high}*Foxp3*-GFP^{+} T-cells expressing *Nr4a3*-Timer at day-7 and -28 of *H. polygyrus* infection. (C) MFI of CD25-Percp and CD44-AF700 at day-7 of infection in CD4^{+}*Foxp3*-GFP^{+} T-cells by *Nr4a3*-Timer Locus. For A and B, Data for day-7 from two independent experiments, n=3 and day-28 from one experiment, n=3. A Student's two sample t-test was used for statistical analysis. Error bars show standard error of the mean. For C, data from two independent experiment, n=3. Error bars show standard deviation of the mean. * signifies p≤ 0.05

4.2.6 TCR signalling may be inhibited by multiple mechanisms

Inhibition of TCR signalling could be occurring through different types of mechanism. For instance, APCs may have a reduced capacity to deliver a TCR signal through down-regulation of MHC-II as seen by Hp-CPI discussed in Chapter 1.2.2. Alternatively, T-cell mechanisms preventing the transduction of TCR signals could be occurring, for instance through ligation of PD-1 on the T-cell surface by PD-L1 or PD-L2, as discussed in Chapter 1.3.1.1. Initially, MHC-II expression on DCs, B-cells and macrophages was assessed by MFI (Figure 4.11A) to assess APC activation. This was assessed within C57BL/6 WT mice during 1^o and 2^o *H. polygyrus* infection. There is some evidence that MHC-II expression may be decreased in both 1^o and 2^o infection on DCs and macrophages, in accordance with the literature (Segura et al., 2007; Sun et al., 2013). Further, the PD-1 ligand PD-L2 is potentially increased within 1^o infection but not 2^o infection (Figure 4.11B, potentially increasing from an MFI of 311 in Naïve mice to 1186 in 1^o infection, compared to an MFI of 370 in 2^o infection). Increased expression of PD-1 ligands increases the potential for PD-1 ligation and subsequent TCR signal transduction inhibition. If this data were reproducible, this would suggest that TCR signalling and thus T-cell activation may be some-what inhibited within 1^o but not 2^o infection.

PD-L2 ligates PD-1 on the T-cell surface, inducing phosphatase activity that prevents the transduction of the TCR signal and counteracts CD28 co-stimulation (Hui et al., 2017; Mizuno et al., 2019), as discussed in Chapter 1.3.1. I therefore assessed PD-1 expression on T-cells to investigate whether PD-L1/2 mechanisms may be contributing to the decreased TCR signalling observed. PD-1 is upregulated downstream of TCR signalling, and thus I hypothesized that an increased expression of PDL-1/2 would induce PD-1 mediated

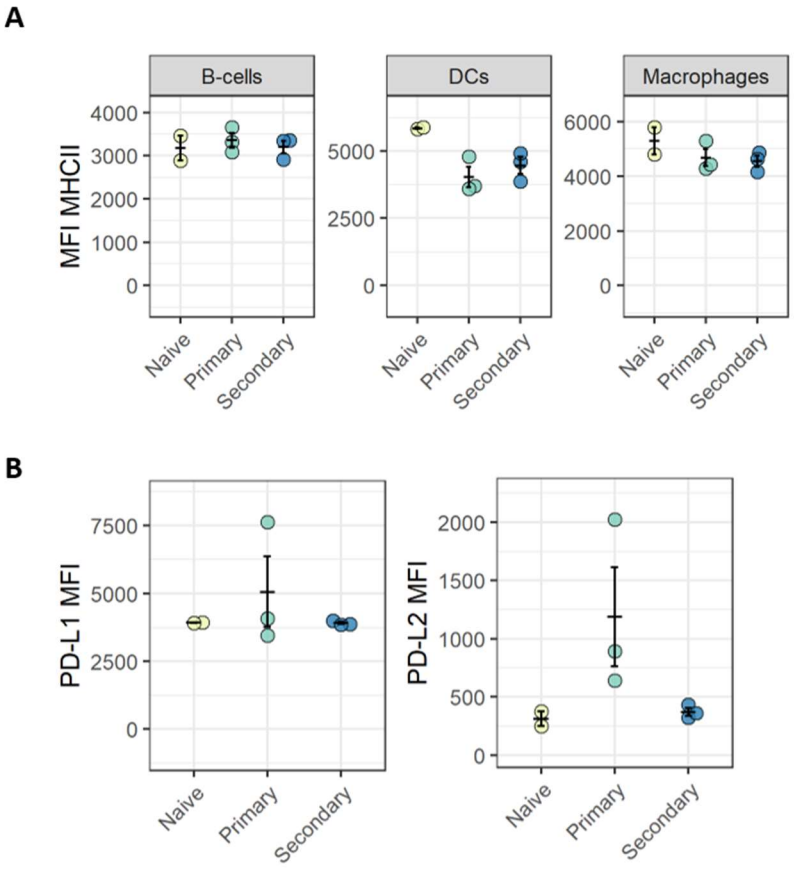


Figure 4.11: MHC-II and PD-1 ligand expression in Antigen-Presenting Cells. (A) Median Fluorescence Intensity (MFI) of MHC-II-APC on B-cells, DCs and macrophages. (B) MFI of PD-L1-PE-Dazzle and PD-L2-PE-Dazzle on DCs. Data from one experiment, n=2/3. Data from C57BL/6 mice. Error bars show standard error of the mean.

suppression of TCR signalling, reducing T-cell expression of PD-1. This was assessed within 1^{o} and 2^{o} *H. polygyrus* infected *Foxp3*-Tocky mice.

The proportion of CD4 T-cells expressing PD-1 (Figure 4.12A) did not appear to decrease in either 1^{o} or 2^{o} *H. polygyrus* infection. Rather, this increased in 2^{o} infection compared to both Naïve mice and 1^{o} infection (increasing from 8.8 % in Naïve mice and 9.7 % in 1^{o} infection to 16.7 % in 2^{o} infection, p=0.02 for both), suggesting that PD-1 mediated suppression is abrogated in 2^{o} infection. Within GITR^{high}CD44^{high} T-cells (Figure 4.12B), the proportion of *Foxp3*-Timer^{-} cells expressing PD-1 did not change in 1^{o} infection but may

potentially be found to decrease in 2^{o} infection if 9 mice per group were used for a power of 80 % (PD-1 was expressed by 52.7 % of *Foxp3*-Timer^{-}GITR^{high}CD44^{high} T-cells in Naïve mice compared to 45.8 % in 2^{o} infection, p=0.2). Within the *Foxp3*-Timer^{+}GITR^{high}CD44^{high} population, the proportion of cells PD-1^{high} potentially decreased from 43.5 % in Naïve mice to 34.6 % in 1^{o} infection (p=0.06) and may be somewhat decreased in 2^{o} infection. Such a finding could be explained by one of two ways; *Foxp3*-Timer^{+}GITR^{high}CD44^{high}PD-1^{high} T-cells may have lost their *Foxp3* expression to become Teff or downregulated their PD-1 expression by PD-1 or another co-inhibitory molecule mediated inhibition.

To investigate whether PD-1 expression was downregulated in the PD-1^{high} T-cell subset, the extent of PD-1 expression was assessed upon PD-1^{high} cells (Figure 4.12C). PD-1 expression was found to be upregulated on *Foxp3*-Timer^{-}GITR^{high}CD44^{high} T-cells in 2^{o} infection (increasing from an MFI of 413 in Naïve mice to 629 in 2^{o} infection, p<0.001) but decreased on *Foxp3*-Timer^{+}GITR^{high}CD44^{high} T-cells in both 1^{o} and 2^{o} infection (decreasing from an MFI of 332 in Naïve mice to 284 in 1^{o}, p=0.02; and 287 in 2^{o} infection, p=0.03). These data suggest that PD-1 may be specifically downregulated on infection-reactive Treg, likely via PD-1 ligation, but not on infection-reactive non-regulatory T-cells. This may reduce somewhat Treg suppressive activities.

4.2.7 Tfh increase in secondary but not primary *H. polygyrus* infection

PD-1 is expressed on activated T-cells, and to a high degree on Tfh (Haynes et al., 2007) due to the frequent B-T-cell interactions driving PD-1 expression. In Tfh, PD-1 is thought to primarily function to prevent proliferation and the resultant overcrowding of the germinal

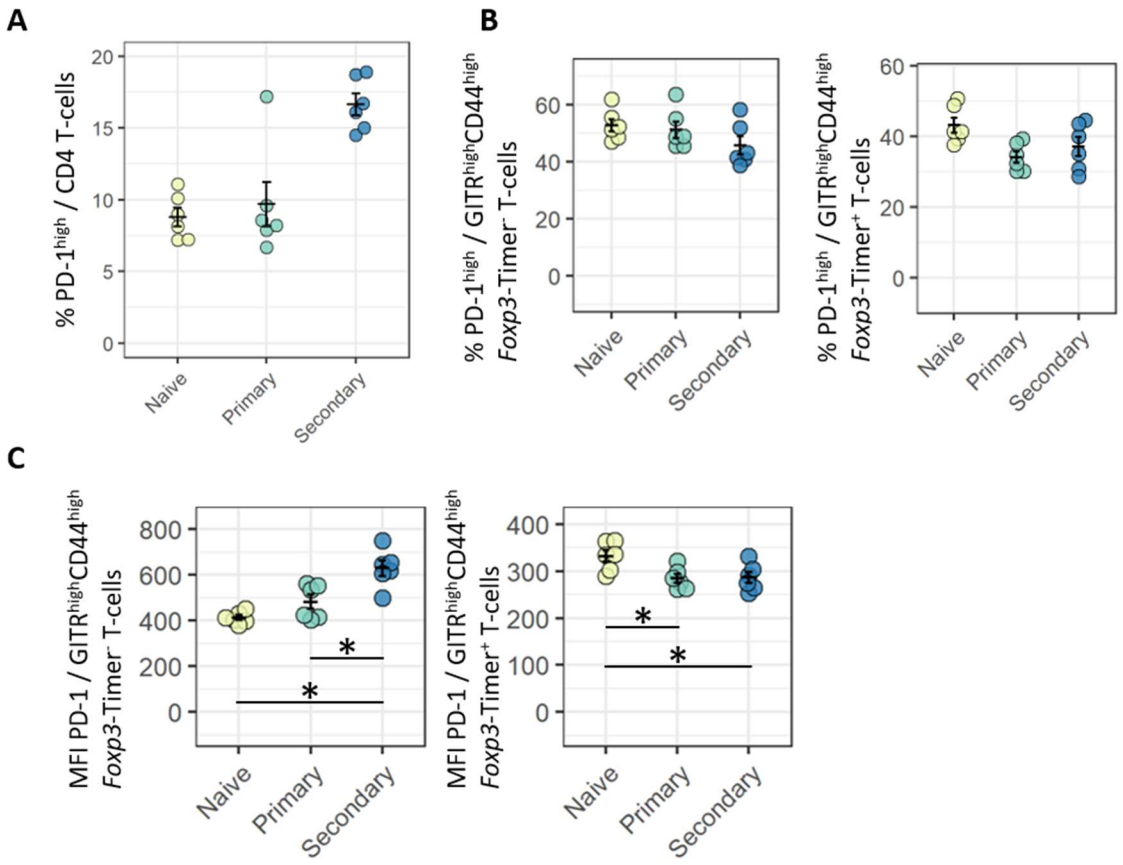


Figure 4.12: PD-1 expression is specifically decreased in GITR^{high}CD44^{high}Foxp3^{+} T-cells and not GITR^{high}CD44^{high}Foxp3^{-} T-cells. (A) Percentage of CD4 T-cells expressing PD-1. (B) Percentage of GITR^{high}CD44^{high}*Foxp3*$^{+/-}$ T-cells expressing PD-1. (C) Median Fluorescence Intensity (MFI) of PD-1 in GITR^{high}CD44^{high}*Foxp3*$^{+/-}$ populations. Data from *Foxp3*-Tocky mice, two independent experiments, n=6. A Kruskal Wallis followed by a Dunn Test was performed for statistics, * signifies p≤ 0.05. Error bars show standard error of the mean.

centre (Crotty, 2011), aid localisation of Tfh to the germinal centre (Shi et al., 2018), and promoted B-cell survival (Good-Jacobson et al., 2010). Consequently, Tfh express very high levels of PD-1, along with CXCR5. Importantly, Tfh have been noted as key effector T-cells in *H. polygyrus* infection (King and Mohrs, 2009), as discussed in Chapter 4.1.

Based on the increased PD-1 expression observed in non-regulatory T-cells in 2^{o} infection, here I investigated whether Tfh differentiation was induced upon 2^{o} infection within *Foxp3*-Tocky mice. Accordingly, Tfh were assessed within 1^{o} and 2^{o} infection (Figure

4.13A, B). The proportion of CD4 T-cells identified as Tfh expanded by 6-fold in 2° infection, from 0.3 % in both Naïve mice and 1° infection to 1.7 % in 2° infection (p=0.006). The lack of Tfh expansion in 1° infection supports the consensus in the literature that a successful anti-parasite T-cell response is not observed as early as day-7 of infection. Expansion of the Tfh population at day-7 of 2° infection implies a rapid memory T-cell response as expected.

Quantifying the percentage of GITR^{high}CD44^{high} T-cells that can be classified as Tfh (Figure 4.13C) identifies that Tfh differentiated within this GITR^{high}CD44^{high} T-cell population; where these cells are enriched with infection-reactive T-cells and subsequently Tmem. No increase in the Tfr (GITR^{high}CD44^{high}*Foxp3*-Timer^{+} PD-1$^{very\text{-}high}$CXCR5^{high}) population was observed in 2° infection, likely allowing for efficient Tfh activity. This would suggest that the essential Tfh population required for parasite clearance are able to act relatively uninhibited.

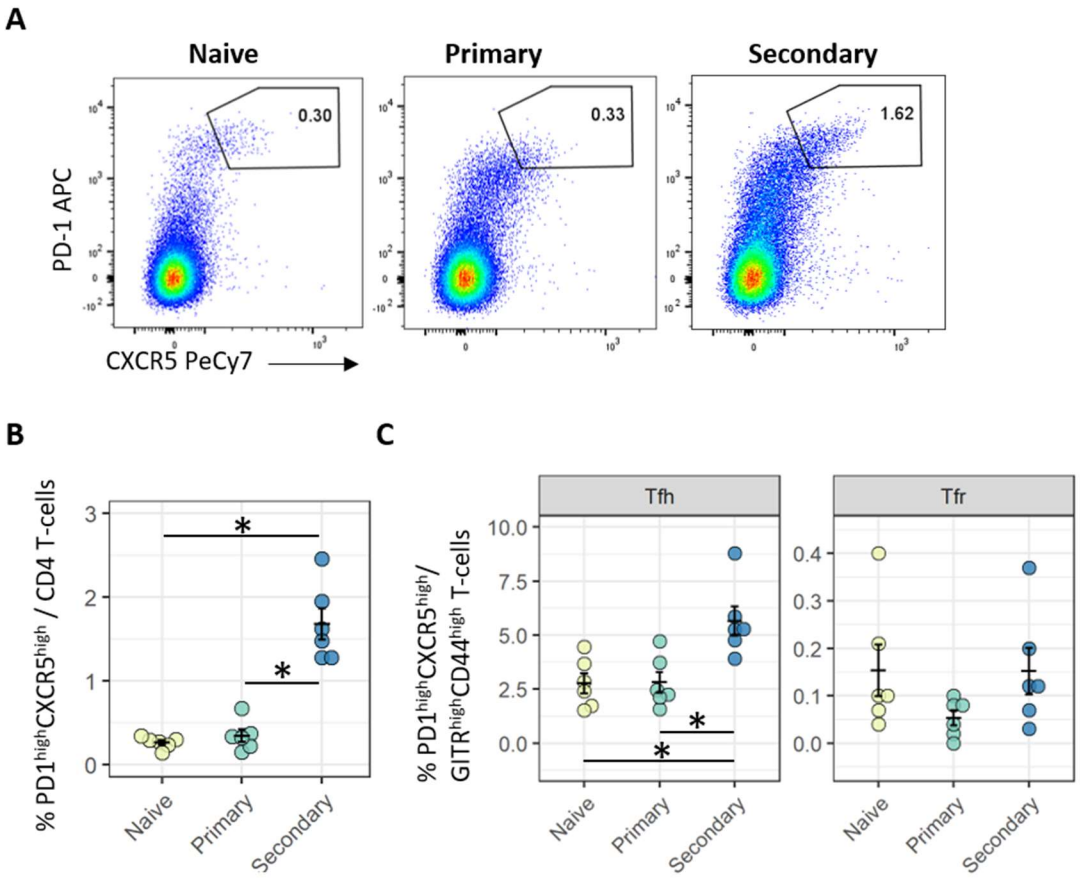


Figure 4.13: Tfh increase in 2^o but not 1^o H. polygyrus infection. (A) Representative plots for CD4 T-cells, where Tfh are identified as PD-1$^{very\text{-}high}$ and CXCR5^{high}. (B) Percentage of CD4 T-cells classified as Tfh. (C) Percentage of GITR^{high}CD44^{high} T-cells classified as Tfh (PD-1$^{very\text{-}high}$CXCR5^{high}*Foxp3*-Timer$^-$) or Tfr (PD-1$^{very\text{-}high}$CXCR5^{high}*Foxp3*-Timer$^+$). Data from two independent experiments, using *Foxp3*-Tocky mice. n=6. For statistics, a one-way ANOVA was performed followed by Tukey's honestly significant difference post hoc analysis. * signifies p≤ 0.05. Error bars show standard error of the mean.

TCR signalling in *Nr4a3*-Tocky mice during 1^o and 2^o infection was then analysed within CD44^{high} populations expressing levels of PD-1; PD-1^{low}, PD-1^{mid} and PD-1^{high}, where PD-1^{high} equates to the level of PD-1 seen within Tfh cells (Figure 4.14A, B). As the proportion of antigen-reactive CD44^{high}*Foxp3*-GFP$^-$ T-cells increased, as defined by their receiving of a TCR signal, PD-1 increased (p<0.001, Figure 4.14B). This finding supports that PD-1 increased as a consequence of TCR signalling, as expected. It is of note that whilst not statistically significant, a slight decrease may be observed in the proportion of PD-1^{mid} and PD-1^{high} cells that have received TCR signalling in both 1^o and 2^o infection compared to Naïve mice. This trend towards a decrease in TCR signalling could be associated with apoptosis, however, PD-1 ligation inhibits TCR signalling, and upregulation of PD-1 expression increases the likelihood of PD-1 ligation. Thus, in *H. polygyrus* infection where a potential increase in PD-1 ligand/s is observed, the likelihood of PD-1 mediated suppression is increased. This was further explored by Timer Locus analysis.

Upon analysis of *Nr4a3*-Timer expression by Timer locus (Figure 4.14C), it is apparent that TCR signalling dynamics differ between PD-1^{mid} and PD-1^{high} cells. This is apparent within the Persistent and PAt loci, where there are significantly more PD-1^{high} cells than PD-1^{mid} cells (p=0.02 for both Persistent and PAt loci). This further identifies that higher PD-1 expression is associated with more active TCR signalling. No significant differences were found between

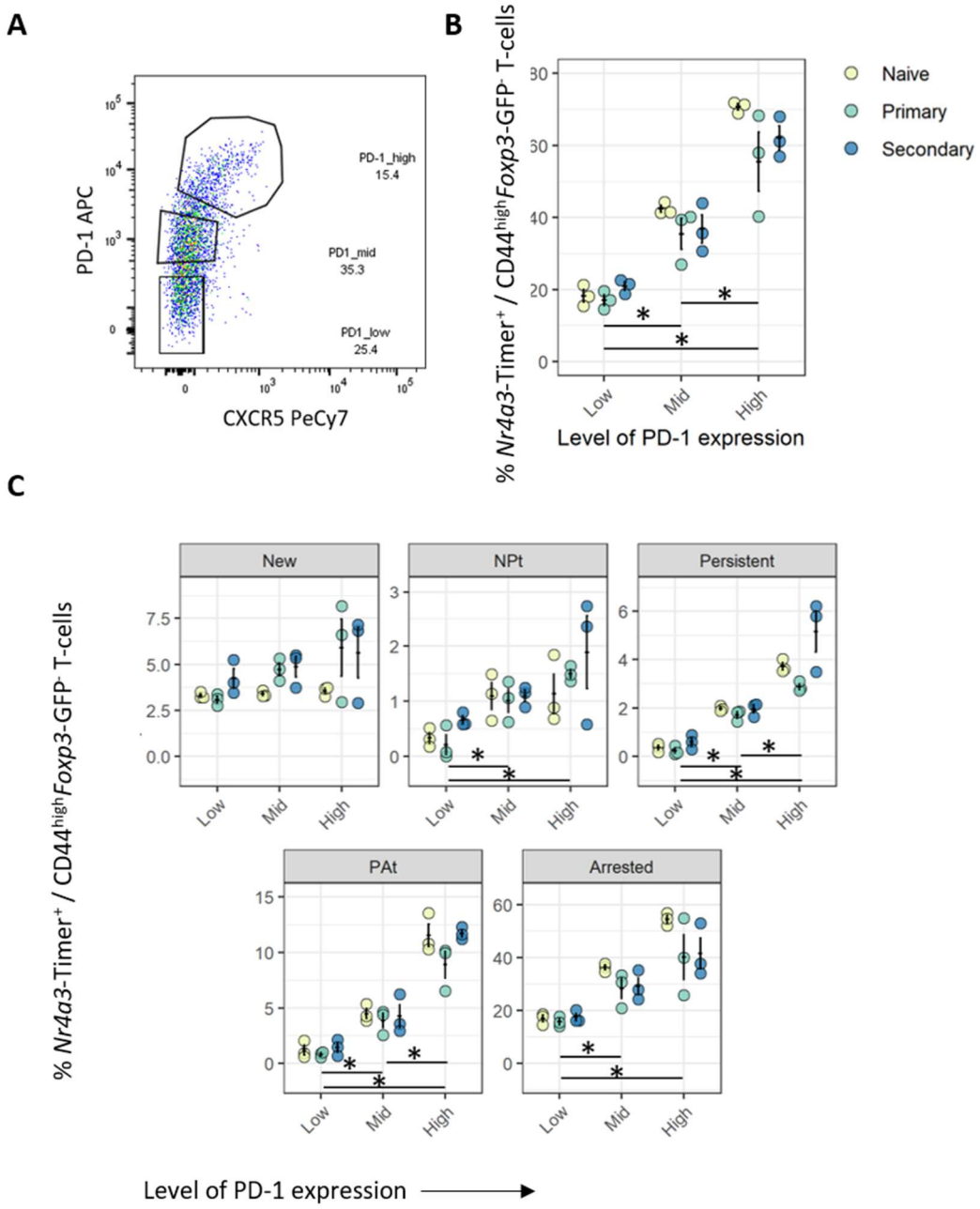


Figure 4.14: TCR signalling increases with PD-1 expression in CD44^{high}Foxp3-GFP^{-} T-cells. (A) Representative plot of CD44^{high}*Foxp3*-GFP^{-} T-cells divided into PD-1 subsets, PD-1^{low}, PD-1^{mid} and PD-1^{high}. (B) % of CD44^{high}*Foxp3*-GFP^{-} T-cells expressing *Nr4a3*-Timer, per PD-1 subset. (C) *Nr4a3*-Timer Locus analysis of PD-1 subsets of CD44^{high}*Foxp3*-GFP^{-} T-cells. Data from one experiment, using *Nr4a3*-Tocky mice. n=3. For statistics, a Kruskal-Wallis test was performed followed by a Dunn Test for multiple comparisons if the Kruskal Wallis test was significant, * signifies p≤ 0.05. Error bars show standard error of the mean.

Naïve mice and those with 1^{o} or 2^{o} *H. polygyrus* infection at any Timer Locus or level of PD-1 expression. However, there does appear to be a trend towards an increase in NPt and Persistent *Nr4a3*-Timer expressing cells within the PD-1^{high} population in 2^{o} infection compared to Naïve mice. A larger number of mice would be required to confirm or deny this trend by increasing statistical power to 80 %. Such a finding, if confirmed, would suggest that these cells may be highly activated within 2^{o} infection. It would thus appear that any PD-1 suppression here is inadequate to prevent Persistent TCR signalling.

Conversely, a potential trend towards a decreased population of PD-1^{high} T-cells receiving Persistent TCR signalling may be observed within 1^{o} infection compared to Naïve mice. Considering no such decrease is observed within the New Timer Locus, nor the PD-1^{mid} populations, this likely suggests that PD-1 induced TCR signalling suppression may potentially be occurring within 1^{o} infection. This would correlate with the potential increase in PD-L2 expression on DCs found in Chapter 4.2.6.

Within CD44^{high}*Foxp3*-GFP^{+} Treg, PD-1 expression was again associated with an increased proportion of antigen-reactive cells (p<0.001, Figure 4.15A). Upon Timer Locus analysis (Figure 4.15B), there was again an increase in the Persistent and PAt loci as PD-1 increased, similar to that of the *Foxp3*-GFP^{-} population in Figure 4.14 (p<0.001 for each).

No significant statistical difference was found at any Timer Locus between infection states, other than within the PAt locus. Here, a modest increase in PD-1^{mid} cells is observed in 2^{o} infection compared to Naïve mice, increasing from 9.0 % in Naïve mice to 11.6 % in 2^{o} infection, p=0.05. There is a further trend towards an increased proportion of cells in 2^{o} infection compared to Naïve mice in the PD-1^{mid} population in the New and NPt loci, but not necessarily the Persistent loci. This may suggest that in 2^{o} infection, CD44^{high}*Foxp3*-GFP^{+}PD-

1^{mid} cells likely receive an increase in TCR signalling, but this is not sustained. There is no evidence of such an increase in 1^{o} infection.

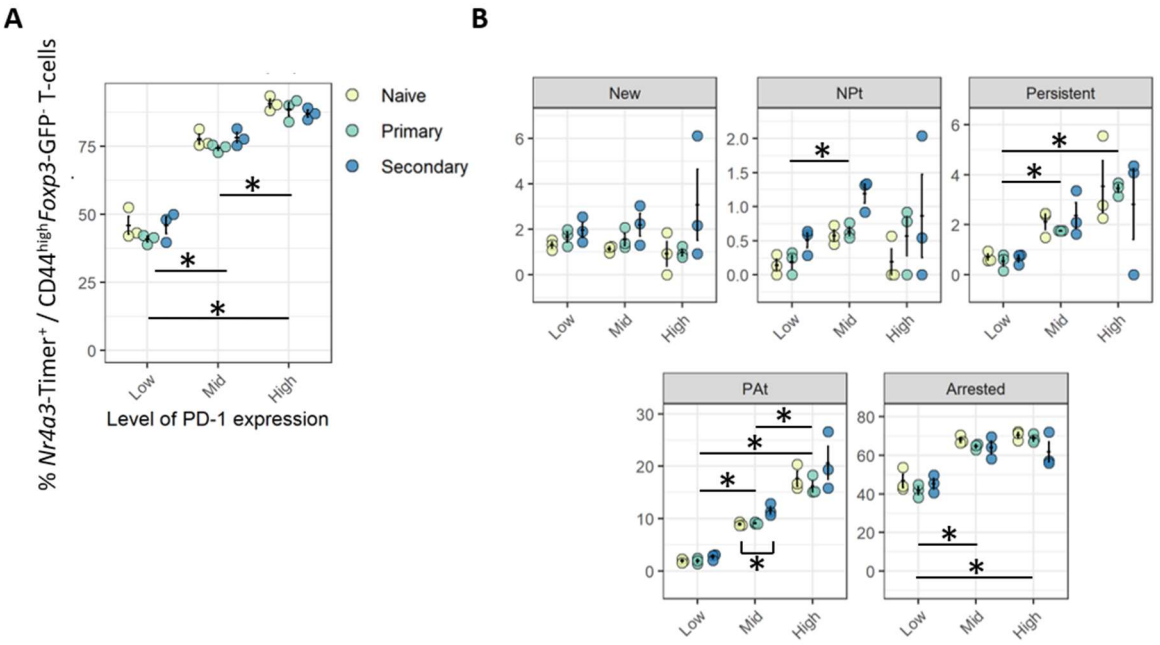


Figure 4.15: TCR signalling increases with PD-1 expression in CD44^{high}Foxp3-GFP^{+} T-cells. (A) % of CD44^{high}*Foxp3*-GFP^{+} T-cells expressing *Nr4a3*-Timer, per PD-1 subset. (B) *Nr4a3*-Timer Locus analysis of PD-1 subsets of CD44^{high}Foxp3-GFP^{+} T-cells. Data from one experiment, using *Nr4a3*-Tocky mice. n=3. For statistics, a Kruskal-Wallis test was performed followed by a Dunn Test for multiple comparisons if the Kruskal Wallis test was significant, * signifies p≤ 0.05. Error bars show standard error of the mean.

4.3 Discussion

This chapter set out to explore the peripheral dynamics of the Treg and memory type T-cell responses during 1° and 2° *H. polygyrus* infection. I found a marked expansion in non-regulatory T-cells during 2° *H. polygyrus* infection and an expanded Tfh subpopulation within this, suggesting that negative regulatory mechanisms are insufficient in preventing an anti-parasite T-cell response. Surprisingly, I found that active *Foxp3*-Timer transcription occurs in 2° *H. polygyrus* infection, similar to that in 1° infection.

C57BL/6 mice are readily infected in 1° *H. polygyrus* infection and resistant to 2° infection. At 7-days post infection, the *H. polygyrus* larvae reside within the intestinal tissue of the small intestine. In 1° infection, the mouse host is unable to clear the *H. polygyrus* larvae at this stage; parasite clearance occurs of the mature parasite within the intestinal lumen later in infection. However, in 2° infection, an effective anti-parasite response is seen during early infection, reducing the adult parasite burden later. This infection model therefore provides a physiological model in which to study both regulatory and memory type T-cell dynamics.

I identify that the GITR^{high}CD44^{high} T-cell population, believed to be enriched with parasite-reactive T-cells, expands within 2° infection. A greater increase occurs in the non-regulatory T-cell fraction of this population, which include Tmem, than Treg. This suggests that a memory response is occurring within 2° infection, as expected. Whilst the proportion of GITR^{high}CD44^{high} T-cells expressing *Foxp3*-Timer decreases in 2° infection, I show that as a proportion of CD4 T-cells, the GITR^{high}CD44^{high}*Foxp3*-Timer^{+} population does expand. Expansion of the *Foxp3*-Timer^{+} population to a smaller extent than the non-regulatory population suggests that Treg expansion may be delayed compared to the Tmem population, which would support the theory that Treg develop subsequent to T-cell activation.

Considering that GITR is a TNFRSF member and co-stimulatory receptor, and is required for tTreg differentiation, GITR signalling may be involved in the differentiation of Teff and Treg in the periphery. It would be of interest to analyse expression of its ligand, GITRL, within 1^o and 2^o infection.

Expansion of the non-regulatory T-cell pool faster than the Treg pool may be somewhat explained by Pelley *et al.*; whereby in 2^o infection, Treg appear to re-differentiate into Th2-like cells dependent on IL-4, with effector Th2 function. The authors further demonstrate that some ex-Treg may later up-regulate *Foxp3* expression again, showing a high level of plasticity. This was further demonstrated by adoptive transfer of Treg into lymphopenic hosts, and therefore the findings are likely reliable (Pelly et al., 2017). In this way, it is possible that parasite-reactive Th2 cells develop from the memory Treg pool in 2^o infection, joining the non-regulatory pool, whilst the Treg population increases at a lower rate downstream of T-cell activation. It is possible that some of the cells within the *Foxp3*-Timer Arrested locus in 2^o infection have become ex-Treg by this process. To fully understand the dynamics at play, single-cell RNAseq would be important.

Surprisingly, *Foxp3*-Timer transcription within the $GITR^{high}CD44^{high}$*Foxp3*-$Timer^+$ Treg subset appears to be active in 2^o infection. This is surprising considering that negative-regulatory mechanisms are likely overcome for an effective anti-parasite response and the potential for Treg to re-differentiate into ex-Treg. Anecdotally, the level of inflammation in the small intestine during 2^o infection and the size of the mLN was increased over that seen in 1^o infection. This led to the hypothesis that *Foxp3* expression may be induced to limit the T-cell response to self-antigen released during parasite migration, preventing excessive damage to the intestinal tissue. Indeed, evidence supporting a role for *Foxp3* expressing Treg

in limiting intestinal pathology was previously identified within *H. polygyrus* infection (Rausch et al., 2009).

Within GITR^{high}CD44^{high} T-cells, newly-initiated *Foxp3*-Timer expression is observed in both 1^{o} and 2^{o} infection, suggesting an increased repertoire of T-cells may be becoming Treg, or that *Foxp3* transcription could be re-initiated in ex-Treg during 2^{o} infection. I further observe an increase in the proportion of GITR^{high}CD44^{high} T-cells that are classified with PAt transcription in 2^{o} infection, and there is some evidence that this may also be elevated in 1^{o} infection. PAt cells have a higher ratio of *Foxp3*-Timer Red to Blue fluorescence than Persistent cells but still transcribe *Foxp3*-Timer. This increase likely correlates with a decreased proportion of GITR^{high}CD44^{high} T-cells classified as Arrested Treg. This may suggest that Arrested Treg have upregulated *Foxp3*-Timer transcription in response to infection. Bending *et al.* previously hypothesised that cells within the *Foxp3*-Timer PAt and Arrested loci are likely predominantly part of the memory T-cell pool against self-antigen (Bending et al., 2018b). In accordance with this hypothesis, self-reactive T-cells may be upregulating *Foxp3*-Timer expression in response to *H. polygyrus* infection. The ability to reliably distinguish helminth-reactive Treg and self-reactive Treg would allow investigation into specific targeting of aberrant Treg within a heterogenous Treg population. Further investigation would be required to fully determine whether the Treg in this study may be identified as helminth-reactive or self-reactive based on their *Foxp3*-Timer expression; this is why the term "infection-reactive" is used, encompassing both helminth-reactive Treg and self-reactive Treg recognising self-antigen released during tissue damage.

Within 2^{o} *H. polygyrus* infection, newly-initiated and Persistent TCR signalling appeared to be increased compared to both Naïve and 1^{o} infected mice. Whilst this data is

from three individual mice, these were analysed in the same experiment, and therefore a second independent experiment would be required to confirm that the results are reproducible. If these results were reproducible, such an increase in newly-initiated and Persistent TCR signalling in 2^o infection could suggest that an increased repertoire of antigen is available. Alternatively, APCs could be expanded and/or more efficient. Considering that my data finds a similar trend towards decreased MHC-II expression, and thus activation, of DCs and macrophages in both 1^o and 2^o infection compared to Naïve mice, an expanded antigen repertoire is more likely.

An increased sensitivity to antigen may be suggested largely based on the presence of newly-initiated TCR signalling. *Nr4a3*-Timer reports a TCR signal that is transduced by the presence of cognate antigen, and not simply brief binding of antigen that is seen in incompatible antigen scanning. Upon T-cell proliferation, Timer protein is split between daughter cells and the Timer Angle or ratio of Timer Blue to Timer Red protein has been reported to reflect that of the parent cell (Bending et al., 2018a). T-cells with newly-initiated *Nr4a3*-Timer expression therefore have most likely received a TCR signal from their cognate antigen for the first time in *Nr4a3*-Timer memory; where *Nr4a3*-Timer memory refers to the time that Timer-Red fluorescence may be detected. Alternatively, it is possible that after many cell divisions have occurred, Timer-protein may be diluted out of daughter cells. Assuming the first scenario, this would imply an increased repertoire of antigen is available within 2^o infection than in 1^o infection. Considering that *H. polygyrus* associated antigen would be incredibly unlikely to change so quickly, a different source of antigen is likely, such as self-antigen.

I further find a decreased proportion of GITR^{high}CD44^{high}*Foxp3*-Timer^{-} T-cells express CD25 in 2^{o} infection. During the contraction phase of the T-cell response in 1^{o} infection, infection-reactive Tmem differentiate from infection-reactive Teff. Upon differentiation, activation markers, including CD25, are downregulated in Tmem as effector mechanisms are not immediately required. Considering that a large proportion of non-regulatory T-cells do not yet express CD25 in 2^{o} infection, this would suggest that a large portion of the expanded population are infection-reactive Tmem; where Tmem are able to proliferate rapidly. Alternatively, or perhaps additionally, upon T-cell activation for the first time, T-cells within 2^{o} *H. polygyrus* infection could rapidly up-regulate GITR, prior to the upregulation of CD25.

Whilst my data suggests that it is highly likely that the GITR^{high}CD44^{high}*Foxp3*-Timer^{-} population contains cells in the early stages of activation or re-activation in 2^{o} infection, low CD25 expression is also associated with Tfh (Ballesteros-Tato et al., 2012). Tfh are considered important for the anti-parasite B-cell response in 2^{o} infection and are reported to increase. Indeed, we found that the proportion of GITR^{high}CD44^{high}*Foxp3*-Timer^{-} T-cells classified as Tfh did expand. These two scenarios are not mutually exclusive, indeed, the percentage of GITR^{high}CD44^{high}*Foxp3*-Timer^{-} T-cells expressing CD25 drops by approximately 10 %, whilst the Tfh subpopulation increased by approximately 2 %. It is therefore likely that both are occurring.

It is reported in the literature that anti-parasite CD4 T-cells secreting IL-4 are found exclusively within the B-cell compartment of the mLN during 2^{o} infection and display markers associated with Tfh (King and Mohrs, 2009). The authors found that these cells may be identified as Tfh by expression of PD-1 and CXCR5. Accordingly, we used these markers to identify Tfh within *H. polygyrus* infection. In 2^{o} infection, my data identified expansion of the

Tfh population, but not the Tfr population. This would suggest that unlike 1^{o} infection, where I suggest *Foxp3*-Timer expression is induced within parasite-reactive T-cells preventing an effective T-cell response (Chapter 3), negative regulatory mechanisms are likely to have been overcome in this specific T-cell subpopulation.

Further to Chapter 3, my comparison of 1^{o} and 2^{o} infection supports that Treg polarisation in 1^{o} infection is likely promoted by soluble factors, most likely from *H. polygyrus*, rather than a downstream consequence of repeated TCR signalling. Whilst multiple factors are required for Treg polarisation, such as TCR signalling, IL-2 signalling and signalling through the TGF-βR, soluble factors such as *Hp*-TGM may reduce the threshold level required of these factors. Indeed, my data finds no increase in TCR signalling at day-7 of 1^{o} infection, despite an increase in *Foxp3* transcriptional activity. At day-7 of infection, the larvae have resided within the muscularis externa for approximately six days. I have shown that increased TCR signalling may be detected using *Nr4a3*-Timer by 72-hours post antigen administration in the form of ovalbumin, and so the decrease in TCR signalling is unlikely to be a consequence of a physiological delay in antigen presentation. It is therefore surprising that no increase in TCR signalling is observed in 1^{o} infection; this is indicative of TCR signalling inhibition.

Additional data supports a mechanism of TCR signalling inhibition that may be helminth-mediated within 1^{o} infection. Upon DCs expressing MHC-II, the extent of expression appears to have potentially decreased in both 1^{o} and 2^{o} infection. This would suggest a reduced activation state of the DC. Any such decreased activation state could be further explored by analysis of co-receptor ligands CD80/86. A reduced activation state and lower expression of MHC-II would most likely correlate with a reduced capacity to present antigen to T-cells and subsequently induce activation. Reduced MHC-II expression has previously been

noted within *H. polygyrus* infection, and hypothesised to reduce T-cell activation (Axtner and Sommer, 2011). Further, MHC-II genotype appears to be a cause of strain variation in *H. polygyrus* infection susceptibility (Behnke and Wahid, 1991; Reynolds et al., 2012).

At the L4 *H. polygyrus* stage, Hewitson *et al.* identified that the ShK/SXC domain containing proteins can be found within the HES, and to a greater extent than in the adult stage (Hewitson et al., 2013). ShK/SXC domains can inhibit calcium-dependent T-cell activation downstream of TCR signalling (Chi et al., 2012). Transcription of *Nr4a3* occurs as a result of the PI_3K pathway and the NFAT transcription factor, which are calcium-dependent. The potential reduction in TCR signalling our data found in 1^o infection therefore supports an active role for such proteins. It would be of great interest to identify whether transcription of *Nr4a1* is reduced during 1^o infection. Jennings *et al.* propose that *Nr4a1* is not associated with the PI_3K TCR signalling pathway (Jennings et al., 2019), and therefore calcium-independent. A reduction in *Nr4a1* transcription would suggest that other factors may also be inhibiting TCR signalling. It is likely that more than one mechanism is at play, considering the potential decrease in DC MHC-II expression and increased PD-L2.

PD-L2 is one ligand for PD-1. PD-1 ligation is well known to limit T-cell activation, and this occurs through inhibition of TCR signalling (Mizuno et al., 2019). PD-L2 is poorly characterised, with the most well-known ligand of PD-1 being PD-L1. However, PD-L2 is known to inhibit TCR mediated proliferation and cytokine production associated with T-cell activation. It is suggested that PD-L1 and PD-L2 have largely overlapping roles (Latchman et al., 2001). It is possible that a PD-L2 related mechanism may be additionally preventing T-cell activation in 1^o infection. Such possible inhibition appears to be overcome in *H. polygyrus* 2^o infection, where more active TCR signalling is potentially identified. It would again be of

interest to analyse CD80/86 expression on APCs in 2^{o} infection, as high expression of these CD28 ligands on the APC surface abrogate PD-1 mediated TCR signalling inhibition (Sugiura et al., 2019).

I identified that PD-1 expression may be specifically decreased on infection-reactive Treg, but not non-regulatory T-cells in *H. polygyrus* infection. Based on the feedback control perspective, pTreg may typically be considered as T-cells with a high state of T-cell activation (Ono and Tanaka, 2015). PD-1 expression is linked to the T-cell activation state, as reviewed by Keir *et al*. (Keir et al., 2008), and so this could suggest that Treg during *H. polygyrus* infection are more susceptible to PD-1 mediated suppression, thus downregulating PD-1 in response to PD-1 ligation. It is possible that PD-1 may have been downregulated by an alternative mechanism without reducing the Treg activation state, lowering the capacity of these Treg to undergo PD-1 mediated suppression. Alternatively, PD-1 expression may have not been upregulated on the Treg precursor cells, further discussed in Chapter 5.1.2.

In conclusion, this chapter finds that *H. polygyrus* infection provides an excellent model in which to study T-cell dynamics. I identify that TCR signalling is likely inhibited within 1^{o} infection, but such mechanisms appear to be overcome in 2^{o} infection. Further, I find that *Foxp3* transcriptional dynamics in 2^{o} infection are very similar to those in 1^{o} infection, however, these infection-reactive Treg may be overshadowed by a disproportionate expansion of infection-reactive memory-phenotype T-cells.

5 Chapter Five: Discussion

5.1 Key findings in context

I identify that *Foxp3* transcription appears to be initiated, maintained and actively regulated within activated T-cells during early 1^{o} *H. polygyrus* infection. These activated T-cells are most likely infection-reactive, where infection-reactive T-cells include both helminth-reactive and self-reactive T-cells from tissue damage. I further find that *Foxp3* transcription is most likely upregulated within Treg that have Arrested *Foxp3* transcription, which are likely to be tTreg, in response to infection. Previous studies have identified tTreg expansion, according to Helios expression, in response to *H. polygyrus* infection (Smith et al., 2016), however, *Foxp3* expression within activated T-cells in the context of *H. polygyrus* infection is a novel finding. I hypothesise that within the C57BL/6 mouse background, and potentially other Th1 skewed backgrounds, *Foxp3* transcription occurs within activated T-cells as a mechanism to prevent their individual function, whether that be anti-parasite in nature or a cause of tissue pathology. Indeed, Smith *et al.* describe that expansion of Treg during early infection is required for susceptibility to 1^{o} *H. polygyrus* infection (Smith et al., 2016); my hypothesis would support these findings.

I have further identified that *Foxp3* transcription is activated and maintained in 2^{o} infection, similar to 1^{o} infection. In addition, I have shown disproportionate expansion of the non-regulatory T-cell population, which are enriched with memory-phenotype T-cells. Considering both newly initiated and Persistent *Foxp3* transcription occurs within CD4^{+} T-cells upon 2^{o} infection, it is unlikely that Treg expansion or polarisation is prevented by direct

inhibition of *Foxp3* transcription. It is more likely that an indirect mechanism selectively allows the rapid expansion of memory-phenotype T-cells. Indeed, it is of note that CD25 expression, where CD25 is highly expressed on Treg precursors, is greatly reduced in non-regulatory T-cells but not Treg during 2^o infection; this may be a key indicator of a potential mechanism, further discussed in Chapter 5.1.1.

I find evidence for TCR signalling inhibition in 1^o infection. This finding was in line with a decreased activation state and increased PD-L2 expression on DCs in my data. In the literature, the APC activation state has been found to be modified by *H. polygyrus* secretions (Balic et al., 2009; Sun et al., 2013). However, decreased TCR signalling is in contrast to the increase in *Foxp3* transcription in my data, as *Foxp3* expression and TCR signalling are considered intrinsically linked (Bandukwala and Rao, 2013). There therefore appears to be a change in the relationship between TCR signalling and *Foxp3* transcription induced by *H. polygyrus* infection. This could be a consequence of *Hp*-TGM, as *Hp*-TGM signalling was identified to induce higher *Foxp3* expression than TGF-β signalling (Johnston et al., 2017).

Ono and Tanaka suggest that post-infection resolution, a small proportion of Teff and Treg survive as Tmem and memory Treg; and that these cells are likely to exist as either of these forms dependent on *Foxp3* regulation at any one time (Ono and Tanaka, 2015). This hypothesis fits with the findings of Pelly *et al.* who describe that ex-Treg in 2^o *H. polygyrus* infection gain an effector Th2 phenotype and contribute to the effective anti-parasite T-cell response (Pelly et al., 2017). Considering that my data identified *Foxp3* expression within activated T-cells, we can assume that these cells contain anti-helminth T-cells. Loss of *Foxp3* transcription, particularly within anti-helminth T-cells but also the wider infection-reactive

memory Treg pool, would thus allow for effector Th2 mechanisms upon re-infection. In this way, the findings of Pelly *et al.* support the data presented in this thesis.

5.1.1 A potential model explaining the delayed Treg response

Once 1^{o} infection has resolved, the pool of activated T-cells must contract to prevent excessive tissue damage and chronic inflammation. Most effector T-cells undergo apoptosis, whilst a fraction remains to differentiate into the memory T-cell pool. In the absence of cognate antigen, effector T-cell activity is not required and receptors such as CD25 are downregulated on memory T-cells. Expression of GITR most likely remains within the memory T-cell pool. The presence of GITR on the memory T-cell surface would allow for rapid T-cell proliferation upon re-stimulation with cognate antigen. Indeed, van Olffen *et al.* described that GITR ligation by its ligand, GITRL, enhances proliferation of both Teff and Treg impartially, rather than promoting differentiation from naïve T-cells (van Olffen et al., 2009).

In this thesis, I identified a significant decrease in the proportion of non-regulatory T-cells expressing CD25 in 2^{o} infection. The non-regulatory T-cell population within 2^{o} infection is likely predominantly composed of infection-reactive Tmem, since this population expanded rapidly upon re-infection. However, it is important to note that the non-regulatory T-cell pool here is likely comprised of parasite-specific and self-antigen reactive Tmem and Teff, in addition to self-reactive memory-like T-cells. Nonetheless, expansion of this pool would suggest that Tmem are able to proliferate in response to cognate antigen prior to the upregulation of CD25. This finding is fundamentally important; IL-2 signalling through the high affinity IL-2R promotes *Foxp3* transcription, likely acting as a downstream negative feedback mechanism of T-cell activation (Burchill et al., 2007; Ono and Tanaka, 2015; Soper et al., 2007;

Yao et al., 2007). As such, a delay in the upregulation of CD25 allows the proliferation of Tmem before *Foxp3* transcription can limit the response.

When taken in combination with the findings of Pelly *et al.* and the proposed memory T-cell dynamics from Ono and Tanaka, (Ono and Tanaka, 2015; Pelly et al., 2017), I hypothesise that upon infection resolution, the infection-reactive memory T-cell pool is formed of Tmem and Treg. A proportion of Treg arrest their *Foxp3* expression, becoming Tmem. Thus, a larger proportion of the memory T-cell pool are Tmem than Treg. Upon re-infection and stimulation with cognate antigen, the larger Tmem population is thus able to expand much more than the Treg population. Augmenting this effect, ligation of GITR allows the proliferation of the Tmem population before the expression of CD25, thus delaying Treg "differentiation" and enabling an effective and efficient anti-parasite response (Figure 5.1).

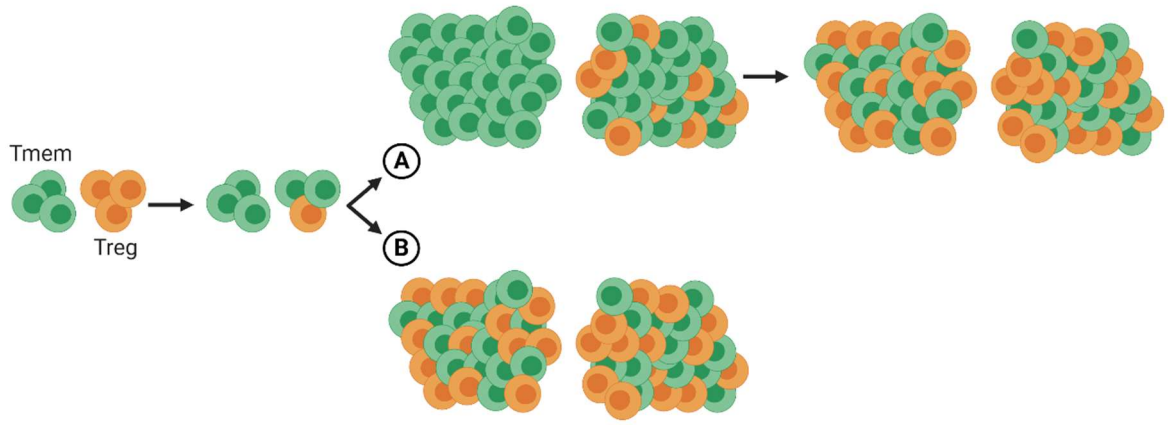


Figure 5.1: Proposed mechanism of an efficient memory T-cell response to H. polygyrus infection. Post-infection resolution, Treg (orange) may arrest their *Foxp3* transcriptional activities, joining the memory T-cell (Tmem, green) pool. As a result, the helminth-reactive Tmem pool is larger than the Treg pool. Upon re-infection, cognate antigen for the Tmem and Treg pool is presented by APCs. During antigen presentation and recognition, GITR on the Tmem and Treg cell surface is ligated, resulting in the rapid proliferation of Tmem and Treg cells before upregulation of CD25 can occur (A). The large number of Tmem cells are thus able to launch an efficient anti-helminth response on a large scale. Once CD25 is expressed on the T-cell surface, IL-2 signalling through the high affinity IL-2R promotes *Foxp3* transcription. A proportion of cells will develop the Treg phenotype, suppressing the anti-helminth response. If GITR ligation did not occur (B) an inefficient anti-helminth response would occur. Upon antigen stimulation, the Tmem and Treg would up-regulate CD25, promoting proliferation through IL-2 signalling. However, *Foxp3* transcription would also be promoted, reducing the ratio of Tmem to Treg and thus limiting the anti-helminth response.

5.1.2 Combining *Foxp3*-Timer and *Nr4a3*-Timer analyses

In my data, a trend is observed towards an increase in CD25 expression within the *Foxp3*-Timer Persistent locus, compared to the New and Arrested loci (Figure 3.3). Upon further confirmation, this would imply that Persistent, and thus sustained *Foxp3* transcription is associated with increased CD25 expression. CD25 expression is directly associated with T-cell activation and is another component transcribed downstream of TCR signalling. Indeed, within *Foxp3*-GFP$^+$ T-cells expressing *Nr4a3*-Timer, a subtle but similar trend is observed, where CD25 expression appears higher within the *Nr4a3*-Timer Persistent locus than the New or Arrested loci (Figure 4.10). This would suggest that the *Foxp3*-GFP$^+$ T-cells in the *Nr4a3*-Timer Persistent locus, and thus receiving sustained TCR signalling, are more activated than those in the New or Arrested loci. This trend is more subtle due to the inability to separate cells that had Arrested *Foxp3* transcription. It is likely that analysis of *Foxp3*-GFP$^+$ cells, excluding Arrested *Foxp3* transcription if it were possible, would show a higher association between the *Nr4a3*-Timer locus and CD25 expression in *Foxp3*-GFP$^+$ cells. Such a finding would suggest that a higher level of CD25 expression in Treg is associated with repeated TCR signalling. Based on the similar trends in CD25 expression, I hypothesise that the Treg within the *Foxp3*-Timer Persistent locus are likely the same cells as the *Foxp3*-GFP$^+$ T-cells within the Persistent *Nr4a3*-Timer locus, and that these Treg would have an effector Treg phenotype.

I identify that *Foxp3* transcription is induced at day-7 of infection, despite no increase in Persistent TCR signalling. Within the thymus, Persistent TCR signalling is associated with tTreg polarisation (Bending et al., 2018a). I hypothesise that the same occurs within the periphery, considering that both the thymus and the periphery require cognate antigen signalling for Treg polarisation. The threshold level of TCR signalling required for *Foxp3*

expression and therefore Treg polarisation could thus be reduced in *H. polygyrus* infection, likely by a soluble factor such as *Hp*-TGM. By reducing the threshold level, T-cells would be polarised to Treg earlier during inflammation and would thus have limited upregulation of co-inhibitory receptors, the expression of which is driven by TCR signalling. In line with this theory, I identify reduced expression of PD-1 within Treg during *H. polygyrus* infection. Reduced PD-1 expression would make these Treg less susceptible to PD-1 mediated suppression than Treg from other inflammatory conditions, thus allowing more efficient proliferation and potentially an enhanced Treg phenotype, as seen during PD-1 signalling blockade in a tumour model (Kamada et al., 2019). Reduced susceptibility to PD-1 mediated suppression could help to explain the findings that adoptive transfer of Treg from *H. polygyrus* infected mice into inflammatory models efficiently suppress the T-cell response to unrelated antigens (Bashir et al., 2002; Donskow-Lysoniewska et al., 2012; Hartmann et al., 2009; Kitagaki et al., 2006; Wilson et al., 2005). I hypothesise that Treg arising from *H. polygyrus* infection would have lower PD-1 expression than Treg from other inflammatory models, and thus a higher suppressive capacity. This hypothesis could be tested by harvesting Treg polarised *in vivo* at the contraction phase of a helminth-unrelated infection and comparing the PD-1 expression on these Treg to those within *H. polygyrus* infection. It would then be important to directly compare the suppressive capacity of these Treg *in vivo*, where Treg from helminth infection would be expected to be more immunosuppressive.

5.2 Mouse strain variation

Here, I used the C57BL/6 mouse strain to investigate T-cell responses to *H. polygyrus* infection. However, most studies regarding *H. polygyrus* utilise the BALB/c mouse strain. The

C57BL/6 mouse strain is widely associated with having a Th1 biased immune response, compared to a Th2 bias found in BALB/c mice (Kelso et al., 1991; Mills et al., 2000; Watanabe et al., 2004). Indeed, upon antigenic stimulation with the mitogen Con-A, splenic T-cells from C57BL/6 mice express high levels of IFN-γ and low levels of IL-4, associated with a Th1 phenotype, whereas BALB/c T-cells preferentially expressed IL-4 with only low levels of IFN-γ (Mills et al., 2000). A Th2 response is typically associated with helminth infections, and thus BALB/c mice would be expected to clear *H. polygyrus* infection more efficiently than C57BL/6 mice. This is reflected within the strain susceptibility to *H. polygyrus* infection, where C57BL/6 mice are susceptible and subject to chronic infection, whilst BALB/c mice are partially resistant and exhibit a much lower *H. polygyrus* burden by day-28 of infection (Reynolds et al., 2016; Smith et al., 2016).

Alongside the Th2 bias, BALB/c mice have also been shown to have a higher frequency of $CD4^+CD25^+Foxp3^+$ Treg than C57BL/6 mice (Chen et al., 2005). The decreased proportion of Treg induced within C57BL/6 mice is likely due to a reported reduction in IL-2 expression in these mice compared to BALB/c. IL-2 is essential for lymphocyte proliferation, and the polarisation of Treg, and thus the Treg proportion may be limited in this way (Chen et al., 2005; Malek, 2003). Most experiments regarding *H. polygyrus* infection utilise the BALB/c mouse strain for its evident Treg expansion, however, it is important to assess both a Th1 biased and Th2 biased immune response to obtain a full picture.

It is possible that the same *Foxp3* mechanisms identified within this thesis are occurring within BALB/c mice, potentially on a larger scale due to the higher expression of IL-2 and the association of IL-2 with both T-cell proliferation and with Treg. Alternatively, *Foxp3* mechanisms may differ greatly between strains. It would be of interest to look for the

proposed mechanism in Chapters 5.1.1 and 5.1.2 within BALB/c mice, as a higher endogenous level of IL-2 may result in earlier expression of CD25 and faster upregulation of co-inhibitory molecules. Further, key genetic differences, including MHC-II haplotype, may influence *Foxp3* expression, considering that *Foxp3* expression is downstream of TCR signalling and thus antigen presentation.

5.3 Use of the Tocky system

This thesis studied *H. polygyrus* infection using the Tocky system, allowing analysis of *in vivo* transcriptional dynamics of key genes; *Foxp3* and *Nr4a3*. Other fluorescent reporter systems are associated with a long fluorescence half-life, and therefore are unable to report real-time dynamics in the same way as the Tocky system, limiting such observations. The Tocky system has thus far been utilised to investigate central tolerance within the thymus (Bending et al., 2018a) and T-cell dynamics within the periphery in both a skin inflammatory setting and EAE (Bending et al., 2018b). This thesis studied peripheral tolerance within the intestinal system, an environment known for its tolerogenic nature. The potential use of the Tocky system within *in vivo* models is highly diverse and would form an extremely powerful tool when used in combination with other cutting-edge techniques. Indeed, I suggested that the use of the Tocky system in combination with single-cell RNA-seq and downstream analyses such as RNA-velocity could be incredibly informative regarding T-cell differentiation or plasticity during infection.

5.4 Overall conclusions

I aimed to further understand the mechanisms of T-cell regulation *in vivo*. I demonstrate that in primary *H. polygyrus* infection of C57BL/6 mice, activated T-cells express *Foxp3* for the first time, likely as a mechanism to prevent their own anti-helminth response. This new T-cell expression of *Foxp3* is in addition to pre-existing Treg, which are likely tTreg, upregulating *Foxp3* transcription in response to infection. Further elucidation of the contribution of these two responses to the helminth's ability to establish chronic infection could aid immunotherapeutic strategies in the future. For instance, key markers could identify more efficacious Treg for immunotherapy, potentially improving outcomes.

I also aimed to investigate the relationship between T-cell regulation and the memory response *in vivo*, where helminth clearance is efficient in secondary infection. I found that *Foxp3* transcriptional dynamics were similar in primary and secondary infection, making direct inhibition of *Foxp3* transcription and thus Treg activity unlikely. I identify that the non-regulatory T-cell population, enriched with Tmem, disproportionately expanded compared to Treg, likely explaining the lack of Treg response. To address this, I proposed a mechanism that would allow for the Tmem population to expand more rapidly than the Treg population upon re-infection. Further work would be required to establish whether this mechanism would be limited to *H. polygyrus* infection or could be applied to other inflammatory models.

My thesis utilised helminth infection to investigate T-cell responses. Helminths are incredibly successful pathogens world-wide, with many exploiting the same or similar mechanisms to evade the host immune response. There are therefore lessons that can be learnt through helminth infection that are not limited to anti-helminth therapies, but also may be applied to the development of immunotherapeutic strategies.

6 References

Akimova, T., Beier, U.H., Wang, L., Levine, M.H., and Hancock, W.W. (2011). Helios expression is a marker of T cell activation and proliferation. PLoS One *6*, e24226.

Anthony, R.M., Urban, J.F., Jr., Alem, F., Hamed, H.A., Rozo, C.T., Boucher, J.L., Van Rooijen, N., and Gause, W.C. (2006). Memory T(H)2 cells induce alternatively activated macrophages to mediate protection against nematode parasites. Nat Med *12*, 955-960.

Axtner, J., and Sommer, S. (2011). Heligmosomoides polygyrus infection is associated with lower MHC class II gene expression in Apodemus flavicollis: indication for immune suppression? Infect Genet Evol *11*, 2063-2071.

Balic, A., Smith, K.A., Harcus, Y., and Maizels, R.M. (2009). Dynamics of CD11c(+) dendritic cell subsets in lymph nodes draining the site of intestinal nematode infection. Immunol Lett *127*, 68-75.

Ballesteros-Tato, A., Leon, B., Graf, B.A., Moquin, A., Adams, P.S., Lund, F.E., and Randall, T.D. (2012). Interleukin-2 inhibits germinal center formation by limiting T follicular helper cell differentiation. Immunity *36*, 847-856.

Bandukwala, H.S., and Rao, A. (2013). 'Nurr'ishing Treg cells: Nr4a transcription factors control Foxp3 expression. Nature immunology *14*, 201-203.

Bashir, M.E., Andersen, P., Fuss, I.J., Shi, H.N., and Nagler-Anderson, C. (2002). An enteric helminth infection protects against an allergic response to dietary antigen. J Immunol *169*, 3284-3292.

Bauché, D., and Marie, J.C. (2017). Transforming growth factor β: a master regulator of the gut microbiota and immune cell interactions. Clinical & Translational Immunology *6*, e136.

Bauquet, A.T., Jin, H., Paterson, A.M., Mitsdoerffer, M., Ho, I.C., Sharpe, A.H., and Kuchroo, V.K. (2009). The costimulatory molecule ICOS regulates the expression of c-Maf and IL-21 in the development of follicular T helper cells and TH-17 cells. Nat Immunol *10*, 167-175.

Bedoret, D., Singh, A.K., Shaw, V., Hoyte, E.G., Hamilton, R., DeKruyff, R.H., Schneider, L.C., Nadeau, K.C., and Umetsu, D.T. (2012). Changes in antigen-specific T-cell number and function during oral desensitization in cow's milk allergy enabled with omalizumab. Mucosal Immunol *5*, 267-276.

Behnke, J.M., and Wahid, F.N. (1991). Immunological relationships during primary infection with Heligmosomoides polygyrus (Nematospiroides dubius): H-2 linked genes determine worm survival. Parasitology *103 Pt 1*, 157-164.

Behnke, J.M., Wahid, F.N., Grencis, R.K., Else, K.J., Ben-Smith, A.W., and Goyal, P.K. (1993). Immunological relationships during primary infection with Heligmosomoides polygyrus (Nematospiroides dubius): downregulation of specific cytokine secretion (IL-9 and IL-10) correlates with poor mastocytosis and chronic survival of adult worms. Parasite Immunol *15*, 415-421.

Behnke, J.M., and Wakelin, D. (1977). Nematospiroides dubius: stimulation of acquired immunity in inbred strains of mice. J Helminthol *51*, 167-176.

Bending, D., Martín, P.P., Paduraru, A., Ducker, C., Marzaganov, E., Laviron, M., Kitano, S., Miyachi, H., Crompton, T., and Ono, M. (2018a). A timer for analyzing temporally dynamic changes in transcription during differentiation in vivo. The Journal of Cell Biology *217*, 2931-2950.

Bending, D., Paduraru, A., Ducker, C.B., Prieto Martin, P., Crompton, T., and Ono, M. (2018b). A temporally dynamic Foxp3 autoregulatory transcriptional circuit controls the effector Treg programme. Embo j *37*.

Bour-Jordan, H., Esensten, J.H., Martinez-Llordella, M., Penaranda, C., Stumpf, M., and Bluestone, J.A. (2011). Intrinsic and extrinsic control of peripheral T-cell tolerance by costimulatory molecules of the CD28/ B7 family. Immunological Reviews *241*, 180-205.

Bryant, V. (1973). The life cycle of Nematospiroides dubius, Baylis, 1926 (Nematoda: Heligmosomidae). J Helminthol *47*, 263-268.

Buck, A.H., Coakley, G., Simbari, F., McSorley, H.J., Quintana, J.F., Le Bihan, T., Kumar, S., Abreu-Goodger, C., Lear, M., Harcus, Y.*, et al.* (2014). Exosomes secreted by nematode parasites transfer small RNAs to mammalian cells and modulate innate immunity. Nat Commun *5*, 5488.

Burchill, M.A., Yang, J., Vogtenhuber, C., Blazar, B.R., and Farrar, M.A. (2007). IL-2 receptor beta-dependent STAT5 activation is required for the development of Foxp3+ regulatory T cells. J Immunol *178*, 280-290.

Busse, D., de la Rosa, M., Hobiger, K., Thurley, K., Flossdorf, M., Scheffold, A., and Höfer, T. (2010). Competing feedback loops shape IL-2 signaling between helper and regulatory T lymphocytes in cellular microenvironments. Proceedings of the National Academy of Sciences of the United States of America *107*, 3058-3063.

Campbell, D.J., and Butcher, E.C. (2002). Rapid Acquisition of Tissue-specific Homing Phenotypes by CD4+ T Cells Activated in Cutaneous or Mucosal Lymphoid Tissues. The Journal of Experimental Medicine *195*, 135-141.

Chen, L., and Flies, D.B. (2013). Molecular mechanisms of T cell co-stimulation and co-inhibition. Nature reviews Immunology *13*, 227-242.

Chen, W., Jin, W., Hardegen, N., Lei, K.J., Li, L., Marinos, N., McGrady, G., and Wahl, S.M. (2003). Conversion of peripheral CD4+CD25- naive T cells to CD4+CD25+ regulatory T cells by TGF-beta induction of transcription factor Foxp3. J Exp Med *198*, 1875-1886.

Chen, W., and Konkel, J.E. (2015). Development of thymic Foxp3(+) regulatory T cells: TGF-β matters. European journal of immunology *45*, 958-965.

Chen, X., Oppenheim, J.J., and Howard, O.M. (2005). BALB/c mice have more CD4+CD25+ T regulatory cells and show greater susceptibility to suppression of their CD4+CD25- responder T cells than C57BL/6 mice. J Leukoc Biol *78*, 114-121.

Chi, V., Pennington, M.W., Norton, R.S., Tarcha, E.J., Londono, L.M., Sims-Fahey, B., Upadhyay, S.K., Lakey, J.T., Iadonato, S., Wulff, H.*, et al.* (2012). Development of a sea anemone toxin as an immunomodulator for therapy of autoimmune diseases. Toxicon *59*, 529-546.

Clouthier, D.L., and Watts, T.H. (2014). Cell-specific and context-dependent effects of GITR in cancer, autoimmunity, and infection. Cytokine & Growth Factor Reviews *25*, 91-106.

Coakley, G., McCaskill, J.L., Borger, J.G., Simbari, F., Robertson, E., Millar, M., Harcus, Y., McSorley, H.J., Maizels, R.M., and Buck, A.H. (2017). Extracellular Vesicles from a Helminth Parasite Suppress Macrophage Activation and Constitute an Effective Vaccine for Protective Immunity. Cell Rep *19*, 1545-1557.

Corry, D.B., and Kheradmand, F. (1999). Induction and regulation of the IgE response. Nature *402*, B18-23.

Cretney, E., Kallies, A., and Nutt, S.L. (2013). Differentiation and function of Foxp3+ effector regulatory T cells. Trends in Immunology *34*, 74-80.

Croft, M., So, T., Duan, W., and Soroosh, P. (2009). The significance of OX40 and OX40L to T-cell biology and immune disease. Immunological reviews *229*, 173-191.

Crotty, S. (2011). Follicular helper CD4 T cells (TFH). Annu Rev Immunol *29*, 621-663.

Crotty, S. (2014). T follicular helper cell differentiation, function, and roles in disease. Immunity *41*, 529-542.

Curotto de Lafaille, M.A., Lino, A.C., Kutchukhidze, N., and Lafaille, J.J. (2004). CD25- T cells generate CD25+Foxp3+ regulatory T cells by peripheral expansion. J Immunol *173*, 7259-7268.

D'Elia, R., Behnke, J.M., Bradley, J.E., and Else, K.J. (2009). Regulatory T cells: a role in the control of helminth-driven intestinal pathology and worm survival. J Immunol *182*, 2340-2348.

Da'dara, A.A., Bhardwaj, R., Ali, Y.B., and Skelly, P.J. (2014). Schistosome tegumental ecto-apyrase (SmATPDase1) degrades exogenous pro-inflammatory and pro-thrombotic nucleotides. PeerJ *2*, e316.

Donskow-Lysoniewska, K., Krawczak, K., and Doligalska, M. (2012). Heligmosomoides polygyrus: EAE remission is correlated with different systemic cytokine profiles provoked by L4 and adult nematodes. Exp Parasitol *132*, 243-248.

Duarte, J.H., Zelenay, S., Bergman, M.L., Martins, A.C., and Demengeot, J. (2009). Natural Treg cells spontaneously differentiate into pathogenic helper cells in lymphopenic conditions. European Journal of Immunology *39*, 948-955.

Filbey, K.J., Grainger, J.R., Smith, K.A., Boon, L., van Rooijen, N., Harcus, Y., Jenkins, S., Hewitson, J.P., and Maizels, R.M. (2014). Innate and adaptive type 2 immune cell responses in genetically controlled resistance to intestinal helminth infection. Immunol Cell Biol *92*, 436-448.

Finkelman, F.D., Shea-Donohue, T., Goldhill, J., Sullivan, C.A., Morris, S.C., Madden, K.B., Gause, W.C., and Urban, J.F., Jr. (1997). Cytokine regulation of host defense against parasitic gastrointestinal nematodes: lessons from studies with rodent models. Annu Rev Immunol *15*, 505-533.

Finney, C.A., Taylor, M.D., Wilson, M.S., and Maizels, R.M. (2007). Expansion and activation of CD4(+)CD25(+) regulatory T cells in Heligmosomoides polygyrus infection. Eur J Immunol *37*, 1874-1886.

Floess, S., Freyer, J., Siewert, C., Baron, U., Olek, S., Polansky, J., Schlawe, K., Chang, H.-D., Bopp, T., Schmitt, E.*, et al.* (2007). Epigenetic control of the foxp3 locus in regulatory T cells. PLoS biology *5*, e38-e38.

Fontenot, J.D., Gavin, M.A., and Rudensky, A.Y. (2003). Foxp3 programs the development and function of CD4+CD25+ regulatory T cells. NatImmunol *4*, 330-336.

Fort, M.M., Cheung, J., Yen, D., Li, J., Zurawski, S.M., Lo, S., Menon, S., Clifford, T., Hunte, B., Lesley, R.*, et al.* (2001). IL-25 induces IL-4, IL-5, and IL-13 and Th2-associated pathologies in vivo. Immunity *15*, 985-995.

Friedman, A., and Weiner, H.L. (1994). Induction of anergy or active suppression following oral tolerance is determined by antigen dosage. Proc Natl Acad Sci U S A *91*, 6688-6692.

Fujihashi, K., Dohi, T., Rennert, P.D., Yamamoto, M., Koga, T., Kiyono, H., and McGhee, J.R. (2001). Peyer's patches are required for oral tolerance to proteins. Proc Natl Acad Sci U S A *98*, 3310-3315.

Furze, R.C., Culley, F.J., and Selkirk, M.E. (2006). Differential roles of the co-stimulatory molecules GITR and CTLA-4 in the immune response to Trichinella spiralis. Microbes Infect *8*, 2803-2810.

Gaffen, S.L. (2001). Signaling domains of the interleukin 2 receptor. Cytokine *14*, 63-77.

Gause, W.C., Lu, P., Zhou, X.D., Chen, S.J., Madden, K.B., Morris, S.C., Linsley, P.S., Finkelman, F.D., and Urban, J.F. (1996). H. polygyrus: B7-independence of the secondary type 2 response. Exp Parasitol *84*, 264-273.

Gavin, M.A., Rasmussen, J.P., Fontenot, J.D., Vasta, V., Manganiello, V.C., Beavo, J.A., and Rudensky, A.Y. (2007). Foxp3-dependent programme of regulatory T-cell differentiation. Nature *445*, 771-775.

Glatman Zaretsky, A., Taylor, J.J., King, I.L., Marshall, F.A., Mohrs, M., and Pearce, E.J. (2009). T follicular helper cells differentiate from Th2 cells in response to helminth antigens. J Exp Med *206*, 991-999.

Goldstein, J.D., Pérol, L., Zaragoza, B., Baeyens, A., Marodon, G., and Piaggio, E. (2013). Role of cytokines in thymus- versus peripherally derived-regulatory T cell differentiation and function. Frontiers in immunology *4*, 155-155.

Good-Jacobson, K.L., Szumilas, C.G., Chen, L., Sharpe, A.H., Tomayko, M.M., and Shlomchik, M.J. (2010). PD-1 regulates germinal center B cell survival and the formation and affinity of long-lived plasma cells. Nature immunology *11*, 535-542.

Gounaris, K., Selkirk, M.E., and Sadeghi, S.J. (2004). A nucleotidase with unique catalytic properties is secreted by Trichinella spiralis. Mol Biochem Parasitol *136*, 257-264.

Grainger, J.R., Smith, K.A., Hewitson, J.P., McSorley, H.J., Harcus, Y., Filbey, K.J., Finney, C.A.M., Greenwood, E.J.D., Knox, D.P., Wilson, M.S.*, et al.* (2010). Helminth secretions induce de novo T cell Foxp3 expression and regulatory function through the TGF-β pathway. The Journal of experimental medicine *207*, 2331-2341.

Ha, H., Han, D., and Choi, Y. (2009). TRAF-mediated TNFR-family signaling. Curr Protoc Immunol *Chapter 11*, Unit11.19D.

Hammerschmidt, S.I., Ahrendt, M., Bode, U., Wahl, B., Kremmer, E., Forster, R., and Pabst, O. (2008). Stromal mesenteric lymph node cells are essential for the generation of gut-homing T cells in vivo. J Exp Med *205*, 2483-2490.

Hammerschmidt, S.I., Friedrichsen, M., Boelter, J., Lyszkiewicz, M., Kremmer, E., Pabst, O., and Förster, R. (2011). Retinoic acid induces homing of protective T and B cells to the gut after subcutaneous immunization in mice. Journal of Clinical Investigation *121*, 3051-3061.

Haque, A., Stanley, A.C., Amante, F.H., Rivera Fde, L., Zhou, Y., Kuns, R.D., Yardley, V., Sakaguchi, S., Hill, G.R., and Engwerda, C.R. (2010). Therapeutic glucocorticoid-induced TNF receptor-mediated amplification of CD4+ T cell responses enhances antiparasitic immunity. J Immunol *184*, 2583-2592.

Hartmann, S., Schnoeller, C., Dahten, A., Avagyan, A., Rausch, S., Lendner, M., Bocian, C., Pillai, S., Loddenkemper, C., Lucius, R.*, et al.* (2009). Gastrointestinal nematode infection interferes with experimental allergic airway inflammation but not atopic dermatitis. Clin Exp Allergy *39*, 1585-1596.

Haynes, N.M., Allen, C.D., Lesley, R., Ansel, K.M., Killeen, N., and Cyster, J.G. (2007). Role of CXCR5 and CCR7 in follicular Th cell positioning and appearance of a programmed cell death gene-1high germinal center-associated subpopulation. J Immunol *179*, 5099-5108.

Hepworth, M.R., Maurer, M., and Hartmann, S. (2012). Regulation of type 2 immunity to helminths by mast cells. Gut Microbes *3*, 476-481.

Hewitson, J.P., Filbey, K.J., Grainger, J.R., Dowle, A.A., Pearson, M., Murray, J., Harcus, Y., and Maizels, R.M. (2011a). Heligmosomoides polygyrus elicits a dominant nonprotective antibody response directed against restricted glycan and peptide epitopes. J Immunol *187*, 4764-4777.

Hewitson, J.P., Harcus, Y., Murray, J., van Agtmaal, M., Filbey, K.J., Grainger, J.R., Bridgett, S., Blaxter, M.L., Ashton, P.D., Ashford, D.A.*, et al.* (2011b). Proteomic analysis of secretory products from the model gastrointestinal nematode Heligmosomoides polygyrus reveals dominance of venom allergen-like (VAL) proteins. J Proteomics *74*, 1573-1594.

Hewitson, J.P., Ivens, A.C., Harcus, Y., Filbey, K.J., McSorley, H.J., Murray, J., Bridgett, S., Ashford, D., Dowle, A.A., and Maizels, R.M. (2013). Secretion of protective antigens by tissue-stage nematode larvae revealed by proteomic analysis and vaccination-induced sterile immunity. PLoS Pathog *9*, e1003492.

Hori, S., Nomura, T., and Sakaguchi, S. (2003). Control of regulatory T cell development by the transcription factor Foxp3. Science *299*, 1057-1061.

Howard, M., Farrar, J., Hilfiker, M., Johnson, B., Takatsu, K., Hamaoka, T., and Paul, W.E. (1982). Identification of a T cell-derived b cell growth factor distinct from interleukin 2. J Exp Med *155*, 914-923.

Hsieh, C.-S., Lee, H.-M., and Lio, C.-W.J. (2012). Selection of regulatory T cells in the thymus. Nature Reviews Immunology *12*, 157-167.

Hui, E., Cheung, J., Zhu, J., Su, X., Taylor, M.J., Wallweber, H.A., Sasmal, D.K., Huang, J., Kim, J.M., Mellman, I.*, et al.* (2017). T cell costimulatory receptor CD28 is a primary target for PD-1-mediated inhibition. Science *355*, 1428-1433.

Igarashi, H., Cao, Y., Iwai, H., Piao, J., Kamimura, Y., Hashiguchi, M., Amagasa, T., and Azuma, M. (2008). GITR ligand-costimulation activates effector and regulatory functions of CD4+ T cells. Biochem Biophys Res Commun *369*, 1134-1138.

Jaensson-Gyllenbäck, E., Kotarsky, K., Zapata, F., Persson, E.K., Gundersen, T.E., Blomhoff, R., and Agace, W.W. (2011). Bile retinoids imprint intestinal CD103(+) dendritic cells with the ability to generate gut-tropic T cells. Mucosal Immunology *4*, 438-447.

Jennings, E., Kanabar, S., Ono, M., Wraith, D.C., and Bending, D. (2019). Distinct regulation of Nr4a receptors by NFAT and ERK signalling during T cell activation. bioRxiv, 767566.

Ji, H.B., Liao, G., Faubion, W.A., Abadia-Molina, A.C., Cozzo, C., Laroux, F.S., Caton, A., and Terhorst, C. (2004). Cutting edge: the natural ligand for glucocorticoid-induced TNF receptor-related protein abrogates regulatory T cell suppression. J Immunol *172*, 5823-5827.

Johansson-Lindbom, B., Svensson, M., Pabst, O., Palmqvist, C., Marquez, G., Förster, R., and Agace, W.W. (2005). Functional specialization of gut CD103+ dendritic cells in the regulation of tissue-selective T cell homing. Journal of Experimental Medicine *202*, 1063-1073.

Johnston, C.J.C., Smyth, D.J., Kodali, R.B., White, M.P.J., Harcus, Y., Filbey, K.J., Hewitson, J.P., Hinck, C.S., Ivens, A., Kemter, A.M.*, et al.* (2017). A structurally distinct TGF-beta mimic from an intestinal helminth parasite potently induces regulatory T cells. Nat Commun *8*, 1741.

Jordan, M.S., Boesteanu, A., Reed, A.J., Petrone, A.L., Holenbeck, A.E., Lerman, M.A., Naji, A., and Caton, A.J. (2001). Thymic selection of CD4+CD25+ regulatory T cells induced by an agonist self-peptide. Nat Immunol *2*, 301-306.

Kamada, T., Togashi, Y., Tay, C., Ha, D., Sasaki, A., Nakamura, Y., Sato, E., Fukuoka, S., Tada, Y., Tanaka, A.*, et al.* (2019). PD-1(+) regulatory T cells amplified by PD-1 blockade promote hyperprogression of cancer. Proceedings of the National Academy of Sciences of the United States of America *116*, 9999-10008.

Kanamaru, F., Youngnak, P., Hashiguchi, M., Nishioka, T., Takahashi, T., Sakaguchi, S., Ishikawa, I., and Azuma, M. (2004). Costimulation via glucocorticoid-induced TNF receptor in both conventional and CD25+ regulatory CD4+ T cells. J Immunol *172*, 7306-7314.

Keir, M.E., Butte, M.J., Freeman, G.J., and Sharpe, A.H. (2008). PD-1 and its ligands in tolerance and immunity. Annu Rev Immunol *26*, 677-704.

Kelso, A., Troutt, A.B., Maraskovsky, E., Gough, N.M., Morris, L., Pech, M.H., and Thomson, J.A. (1991). Heterogeneity in lymphokine profiles of CD4+ and CD8+ T cells and clones activated in vivo and in vitro. Immunol Rev *123*, 85-114.

Khattri, R., Cox, T., Yasayko, S.A., and Ramsdell, F. (2003). An essential role for Scurfin in CD4+CD25+ T regulatory cells. Nat Immunol *4*, 337-342.

Kim, H.P., Imbert, J., and Leonard, W.J. (2006). Both integrated and differential regulation of components of the IL-2/IL-2 receptor system. Cytokine Growth Factor Rev *17*, 349-366.

King, I.L., Mohrs, K., and Mohrs, M. (2010). A nonredundant role for IL-21 receptor signaling in plasma cell differentiation and protective type 2 immunity against gastrointestinal helminth infection. J Immunol *185*, 6138-6145.

King, I.L., and Mohrs, M. (2009). IL-4-producing CD4+ T cells in reactive lymph nodes during helminth infection are T follicular helper cells. J Exp Med *206*, 1001-1007.

Kitagaki, K., Businga, T.R., Racila, D., Elliott, D.E., Weinstock, J.V., and Kline, J.N. (2006). Intestinal helminths protect in a murine model of asthma. J Immunol *177*, 1628-1635.

Krummel, M.F., and Allison, J.P. (1995). CD28 and CTLA-4 have opposing effects on the response of T cells to stimulation. The Journal of experimental medicine *182*, 459-465.

La Manno, G., Soldatov, R., Zeisel, A., Braun, E., Hochgerner, H., Petukhov, V., Lidschreiber, K., Kastriti, M.E., Lonnerberg, P., Furlan, A*., et al.* (2018). RNA velocity of single cells. Nature *560*, 494-498.

Latchman, Y., Wood, C.R., Chernova, T., Chaudhary, D., Borde, M., Chernova, I., Iwai, Y., Long, A.J., Brown, J.A., Nunes, R*., et al.* (2001). PD-L2 is a second ligand for PD-1 and inhibits T cell activation. Nat Immunol *2*, 261-268.

Liao, G., Nayak, S., Regueiro, J.R., Berger, S.B., Detre, C., Romero, X., de Waal Malefyt, R., Chatila, T.A., Herzog, R.W., and Terhorst, C. (2010). GITR engagement preferentially enhances proliferation of functionally competent CD4+CD25+FoxP3+ regulatory T cells. Int Immunol *22*, 259-270.

Liao, W., Lin, J.-X., and Leonard, W.J. (2011). IL-2 family cytokines: new insights into the complex roles of IL-2 as a broad regulator of T helper cell differentiation. Current opinion in immunology *23*, 598-604.

Liao, W., Schones, D.E., Oh, J., Cui, Y., Cui, K., Roh, T.Y., Zhao, K., and Leonard, W.J. (2008). Priming for T helper type 2 differentiation by interleukin 2-mediated induction of interleukin 4 receptor alpha-chain expression. Nat Immunol *9*, 1288-1296.

Lin, J.X., and Leonard, W.J. (2000). The role of Stat5a and Stat5b in signaling by IL-2 family cytokines. Oncogene *19*, 2566-2576.

Lippolis, J.D., White, F.M., Marto, J.A., Luckey, C.J., Bullock, T.N., Shabanowitz, J., Hunt, D.F., and Engelhard, V.H. (2002). Analysis of MHC class II antigen processing by quantitation of peptides that constitute nested sets. J Immunol *169*, 5089-5097.

Liu, Y., Beyer, A., and Aebersold, R. (2016). On the Dependency of Cellular Protein Levels on mRNA Abundance. Cell *165*, 535-550.

Liu, Y., Zhang, P., Li, J., Kulkarni, A.B., Perruche, S., and Chen, W. (2008). A critical function for TGF-beta signaling in the development of natural CD4+CD25+Foxp3+ regulatory T cells. Nat Immunol *9*, 632-640.

Loke, P., Gallagher, I., Nair, M.G., Zang, X., Brombacher, F., Mohrs, M., Allison, J.P., and Allen, J.E. (2007). Alternative activation is an innate response to injury that requires CD4+ T cells to be sustained during chronic infection. J Immunol *179*, 3926-3936.

Long, M., Park, S.-G., Strickland, I., Hayden, M.S., and Ghosh, S. (2009). Nuclear Factor-κB Modulates Regulatory T Cell Development by Directly Regulating Expression of Foxp3 Transcription Factor. Immunity *31*, 921-931.

Loser, S., Smith, K.A., and Maizels, R.M. (2019). Innate Lymphoid Cells in Helminth Infections-Obligatory or Accessory? Front Immunol *10*, 620.

Love, M.I., Huber, W., and Anders, S. (2014). Moderated estimation of fold change and dispersion for RNA-seq data with DESeq2. Genome Biol *15*, 550.

MacDonald, A.S., and Maizels, R.M. (2008). Alarming dendritic cells for Th2 induction. J Exp Med *205*, 13-17.

MacLeod, M.K.L., Clambey, E.T., Kappler, J.W., and Marrack, P. (2009). CD4 memory T cells: what are they and what can they do? Seminars in immunology *21*, 53-61.

Mahmud, S.A., Manlove, L.S., Schmitz, H.M., Xing, Y., Wang, Y., Owen, D.L., Schenkel, J.M., Boomer, J.S., Green, J.M., Yagita, H.*, et al.* (2014). Costimulation via the tumor-necrosis factor receptor superfamily couples TCR signal strength to the thymic differentiation of regulatory T cells. Nature Immunology *15*, 473-481.

Maizels, R.M., Hewitson, J.P., Murray, J., Harcus, Y.M., Dayer, B., Filbey, K.J., Grainger, J.R., McSorley, H.J., Reynolds, L.A., and Smith, K.A. (2012). Immune modulation and modulators in Heligmosomoides polygyrus infection. Experimental parasitology *132*, 76-89.

Malek, T.R. (2003). The main function of IL-2 is to promote the development of T regulatory cells. J Leukoc Biol *74*, 961-965.

Mantel, P.Y., Ouaked, N., Ruckert, B., Karagiannidis, C., Welz, R., Blaser, K., and Schmidt-Weber, C.B. (2006). Molecular Mechanisms Underlying FOXP3 Induction in Human T Cells. *176*, 3593-3602.

Marie, J.C., Letterio, J.J., Gavin, M., and Rudensky, A.Y. (2005). TGF-beta1 maintains suppressor function and Foxp3 expression in CD4+CD25+ regulatory T cells. J Exp Med *201*, 1061-1067.

McCoy, K.D., Stoel, M., Stettler, R., Merky, P., Fink, K., Senn, B.M., Schaer, C., Massacand, J., Odermatt, B., Oettgen, H.C.*, et al.* (2008). Polyclonal and specific antibodies mediate protective immunity against enteric helminth infection. Cell Host Microbe *4*, 362-373.

McSorley, H.J., and Maizels, R.M. (2012). Helminth infections and host immune regulation. Clin Microbiol Rev *25*, 585-608.

McSorley, H.J., O'Gorman, M.T., Blair, N., Sutherland, T.E., Filbey, K.J., and Maizels, R.M. (2012). Suppression of type 2 immunity and allergic airway inflammation by secreted products of the helminth Heligmosomoides polygyrus. European Journal of Immunology *42*, 2667-2682.

Mills, C.D., Kincaid, K., Alt, J.M., Heilman, M.J., and Hill, A.M. (2000). M-1/M-2 macrophages and the Th1/Th2 paradigm. J Immunol *164*, 6166-6173.

Miyao, T., Floess, S., Setoguchi, R., Luche, H., Fehling, H.J., Waldmann, H., Huehn, J., and Hori, S. (2012). Plasticity of Foxp3(+) T cells reflects promiscuous Foxp3 expression in conventional T cells but not reprogramming of regulatory T cells. Immunity *36*, 262-275.

Mizuno, R., Sugiura, D., Shimizu, K., Maruhashi, T., Watada, M., Okazaki, I.M., and Okazaki, T. (2019). PD-1 Primarily Targets TCR Signal in the Inhibition of Functional T Cell Activation. Front Immunol *10*, 630.

Mohrs, K., Harris, D.P., Lund, F.E., and Mohrs, M. (2005). Systemic dissemination and persistence of Th2 and type 2 cells in response to infection with a strictly enteric nematode parasite. J Immunol *175*, 5306-5313.

Mohrs, M., Shinkai, K., Mohrs, K., and Locksley, R.M. (2001). Analysis of type 2 immunity in vivo with a bicistronic IL-4 reporter. Immunity *15*, 303-311.

Mora, J.R., Bono, M.R., Manjunath, N., Weninger, W., Cavanagh, L.L., Rosemblatt, M., and Von Andrian, U.H. (2003). Selective imprinting of gut-homing T cells by Peyer's patch dendritic cells. Nature *424*, 88-93.

Moran, A.E., Holzapfel, K.L., Xing, Y., Cunningham, N.R., Maltzman, J.S., Punt, J., and Hogquist, K.A. (2011). T cell receptor signal strength in Treg and iNKT cell development demonstrated by a novel fluorescent reporter mouse. J Exp Med *208*, 1279-1289.

Moriggl, R., Topham, D.J., Teglund, S., Sexl, V., McKay, C., Wang, D., Hoffmeyer, A., van Deursen, J., Sangster, M.Y., Bunting, K.D.*, et al.* (1999). Stat5 is required for IL-2-induced cell cycle progression of peripheral T cells. Immunity *10*, 249-259.

Mowat, A.M. (2003). Anatomical basis of tolerance and immunity to intestinal antigens. Nature Reviews Immunology *3*, 331-341.

Nurieva, R.I., Chung, Y., Hwang, D., Yang, X.O., Kang, H.S., Ma, L., Wang, Y.H., Watowich, S.S., Jetten, A.M., Tian, Q.*, et al.* (2008). Generation of T follicular helper cells is mediated by interleukin-21 but independent of T helper 1, 2, or 17 cell lineages. Immunity *29*, 138-149.

Oderup, C., Cederbom, L., Makowska, A., Cilio, C.M., and Ivars, F. (2006). Cytotoxic T lymphocyte antigen-4-dependent down-modulation of costimulatory molecules on dendritic cells in CD4+ CD25+ regulatory T-cell-mediated suppression. Immunology *118*, 240-249.

Ono, M., Shimizu J Fau - Miyachi, Y., Miyachi Y Fau - Sakaguchi, S., and Sakaguchi, S. (2006). Control of autoimmune myocarditis and multiorgan inflammation by glucocorticoid-induced TNF receptor family-related protein(high), Foxp3-expressing CD25+ and CD25- regulatory T cells. Journal of Immunology *176*, 4748-4756.

Ono, M., and Tanaka, R.J. (2015). Controversies concerning thymus-derived regulatory T cells: fundamental issues and a new perspective. Immunology and Cell Biology *94*, 3-10.

Osborne, B.A., Smith, S.W., Liu, Z.G., McLaughlin, K.A., Grimm, L., and Schwartz, L.M. (1994). Identification of genes induced during apoptosis in T lymphocytes. Immunol Rev *142*, 301-320.

Osbourn, M., Soares, D.C., Vacca, F., Cohen, E.S., Scott, I.C., Gregory, W.F., Smyth, D.J., Toivakka, M., Kemter, A.M., le Bihan, T.*, et al.* (2017). HpARI Protein Secreted by a Helminth Parasite Suppresses Interleukin-33. Immunity *47*, 739-751.e735.

Pabst, O., and Mowat, A.M. (2012). Oral tolerance to food protein. Mucosal Immunol *5*, 232-239.

Pardee, A.B. (1989). G1 events and regulation of cell proliferation. Science *246*, 603-608.

Patel, N., Wu, W., Mishra, P.K., Chen, F., Millman, A., Csoka, B., Koscso, B., Eltzschig, H.K., Hasko, G., and Gause, W.C. (2014). A2B adenosine receptor induces protective antihelminth type 2 immune responses. Cell Host Microbe *15*, 339-350.

Patro, R., Duggal, G., Love, M.I., Irizarry, R.A., and Kingsford, C. (2017). Salmon provides fast and bias-aware quantification of transcript expression. Nat Methods *14*, 417-419.

Pelly, V.S., Coomes, S.M., Kannan, Y., Gialitakis, M., Entwistle, L.J., Perez-Lloret, J., Czieso, S., Okoye, I.S., Rückerl, D., Allen, J.E.*, et al.* (2017). Interleukin 4 promotes the development of ex-Foxp3 Th2 cells during immunity to intestinal helminths. The Journal of experimental medicine *214*, 1809-1826.

Pelly, V.S., Kannan, Y., Coomes, S.M., Entwistle, L.J., Ruckerl, D., Seddon, B., MacDonald, A.S., McKenzie, A., and Wilson, M.S. (2016). IL-4-producing ILC2s are required for the differentiation of TH2 cells following Heligmosomoides polygyrus infection. Mucosal Immunol *9*, 1407-1417.

Phythian-Adams, A.T., Cook, P.C., Lundie, R.J., Jones, L.H., Smith, K.A., Barr, T.A., Hochweller, K., Anderton, S.M., Hammerling, G.J., Maizels, R.M.*, et al.* (2010). CD11c depletion severely disrupts Th2 induction and development in vivo. J Exp Med *207*, 2089-2096.

Picelli, S., Faridani, O.R., Björklund, Å.K., Winberg, G., Sagasser, S., and Sandberg, R. (2014). Full-length RNA-seq from single cells using Smart-seq2. Nature Protocols *9*, 171.

Qureshi, O.S., Zheng, Y., Nakamura, K., Attridge, K., Manzotti, C., Schmidt, E.M., Baker, J., Jeffery, L.E., Kaur, S., Briggs, Z.*, et al.* (2011). Trans-endocytosis of CD80 and CD86: a molecular basis for the cell-extrinsic function of CTLA-4. Science *332*, 600-603.

Rausch, S., Huehn, J., Kirchhoff, D., Rzepecka, J., Schnoeller, C., Pillai, S., Loddenkemper, C., Scheffold, A., Hamann, A., Lucius, R.*, et al.* (2008). Functional analysis of effector and regulatory T cells in a parasitic nematode infection. Infection and immunity *76*, 1908-1919.

Rausch, S., Huehn, J., Loddenkemper, C., Hepworth, M.R., Klotz, C., Sparwasser, T., Hamann, A., Lucius, R., and Hartmann, S. (2009). Establishment of nematode infection despite increased Th2 responses and immunopathology after selective depletion of Foxp3+ cells. Eur J Immunol *39*, 3066-3077.

Reynolds, L.A., Filbey, K.J., and Maizels, R.M. (2012). Immunity to the model intestinal helminth parasite Heligmosomoides polygyrus. Seminars in Immunopathology *34*, 829-846.

Reynolds, L.A., Smith, K.A., Filbey, K.J., Harcus, Y., and James, P. (2016). Commensal-pathogen interactions in the intestinal tract : Lactobacilli promote infection with, and are promoted by, helminth parasites. Gut Microbes *5*, 522-532.

Ronchetti, S., Ricci, E., Petrillo, M.G., Cari, L., Migliorati, G., Nocentini, G., and Riccardi, C. (2015). Glucocorticoid-induced tumour necrosis factor receptor-related protein: a key marker of functional regulatory T cells. Journal of immunology research *2015*, 171520-171520.

Ronchetti, S., Zollo, O., Bruscoli, S., Agostini, M., Bianchini, R., Nocentini, G., Ayroldi, E., and Riccardi, C. (2004). GITR, a member of the TNF receptor superfamily, is costimulatory to mouse T lymphocyte subpopulations. Eur J Immunol *34*, 613-622.

Schmitz, J., Owyang, A., Oldham, E., Song, Y., Murphy, E., McClanahan, T.K., Zurawski, G., Moshrefi, M., Qin, J., Li, X.*, et al.* (2005). IL-33, an interleukin-1-like cytokine that signals via the IL-1 receptor-related protein ST2 and induces T helper type 2-associated cytokines. Immunity *23*, 479-490.

Segura, M., Su, Z., Piccirillo, C., and Stevenson, M.M. (2007). Impairment of dendritic cell function by excretory-secretory products: a potential mechanism for nematode-induced immunosuppression. Eur J Immunol *37*, 1887-1904.

Shevach, E.M., and Thornton, A.M. (2014). tTregs, pTregs, and iTregs: similarities and differences. Immunol Rev *259*, 88-102.

Shi, J., Hou, S., Fang, Q., Liu, X., Liu, X., and Qi, H. (2018). PD-1 Controls Follicular T Helper Cell Positioning and Function. Immunity *49*, 264-274.e264.

Siewert, C., Lauer, U., Cording, S., Bopp, T., Schmitt, E., Hamann, A., and Huehn, J. (2008). Experience-driven development: effector/memory-like alphaE+Foxp3+ regulatory T cells originate from both naive T cells and naturally occurring naive-like regulatory T cells. J Immunol *180*, 146-155.

Smith, K.A., Filbey, K.J., Reynolds, L.A., Hewitson, J.P., Harcus, Y., Boon, L., Sparwasser, T., Hammerling, G., and Maizels, R.M. (2016). Low-level regulatory T-cell activity is essential for functional type-2 effector immunity to expel gastrointestinal helminths. Mucosal Immunol *9*, 428-443.

Smith-Garvin, J.E., Koretzky, G.A., and Jordan, M.S. (2009). T cell activation. Annual review of immunology *27*, 591-619.

Soper, D.M., Kasprowicz, D.J., and Ziegler, S.F. (2007). IL-2Rbeta links IL-2R signaling with Foxp3 expression. Eur J Immunol *37*, 1817-1826.

Spahn, T.W., Weiner, H.L., Rennert, P.D., Lugering, N., Fontana, A., Domschke, W., and Kucharzik, T. (2002). Mesenteric lymph nodes are critical for the induction of high-dose oral tolerance in the absence of Peyer's patches. Eur J Immunol *32*, 1109-1113.

Stephens, G.L., McHugh, R.S., Whitters, M.J., Young, D.A., Luxenberg, D., Carreno, B.M., Collins, M., and Shevach, E.M. (2004). Engagement of glucocorticoid-induced TNFR family-related receptor on effector T cells by its ligand mediates resistance to suppression by CD4+CD25+ T cells. J Immunol *173*, 5008-5020.

Subach, F.V., Subach, O.M., Gundorov, I.S., Morozova, K.S., Piatkevich, K.D., Cuervo, A.M., and Verkhusha, V.V. (2009). Monomeric fluorescent timers that change color from blue to red report on cellular trafficking. Nature Chemical Biology *5*, 118-126.

Sugiura, D., Maruhashi, T., Okazaki, I.M., Shimizu, K., Maeda, T.K., Takemoto, T., and Okazaki, T. (2019). Restriction of PD-1 function by cis-PD-L1/CD80 interactions is required for optimal T cell responses. Science *364*, 558-566.

Sun, C.-M., Hall, J.A., Blank, R.B., Bouladoux, N., Oukka, M., Mora, J.R., and Belkaid, Y. (2007). Small intestine lamina propria dendritic cells promote de novo generation of Foxp3 T reg cells via retinoic acid. The Journal of experimental medicine *204*, 1775-1785.

Sun, Y., Liu, G., Li, Z., Chen, Y., Liu, Y., Liu, B., and Su, Z. (2013). Modulation of dendritic cell function and immune response by cysteine protease inhibitor from murine nematode parasite Heligmosomoides polygyrus. Immunology *138*, 370-381.

Svetic, A., Madden, K.B., Zhou, X.D., Lu, P., Katona, I.M., Finkelman, F.D., Urban, J.F., Jr., and Gause, W.C. (1993). A primary intestinal helminthic infection rapidly induces a gut-associated elevation of Th2-associated cytokines and IL-3. J Immunol *150*, 3434-3441.

Tai, X., Cowan, M., Feigenbaum, L., and Singer, A. (2005). CD28 costimulation of developing thymocytes induces Foxp3 expression and regulatory T cell differentiation independently of interleukin 2. Nature Immunology *6*, 152-162.

Tang, Q., Adams, J.Y., Penaranda, C., Melli, K., Piaggio, E., Sgouroudis, E., Piccirillo, C.A., Salomon, B.L., and Bluestone, J.A. (2008). Central role of defective interleukin-2 production in the triggering of islet autoimmune destruction. Immunity *28*, 687-697.

Taylor, A., Verhagen, J., Blaser, K., Akdis, M., and Akdis, C.A. (2006). Mechanisms of immune suppression by interleukin-10 and transforming growth factor-beta: the role of T regulatory cells. Immunology *117*, 433-442.

Taylor, M.D., LeGoff, L., Harris, A., Malone, E., Allen, J.E., and Maizels, R.M. (2005). Removal of regulatory T cell activity reverses hyporesponsiveness and leads to filarial parasite clearance in vivo. J Immunol *174*, 4924-4933.

Uraushihara, K., Kanai, T., Ko, K., Totsuka, T., Makita, S., Iiyama, R., Nakamura, T., and Watanabe, M. (2003). Regulation of murine inflammatory bowel disease by CD25+ and CD25- CD4+ glucocorticoid-induced TNF receptor family-related gene+ regulatory T cells. J Immunol *171*, 708-716.

Urban, J.F., Jr., Katona, I.M., and Finkelman, F.D. (1991). Heligmosomoides polygyrus: CD4+ but not CD8+ T cells regulate the IgE response and protective immunity in mice. Exp Parasitol *73*, 500-511.

Urban, J.F., Jr., Maliszewski, C.R., Madden, K.B., Katona, I.M., and Finkelman, F.D. (1995). IL-4 treatment can cure established gastrointestinal nematode infections in immunocompetent and immunodeficient mice. J Immunol *154*, 4675-4684.

van Olffen, R.W., Koning, N., van Gisbergen, K.P., Wensveen, F.M., Hoek, R.M., Boon, L., Hamann, J., van Lier, R.A., and Nolte, M.A. (2009). GITR triggering induces expansion of both effector and regulatory CD4+ T cells in vivo. J Immunol *182*, 7490-7500.

Vang, K.B., Yang, J., Pagán, A.J., Li, L.-X., Wang, J., Green, J.M., Beg, A.A., and Farrar, M.A. (2010). Cutting edge: CD28 and c-Rel-dependent pathways initiate regulatory T cell development. Journal of immunology (Baltimore, Md : 1950) *184*, 4074-4077.

Vinuesa, C.G., Linterman, M.A., Yu, D., and MacLennan, I.C. (2016). Follicular Helper T Cells. Annu Rev Immunol *34*, 335-368.

Vitetta, E.S., Ohara, J., Myers, C.D., Layton, J.E., Krammer, P.H., and Paul, W.E. (1985). Serological, biochemical, and functional identity of B cell-stimulatory factor 1 and B cell differentiation factor for IgG1. J Exp Med *162*, 1726-1731.

Vogelzang, A., McGuire, H.M., Yu, D., Sprent, J., Mackay, C.R., and King, C. (2008). A fundamental role for interleukin-21 in the generation of T follicular helper cells. Immunity *29*, 127-137.

Wahid, F.N., and Behnke, J.M. (1993). Immunological relationships during primary infection with Heligmosomoides polygyrus (Nematospiroides dubius): parasite specific IgG1 antibody responses and primary response phenotype. Parasite Immunol *15*, 401-413.

Walker, L.S., and Sansom, D.M. (2011). The emerging role of CTLA4 as a cell-extrinsic regulator of T cell responses. Nat Rev Immunol *11*, 852-863.

Walker, L.S.K. (2017). PD-1 and CTLA4: Two checkpoints, one pathway? Science immunology *2*, eaan3864.

Watanabe, H., Numata, K., Ito, T., Takagi, K., and Matsukawa, A. (2004). Innate immune response in Th1- and Th2-dominant mouse strains. Shock *22*, 460-466.

Waysbort, N., Russ, D., Chain, B.M., and Friedman, N. (2013). Coupled IL-2-dependent extracellular feedbacks govern two distinct consecutive phases of CD4 T cell activation. J Immunol *191*, 5822-5830.

Wilson, M.S., Taylor, M.D., Balic, A., Finney, C.A., Lamb, J.R., and Maizels, R.M. (2005). Suppression of allergic airway inflammation by helminth-induced regulatory T cells. J Exp Med *202*, 1199-1212.

Wojciechowski, W., Harris, D.P., Sprague, F., Mousseau, B., Makris, M., Kusser, K., Honjo, T., Mohrs, K., Mohrs, M., Randall, T.*, et al.* (2009). Cytokine-producing effector B cells regulate type 2 immunity to H. polygyrus. Immunity *30*, 421-433.

Worbs, T. (2006). Oral tolerance originates in the intestinal immune system and relies on antigen carriage by dendritic cells. Journal of Experimental Medicine *203*, 519-527.

Worthington, J.J., Czajkowska, B.I., Melton, A.C., and Travis, M.A. (2011). Intestinal dendritic cells specialize to activate transforming growth factor-β and induce Foxp3+ regulatory T cells via integrin αvβ8. Gastroenterology *141*, 1802-1812.

Xiao, S., Jin, H., Korn, T., Liu, S.M., Oukka, M., Lim, B., and Kuchroo, V.K. (2008). Retinoic acid increases Foxp3+ regulatory T cells and inhibits development of Th17 cells by enhancing TGF-beta-driven Smad3 signaling and inhibiting IL-6 and IL-23 receptor expression. J Immunol *181*, 2277-2284.

Yamazaki, S., Bonito, A.J., Spisek, R., Dhodapkar, M., Inaba, K., and Steinman, R.M. (2007). Dendritic cells are specialized accessory cells along with TGF- for the differentiation of Foxp3+ CD4+ regulatory T cells from peripheral Foxp3 precursors. Blood *110*, 4293-4302.

Yan, Q., Barros, T., Visperas, P.R., Deindl, S., Kadlecek, T.A., Weiss, A., and Kuriyan, J. (2013). Structural basis for activation of ZAP-70 by phosphorylation of the SH2-kinase linker. Molecular and cellular biology *33*, 2188-2201.

Yang, X.P., Ghoreschi, K., Steward-Tharp, S.M., Rodriguez-Canales, J., Zhu, J., Grainger, J.R., Hirahara, K., Sun, H.W., Wei, L., Vahedi, G.*, et al.* (2011). Opposing regulation of the locus encoding IL-17 through direct, reciprocal actions of STAT3 and STAT5. Nat Immunol *12*, 247-254.

Yao, Z., Kanno, Y., Kerenyi, M., Stephens, G., Durant, L., Watford, W.T., Laurence, A., Robinson, G.W., Shevach, E.M., Moriggl, R.*, et al.* (2007). Nonredundant roles for Stat5a/b in directly regulating Foxp3. Blood *109*, 4368-4375.

Younes, S.A., Punkosdy, G., Caucheteux, S., Chen, T., Grossman, Z., and Paul, W.E. (2011). Memory phenotype CD4 T cells undergoing rapid, nonburst-like, cytokine-driven proliferation can be distinguished from antigen-experienced memory cells. PLoS Biol *9*, e1001171.

Zhan, Y., Gerondakis, S., Coghill, E., Bourges, D., Xu, Y., Brady, J.L., and Lew, A.M. (2008). Glucocorticoid-induced TNF receptor expression by T cells is reciprocally regulated by NF-kappaB and NFAT. J Immunol *181*, 5405-5413.

Zhang, B., Chikuma, S., Hori, S., Fagarasan, S., and Honjo, T. (2016). Nonoverlapping roles of PD-1 and FoxP3 in maintaining immune tolerance in a novel autoimmune pancreatitis mouse model. Proceedings of the National Academy of Sciences of the United States of America *113*, 8490-8495.

Zheng, Y., Josefowicz, S., Chaudhry, A., Peng, X.P., Forbush, K., and Rudensky, A.Y. (2010). Role of conserved non-coding DNA elements in the Foxp3 gene in regulatory T-cell fate. Nature *463*, 808-812.

Zhou, B., Comeau, M.R., De Smedt, T., Liggitt, H.D., Dahl, M.E., Lewis, D.B., Gyarmati, D., Aye, T., Campbell, D.J., and Ziegler, S.F. (2005). Thymic stromal lymphopoietin as a key initiator of allergic airway inflammation in mice. Nat Immunol *6*, 1047-1053.

Zhou, P., L'Italien, L., Hodges, D., and Schebye, X.M. (2007). Pivotal roles of CD4+ effector T cells in mediating agonistic anti-GITR mAb-induced-immune activation and tumor immunity in CT26 tumors. J Immunol *179*, 7365-7375.